Radio Resource Management for Unmanned Aerial Vehicle Assisted Wireless Communications and Networking

Junfei Qiu

Doctor of Philosophy

University of York

Electronic Engineering

June 2021

Abstract

In recent years, employing unmanned aerial vehicles (UAVs) as aerial communication platforms or users is envisioned as a promising solution to enhance the performance of the existing wireless communication systems. However, applying UAVs for information technology applications also introduces many new challenges.

This thesis focuses on the UAV-assisted wireless communication and networking, and aims to address the challenges through exploiting and designing efficient radio resource management methods. Specifically, four research topics are studied in this thesis. Firstly, to address the constraint of network heterogeneity and leverage the benefits of diversity of UAVs, a hierarchical air-ground heterogeneous network architecture enabled by software defined networking is proposed, which integrates both high and low altitude platforms into conventional terrestrial networks to provide additional capacity enhancement and expand the coverage of current network systems. Secondly, to address the constraint of link disconnection and guarantee the reliable communications among UAVs as aerial user equipment to perform sensing tasks, a robust resource allocation scheme is designed while taking into account the dynamic features and different requirements for different UAV transmission connections. Thirdly, to address the constraint of privacy and security threat and motivate the spectrum sharing between cellular and UAV operators, a blockchain-based secure spectrum trading framework is constructed where mobile network operators and UAV operators can share spectrum in a distributed and trusted environment based on blockchain technology to protect users' privacy and data security. Fourthly, to address the constraint of low endurance of UAV and prolong its flight time as an aerial base station for delivering communication coverage in a disaster area, an energy efficiency maximization problem jointly optimizing user association, UAV's transmission power and trajectory is studied in which laser charging is exploited to supply sustainable energy to enable the UAV to operate in the sky for a long time.

Table of contents

List of figures

List of tables

Acknowledgements

First and foremost, I would like to express my deepest gratitude to my supervisor, Professor David Grace, for his professional guidance and unconditional support throughout my entire Ph.D. study. I am grateful to him for always believing me, encouraging me to tackle many challenging research problems, giving me so much freedom to explore different research directions, and providing me with tremendous help whenever I needed it. His wide knowledge, strong research enthusiasm and hard-working attitude have inspired me during all my Ph.D. period, and will have a profound effect on my future career. I am extremely lucky to have such a nice supervisor.

I would also like to thank my thesis advisor, Professor Alister G. Burr for the motivating in-depth discussions, valuable comments and suggestions during the periodic research assessments that helped in shaping my research work. I have benefited a lot from the discussions and insightful conversations with him.

I am also grateful to the members of the Communication Technologies Research Group and Department of Electronic Engineering for creating a friendly, supportive, enjoyable and comfortable environment at the workplace. In particular, thanks to my colleagues, Dr. Yi Chu, Dr. Hamed Ahmadi, Dr. Shipra Kapoor, Dr. Danial Zakaria, Dr. Tareq Al Shami, Steve Arum, Kayode Popoola, Qiao Wang, Muheeb Ahmed in the research group for their countless discussions and helpful suggestions. I am also grateful to the department staff, Mrs Camilla Danese and Mrs Helen Smith, for their sincere help for my study and life at the university. Thank you also for all the lab lectures I worked with as a demonstrator. Such an experience enhanced my teaching ability and improved my understanding of the subjects. Many thanks to all my friends at University of York and UK who ever helped me, cared for me, or were there for me, especially during those hard times.

Finally, I would like to thank my family from the bottom of my heart. Thanks to my mother, father and sister, for their supports and concerns.

Declaration

All work presented in this thesis is original to the best knowledge of the author. References and acknowledgements to other researchers have been given as appropriate. This work has not previously been presented for an award at this or any other institution. Some of the research in this thesis has resulted in publications in journals, which are listed as follows:

Publications

- **Junfei Qiu**, David Grace, Guoru Ding, Muhammad D. Zakaria, and Qihui Wu, "Air-Ground Heterogeneous Networks for 5G and Beyond via Integrating High and Low Altitude Platforms," *IEEE Wireless Communications Magazine*, vol. 26, no. 6, pp. 140–148, 2019. (Chapter 2)

- **Junfei Qiu** and David Grace, "Robust Resource Allocation for Air-Ground Integrated Networks with Reliable Connection," *IEEE Transactions on Network Science and Engineering*, under review. (Chapter 3).

- **Junfei Qiu**, David Grace, Guoru Ding, Junnan Yao, and Qihui Wu, "Blockchain-Based Secure Spectrum Trading for Unmanned-Aerial-Vehicle-Assisted Cellular Networks: An Operator's Perspective," *IEEE Internet of Things Journal*, vol. 7, no. 1, pp. 451-466, 2020. (Chapter 4) (**ESI highly cited paper**)

- **Junfei Qiu**, Jingwei Zhang, and David Grace, "Energy Efficiency Optimization for UAV-Assisted Emergency Communication Coverage with Wireless Laser Charging," *IEEE Transactions on Vehicular Technology*, under review. (Chapter 5)

<div align="right">

Junfei Qiu
June 2021

</div>

Acronyms

3D   Three Dimensions

3GPP Third Generation Partnership Project

5G   Fifth Generation

AI   Artificial Intelligence

AWGN Additive White Gaussian Noise

BS   Base Station

CapEx Capital Expenditure

CDF Cumulative Distribution Function

CNNs Convolutional Neural Networks

CoMP Coordinated Multipoint

CSI Channel State Information

D2D Device-to-Device

EE   Energy Efficiency

FSO Free Space Optics

GSM Global System for Mobile Communications

HAP High Altitude Platform

i.i.d. Independent and Identically Distributed

IMT International Mobile Telecommunications

IoT   Internet of Things

IRS   Intelligent Reflecting Surface

ITU   International Telecommunications Union

LAP   Low Altitude Platform

LBC   Laser Beam Charging

LEO   Low Earth Orbit

LoS   Line-of-Sight

LTE   Long Term Evolution

MANET   Mobile Ad Hoc Networks

mmWave   Millimeter Wave

MIMO   Multi-Input and Multi-Output

NFV   Network Function Virtualization

NOMA   Non-Orthogonal Multiple Access

NP-hard   Non-deterministic Polynomial-time hard

OMA   Orthogonal Multiple Access

OpEx   Operational Expenditure

QoE   Quality of Experience

QoS   Quality of Service

RIS   Reconfigurable Intelligent Surface

Rx   Receiver

SDN   Software Defined Networking

SE   Spectral Efficiency

SINR   Signal-to-Interference-plus-Noise Ratio

TDMA   Time Division Multiple Access

TA   Trusted Authority

Tx   Transmitter

U2I   UAV-to-Infrastructure

U2U   UAV-to-UAV

U2X   UAV-to-Everything

UAV   Unmanned Aerial Vehicle

UE   User Equipment

UNs   United Nations

VANET   Vehicular Ad Hoc Networks

Chapter 1

Introduction

Striving to provide universal and affordable access to the Internet has been enshrined by the United Nations (UNs) as one of the 17 sustainable development goals in the 2030 Agenda for Sustainable Development [1]. The fifth generation (5G) cellular networks have been regarded as the dominant technology to deliver worldwide connectivity in the forthcoming years. However, to achieve ubiquitous coverage for anyone, anywhere at any time in a real sense, a number of challenging barriers still need to be tackled. For instance, since network deployments for mobile operators are business and profit-driven, *rural and remote areas* with low population densities and limited income are less appealing for operators to install 5G sites. In such areas, it is hard to generate sufficient revenue for operators to compensate for their capital expenditure (CapEx) and operational expenditure (OpEx). In addition, for some *hotspot areas* such as the Olympic Games venues, traffic demands will temporarily far exceed the capacity density of the ground cellular networks. In this case, further considering deploying new base stations on a permanent basis is not economically feasible. Besides, in *emergency* situations such as natural disasters, terrestrial networks may be destroyed, meaning that fast communication service recovery is hard to provide as it is not practical to install new 5G infrastructure immediately.

To deal with the aforementioned issues, research on employing unmanned aerial vehicles (UAVs) in wireless communication systems has reached an unprecedented peak recently, due to their superior attributes such as mobility, flexibility, adaptive altitude and lower cost [2–8]. They can offer a valid alternative and an efficient complement to traditional terrestrial or satellite-based infrastructure, acting as either aerial user terminals to provide such as information dissemination and data collection, or as flying base stations to enhance coverage and capacity of wireless networks [9, 10].

1.1 Advantages and Characteristics of UAV-aided Wireless Communications

In fact, UAV-aided wireless communication offers one promising solution to provide wireless connectivity for devices without infrastructure coverage due to severe shadowing by urban or mountainous terrain, or damage to the communication infrastructure caused by natural disasters [11–20]. Compared to traditional terrestrial or satellite systems, wireless communications with UAVs have several important advantages.

- Firstly, on-demand UAV systems are more cost-effective and can be much more swiftly deployed, which makes them especially suitable for unexpected or limited-duration missions.

- Secondly, with the aid of low-altitude UAVs, short-range line-of-sight (LoS) communication links can be established in most scenarios, which potentially leads to significant performance improvement over direct communication between source and destination.

- Thirdly, the maneuverability of UAVs offers new opportunities for performance enhancement, through the dynamic adjustment of UAV state to best suit the communication environment.

- Fourthly, adaptive communications can be jointly designed with UAV mobility control to further improve the communication performance. For example, when a UAV experiences good channels with ground terminals, besides transmitting at higher rates, it can also lower its speed to sustain good wireless connectivity to transmit more data to the ground terminals.

These evident benefits make UAV-aided wireless communication a promising integral component of future wireless systems, which need to support more diverse applications with orders-of-magnitude capacity improvement over current systems.

1.2 Applications and Network Scenarios for Integrating UAVs into Wireless Communications

In order to paint a clear picture on how UAVs can indeed be applied in augmenting the existing networks, we overview a number of prospective applications and network scenarios for integrating UAVs into wireless communications.

1.2.1   UAV-assisted Wireless Relays
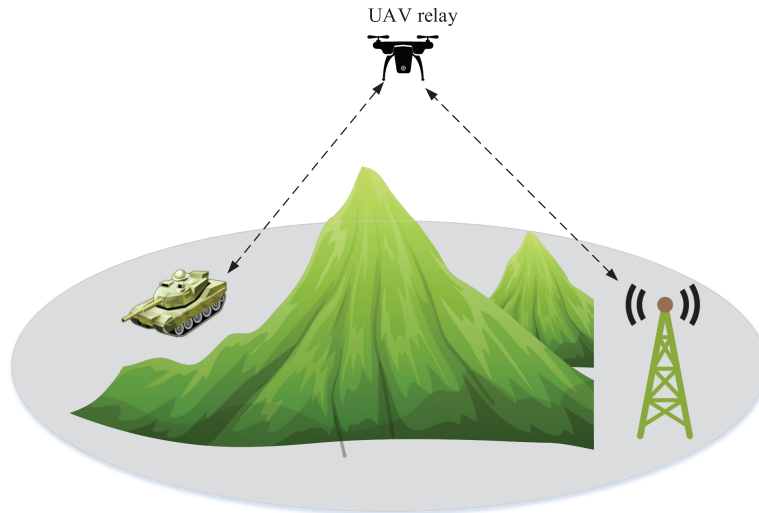
Fig. 1.1 UAV acting as a relay.

In this scenario, a UAV is used to relay information between remote user and base station separated by an obstacle, such as mountain, as shown in Fig. 1.1. As mobile relays, UAVs have several added advantages compared to traditional ground relays. UAV-aided relays are cost-effective and can easily and swiftly be deployed whenever needed, which makes them very suitable for emergency and temporary events. Moreover, UAVs' high mobility provides an opportunity for enhancing network performance through location adjustment to best suit the environment.

Relaying using UAVs can be an effective technique to improve network throughput, reliability, and extend range of communication. In literatures, UAV-aided wireless communication relays are widely studied in [21–39]. These literatures demonstrate the potential of UAVs as mobile relays to improve the performance of wireless networks.

1.2.2   UAVs as Flying Base Stations

After catastrophic natural disasters, or in emergency situations such as political rallies or sports events where there are large gatherings of mobile users, a temporary unmanned aerial base station can be used to provide communication coverage. UAVs mounted with communication devices are suitable for providing such an infrastructure due to their two unique characteristics, namely, low cost and fast speed. Aerial base stations can provide service with very high quality due to their ability to establish a line of sight connection. Their placements can also be optimized to provide maximum coverage and throughput.
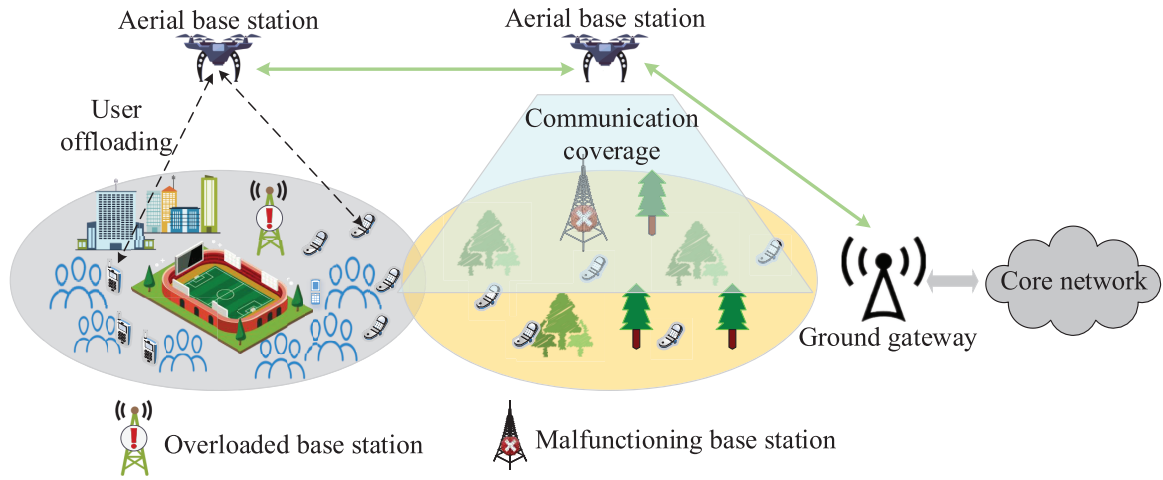
Fig. 1.2 Unmanned aerial base stations providing coverage to ground nodes.

Fig. 1.2 depicts a scenario where UAVs equipped with transceivers provide coverage
to users on the ground. Literatures [40–56] explore wireless communication networks in
which UAVs act as aerial base stations. Deploying UAVs as flying base stations can provide
much better performance in terms of coverage, load balancing, spectral efficiency, and user
experience compared to existing ground based solutions.

1.2.3 Cellular-Connected UAVs as User Equipments
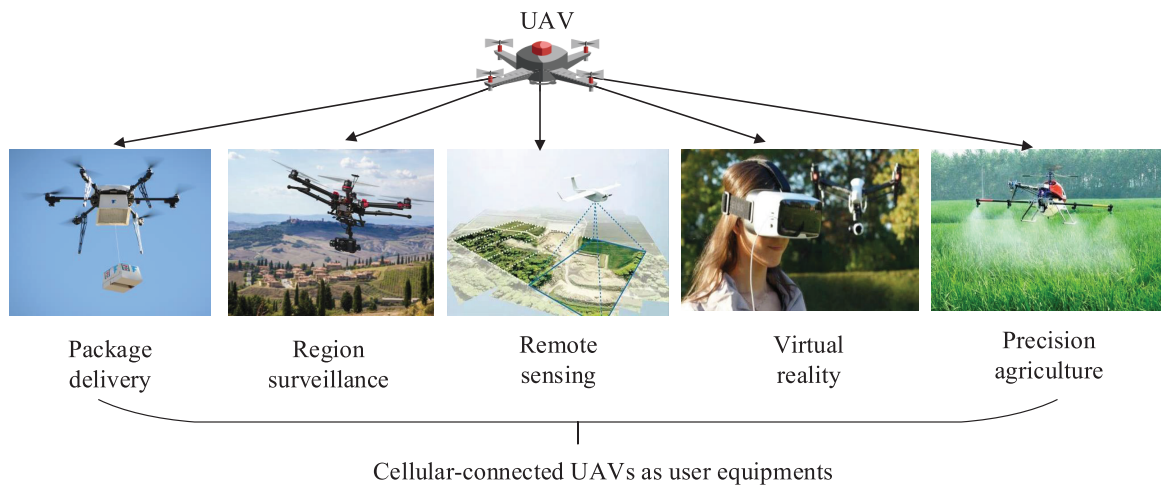
Fig. 1.3 Various UAV applications as aerial user equipments.

Naturally, UAVs can also act as aerial users of the wireless infrastructure [57]. In particu-
lar, UAV-users find their applicability in a wide range of emerging applications with varying
demands and goals, such as package delivery [58–62], region surveillance [63–74], remote

sensing [75–86], virtual reality [87–91] and precision agriculture [92–97] applications, as shown in Fig. 1.3.

Indeed, cellular-connected UAVs, where the UAVs are supported by cellular base stations as new aerial users, will be a key enabler of the Internet of Things (IoT). For instance, for delivery purposes, UAVs are used for Amazon's prime air drone delivery service, and autonomous delivery of emergency drugs [98]. The key advantage of UAV-users is their ability to swiftly move and optimize their path to quickly complete their missions. Besides, UAVs can be also despatched to disseminate (or collect) delay-tolerant information to (from) a wireless sensor network (WSN) with a large number of distributed wireless devices. Because of the unique potential of UAVs in improving WSNs, many works have studied and contributed to the area [99–112]. As described in these works, the integration of UAVs in WSN architecture will enhance the performance and extend lifespan of the network.

1.2.4 Cache-Enabled UAVs
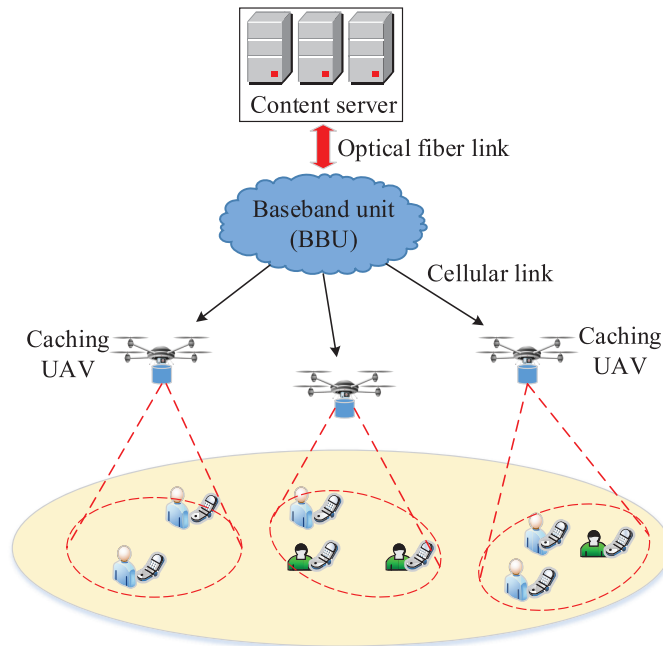
Fig. 1.4 A cellular network with cache-enabled UAVs.

Caching at small base stations has emerged as a promising approach to improve users' throughput and to reduce the transmission delay. However, caching at static ground base stations may not be effective in serving mobile users in cases of frequent handovers (e.g., as in ultra-dense networks with moving users). Hence, to enhance caching efficiency, there is a

need to deploy flexible base stations that can track the users' mobility to effectively deliver
the required contents.

To this end, UAVs can effectively serve mobile users with popular cached contents by
tracking them according to the movement pattern [113]. A typical caching UAV-enabled
network scenario is shown in Fig. 1.4. In fact, the use of cache-enabled UAVs is a promising
solution for traffic offloading in wireless networks [114, 115]. In this case, by leveraging
user-centric information, such as content request distribution and mobility patterns, cache-
enabled UAVs can be optimally moved and deployed to deliver desired services to users.
Another key advantage of deploying cache-enabled UAVs is that the caching complexity can
be significantly reduced compared to a conventional static base station case. It is evident that,
deploying cache-enabled UAVs can enhance quality of experience (QoE) of users, minimize
energy consumption, and reduce congestion in the network [116–132].

1.2.5 UAVs as Flying Wireless Backhaul for Terrestrial Networks
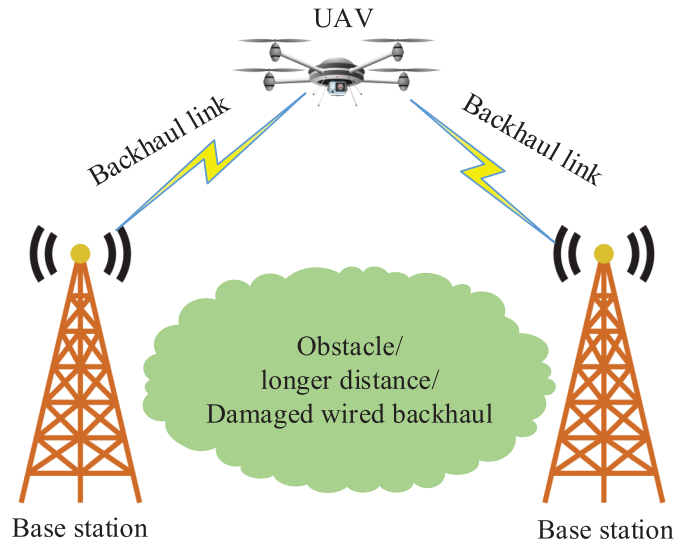
Fig. 1.5 An example scenario where UAV is used for providing wireless backhaul for two
base stations.

Wired backhauling is a common approach for connecting base stations to a core network
in terrestrial networks. However, wired connections can be expensive and infeasible due to
geographical constraints, especially when dealing with ultra dense cellular networks. While
wireless backhauling is a viable and cost-effective solution, it suffers from blockage and
interference that degrade the performance of the radio access network.

In this case, UAVs can play a key role in enabling cost-effective, reliable, and high speed wireless backhaul connectivity for ground networks [133]. In particular, UAVs can be optimally placed to avoid obstacles and establish LoS and reliable communication links. Moreover, the use of UAVs with millimeter wave (mmWave) capabilities can establish high data rate wireless backhaul connections that are needed to cope with high traffic demands in congested areas [134]. UAVs can also create a reconfigurable network in the sky and provide multi-hop LoS wireless backhauling opportunities. Fig. 1.5 shows an example of UAV-based wireless backhauling for two base stations which are either deployed at far distances, or have damaged wired backhaul, or obstructed LoS. Clearly, such flexible UAV-based backhaul networks can significantly improve the reliability, capacity, and operation cost of backhauling in terrestrial networks.

1.3 Challenges of UAV-assisted Wireless Communications and Networking

Despite the many promising benefits, wireless communications with UAVs are also faced with several new design challenges and constraints.

- **Network heterogeneity:** As an emerging network paradigm, UAV-assisted wireless communication system introduces a multi-tier network architecture with aerial and terrestrial segments. Different layers have distinct characteristics such as communication standards and diverse network devices which lead to a more complex network with high heterogeneity.

- **Link disconnection:** Due to the high-speed moving of UAVs, link disconnections of UAV-to-UAV communications may easily occur in the process of data transmission which can adversely affect the network robustness.

- **Privacy security:** There always exist privacy and security threats in the UAV-assisted cellular networks since UAVs operate in a dynamic and distributed environment. Such an issue poses a great challenge to establish trust and protect users' privacy and data security.

- **Low endurance:** The flight time of a UAV is generally short because of the limited onboard battery capacity which significantly affects the performance of UAV communication systems and prevents the wide applications of UAVs for long-time operation tasks.

1.4 Motivations and Contributions

Motivated by the above observations, in this thesis, we focus on investigating more efficient radio resource management schemes for UAV-assisted wireless communications and networking to overcome the aforementioned constraints and challenges. Specifically, the thesis presents four major contributions.

- Firstly, a hierarchical air-ground *heterogeneous network architecture* enabled by software defined networking is discussed, which integrates both *high and low altitude platforms* into conventional terrestrial cellular networks to provide additional capacity and expand the coverage of current network systems. A case study is presented for such an integrated air-ground network system.

- Secondly, dispatching UAVs as *aerial user equipments* to perform sensing and communication tasks, a robust resource allocation scheme is designed to guarantee the *reliable connection* of UAV transmission links while taking into account the dynamic features and different requirements for different types of UAV connections.

- Thirdly, from an operator's perspective, a blockchain-based *secure spectrum trading* model is constructed where mobile network operators and UAV operators can share spectrum in a distributed and trusted environment based on *blockchain* technology to establish trust and protect users' privacy and data security.

- Fourthly, deploying a UAV as a *flying base station* to deliver emergency communication coverage in a disaster area, to address the issue of low endurance of UAV, an energy efficiency maximization problem is studied in which *laser charging* is exploited to supply sustainable energy for the UAV to prolong its flight time.

Based on the aforementioned advanced technologies and methods, it is expected that the UAV will be a key enabler to assist 5G and beyond systems for providing ubiquitous network coverage worldwide and achieving the goal of global access to the Internet for all.

1.5 Thesis Outline

An overview of the thesis structure is shown in Fig. 1.6. The rest of this thesis is organized as follows.

Chapter 2 proposes a novel hierarchical air-ground heterogeneous network architecture to fully exploit the benefits of the distinct features of various UAVs. This chapter focuses on providing a comprehensive comparison and review of different types of UAVs for communication services and constructing a conceptual architecture to demonstrate how the proposed

Radio Resource Management for Unmanned Aerial Vehicle Assisted Wireless Communications and Networking

Chapter 2	Chapter 3	Chapter 4	Chapter 5
Air-Ground Heterogeneous Networks for 5G and Beyond via Integrating High and Low Altitude Platforms	Robust Resource Allocation for Air-Ground Integrated Networks with Reliable Connection	Blockchain-Based Secure Spectrum Trading for UAV-Assisted Cellular Networks	Energy Efficiency Optimization for UAV-Assisted Emergency Communication Coverage with Wireless Laser Charging
Network heterogeneity	Link disconnection	Privacy security	Low endurance

Research on the potential opportunities and challenges bringing by integrating UAVs into next-generation wireless communication networks

Fig. 1.6 An overview of the thesis structure.

multi-tier system operates to address the network heterogeneity and obtains the benefits from both aerial and terrestrial segments.

Chapter 3 studies the potentials of cellular-connected UAVs with UAVs acting as aerial users to perform data sensing in a cellular network, where UAV-to-UAV (U2U) transmit-receive pairs share the same spectrum with the uplink UAV-to-infrastructure (U2I) communication links. Pursuant to differing requirements for different types of links, i.e., high capacity for U2I links and ultra reliability for U2U links, a robust resource allocation algorithm is designed to maximize the sum ergodic capacity of the U2I connections while guaranteeing the reliable connection for each U2U link. This chapter focuses on dealing with the constraint of link disconnection due to the high mobility of UAVs with considering the scenario in which UAVs serve as aerial users.

Chapter 4 presents a spectrum blockchain framework to motivate secure spectrum trading and sharing between mobile and UAV network operators. A utility maximization model is further formulated to study the optimal spectrum pricing and purchasing solutions for different operators. This chapter focuses on tackling the spectrum scarcity issue for UAV communications as well as showing how the blockchain helps to address the constraint of security and privacy threat to improve the spectrum trading environment.

Chapter 5 exploits using laser charging to prolong the UAV's flight time for providing communication coverage in a disaster area as a flying base station. An energy efficiency maximization problem is investigated by optimizing the multiuser communication scheduling and association jointly with the UAV's power allocation strategy and flight trajectory. This chapter focuses on solving the low endurance constraint of UAVs and illustrating the preliminary attempt and practicability to use laser charging for UAV communications.

Chapter 6 concludes the thesis, summarises the novel contributions and provides the recommendation for further extensions of the presented work.

Chapter 2

Air-Ground Heterogeneous Network for 5G and Beyond via Integrating High and Low Altitude Platforms

2.1 Introduction

Although there have been many discussions on utilizing UAVs in cellular networks in the existing recent works as shown in Chapter 1, most just focus on low-altitude UAVs (i.e., low altitude platforms, which typically operate at an altitude not exceeding several kilometers), while neglecting the potential usage of high-altitude UAVs (i.e., high altitude platforms, which operate at the stratospheric altitudes in typically quasi-stationary locations)[1]. Generally speaking, *low altitude platforms* (LAPs) are more cost-effective and can be more swiftly deployed than *high altitude platforms* (HAPs), but HAP-based communications also have several important advantages such as wider coverage and longer endurance since most of them are solar-powered [135, 136]. In fact, the sundry assets of UAVs and their placement options provide a unique potential to create multi-tier heterogeneous aerial networks [137] to inject additional capacity and expand the coverage for 5G terrestrial networks.

Motivated by the above observations, different from existing works focusing on standalone aerial networks, in this chapter, we investigate exploiting the latent opportunities and challenges for integrating both HAPs and LAPs into 5G and beyond (B5G) cellular systems. In order to address the challenges of network heterogeneity and fully leverage the benefits of the distinct features of various UAVs, we propose a novel hierarchical network architecture enabled by software defined networking (SDN), which integrates cross-layer

---

[1]Here, the term "UAV" is a general concept covering the various aerial platforms such as drones, airships, aircraft, balloons, etc.

Table 2.1 Typical features comparison of HAPs and LAPs for communication services [136, 146, 147].

Aerial platforms	Key features	Classification type	Typical performance and specification						Challenges and opportunities for integrating into 5G/B5G
			Payload capabilities	Mobility and station keeping	Power source and endurance	Data rate and capacity	Radio frequency transmit power	Main applications	
High altitude platforms (HAPs)	HAPs are aerial unmanned long-endurance platforms situated at the stratospheric altitudes which can provide multipurpose communications payloads over regional areas of coverage.	Aircraft	<150kg/<500W	Usually fly on a tight circle (about 2 km radius or more)	Solar cells (+fuel cells), 1~3 months	High, capacity can upgrade by increasing the number and changing the size of the spot beams	1~5 W for per cell	Wide area relay and broadcast, environmental monitoring, maritime surveillance, earth observation, internet connectivity	• **Pros**: Wider coverage and longer endurance; high payload capabilities; capacity increases through spot-beam resizing; have licensed spectrum • **Cons**: Deployment cost is a little high; challenging for maintaining station-keeping
		Balloon	<100kg/<100W	Most are stationary (Google Loon can move with the wind speed)	Fuel cells (+solar cells), 1~3 months				
		Airship	<500kg/<5~6kW	Quasi-stationary (only need to compensate for the winds)	Solar cells (+fuel cells), 1~several years				
Low altitude platforms (LAPs)	LAPs typically refer to small fuelled unmanned airplane, having short mission durations and operating at generally modest or low altitudes.	Fixed-wing	Heavy payload, in general up to 100 kg	High speed, maximum speed with 120 km/h, must maintain continuous forward motion to remain aloft	Fuel cells (+solar cells), up to dozens of hours, will be longer with solar power	Relatively low, limited by the platform size	0.1~5 W in general	Emergency communication, military surveillance, caching relay nodes, aerial inspection, temporary events support	• **Pros**: Cost-effective, light weight and more swiftly deployed; short-range line-of-sight (LoS) communication links, closer to mission objectives; good wireless connectivity • **Cons**: Low payload and endurance; limited flight time
		Rotary-wing (helicopter)	Low, depends on size, in general 30~50 kg	Medium speed, 15~40 km/h, can stay stationary in the air	Battery-powered, up to several hours, will be longer if tethered to the ground				
		Rotary-wing (multicopter)	Low, depends on size, in general 10~15 kg	Limited mobility, are able to move in any direction as well as to stay stationary in the air	Battery-powered, up to several hours, will be longer if tethered to the ground				

high and low altitude platforms into conventional terrestrial cellular networks to inject additional capacity and expand the coverage for underserved areas in a flexible, seamless, and cost-effective manner.

Specifically, we first present a comprehensive comparison and review of different types of UAVs for communication services in Section 2.2. Next, in Section 2.3, an integrated HAP-LAP-terrestrial heterogeneous network architecture based on SDN is proposed with discussions about the motivation and feasibility for integration and its potential advantages. In Section 2.4, several key enabling technologies associated with the operation of the integrated air-ground networks are identified. Then, in Section 2.5, we discuss the potential application scenarios where the system can further enhance the performance of traditional terrestrial networks, followed by a case study to demonstrate the effectiveness of the proposed architecture. Finally, the challenges and open issues are given in Section 2.6, followed by the conclusion of this chapter in Section 2.7.

2.2   HAPs vs. LAPs for Communication Services

In general, UAVs can be categorized, based on their altitudes, into HAPs and LAPs [138]. In this section, we mainly provide a comprehensive review and comparison on the existing state-of-the-art developments in HAPs and LAPs for communication services. Table 2.1

Table 2.2 Several well-known projects/products for HAPs and LAPs.

Projects/Products	Description	Leading organizations	Start time
Zephyr (http://www.airbus.com/defence/uav/zephyr.html)	Zephyr is a high altitude pseudo-satellite, running exclusively on solar power with a goal of filling a capability gap between satellites and low-altitude UAVs.	Airbus Defense and Space	2013
Project Loon (https://x.company/loon/)	Project Loon is a network of stratospheric balloons at altitudes between 18 km and 25 km, travelling on the edge of the space to provide Internet access for rural and remote areas worldwide. However, this project is shut down in 2021 after failing to find a sustainable business model.	Google	2012
Aquila (https://code.facebook.com/posts/268598690180189)	Aquila is a solar-powered high-altitude aircraft, intended to act as relay stations to connect areas of the world that traditionally haven't had reliable internet access.	Facebook	2014
StratoBus (http://airstar.aero/en/technologies-for-stratobus/)	Stratobus is an autonomous airship, operating at an altitude of about 20 kilometers with stationary position to carry out a wide range of missions, including observation, security, telecommunications, broadcasting and navigation.	Thales Alenia Space	2010
Skybender (https://www.theguardian.com/technology/2016/jan/29/project-skybender-google-drone-tests-internet-spaceport-virgin-galactic)	Project SkyBender aims to beam 5G internet from solar-powered drones, which is expected to use new millimeter wave technology to deliver data from drones – potentially 40 times faster than 4G.	Google	2016
Flying Cell on Wings (CoW) (http://about.att.com/innovationblog/cows_fly)	Flying CoW is a cell site on a drone, aiming to beam LTE coverage from the sky to customers on the ground during disasters or big events.	AT&T Company	2017

summarizes the typical features of HAPs and LAPs, and Table 2.2 introduces several well-known projects/products of utilizing UAVs to serve communication applications.

2.2.1   HAP-Based Communication Networks

HAPs are aerial unmanned long-endurance platforms situated in the stratosphere (from 17 to 22 km) which can provide multipurpose communications payloads over regional areas of coverage, without the need for significant and expensive ground based infrastructures [139–143]. HAPs for telecommunications were studied extensively in 1990s and 2000s [144]. However, owing to the technology limitations, particularly relating to the solar cell, battery and aeronautics, very few research projects continued. Fortunately, with the improvement of key enabling technologies of materials, battery and energy capture in recent years, accompanied by ample capital investment from several major Internet companies like Google and Facebook, the development of HAPs has been back in the public eye. In contrast to satellites, HAPs have better link budget and higher capacity, lower propagation delays, lower upgrading cost, and shorter landing and takeoff times for maintenance purposes [145]. They have been considered as new radio access platforms for the 5G wireless communication system by the Third Generation Partnership Project (3GPP) [135]. Moreover, in April 2018, the North Sky Research of United States released a comprehensive analysis report of the HAPs market, which claimed that the global HAPs revenue would keep increasing in the next ten years[2].

---

[2]http://www.nsr.com/research-reports/satellite-space-infrastructure/high-altitude-platforms-haps-market-2nd-edition/, High Altitude Platforms (HAPS), 2nd edition, 2018.

In this section, we will discuss the types, advantages, applications, and challenges of HAPs, respectively.

1) Types of HAPs: HAPs may be aircraft, airships or balloons that operate at altitudes in the range of 17-22 km above the Earth's surface [146]. This altitude range is chosen because of its low wind currents and low turbulence which reduce the energy needed to maintain the position of the HAP. Different categories of HAPs have been discussed throughout the history of HAPs as follows:

- **High altitude aircraft:** They typically fly on a circular path in the sky since they cannot stay in the air statically unless they move [147, 148]. They generally have a wide wingspan, are lightweight and are powered by solar cells or fuel such that they can fly at high altitudes for a long time [149–151]. The key limitation of such HAPs is their typical low payload capacity and high operational cost.

- **Balloons:** They are primarily designed to stay still in the air for a long period of time and can be lifted by using hydrogen, helium, ammonia or methane [152–155]. The balloons are often huge, over 100 m, and capable of carrying payloads of 800 kg or more.

- **Airships:** They are huge aerial platforms with lengths of 100 m or more, and are mainly powered by solar panels mounted on the top surface of the airship [146, 156, 157]. In comparison to balloons, airships have station-keeping capability using electric motors and propellers [158].

2) Advantages of HAPs: HAP-based communications have several advantages which are summarized as follows:

- *Large-scale coverage with long endurance:* Compared with LAPs, HAPs have longer endurance since most of them are solar-powered [159]. Furthermore, the capability of HAPs to hover at high altitudes, allowing them to provide services for ground points over an extensive area [160], makes them more favorable in comparison to LAPs and terrestrial networks. A handful of HAPs could cover a whole country (e.g., Japan can be covered by 16 HAPs with an elevation angle of 10° while Greece can be covered by 8 HAPs) [147].

- *Quick response to temporal and spatial traffic demands:* A HAP can achieve cell coverage through *spot beams* delivered by a phased array antenna without using any infrastructures [140]. Moreover, since the size of the spot beam can be optionally adjusted [161], amorphous cells with flexible capacity provision will be available just through resizing the spot beam. HAPs are ideally suited to the provision of centralised adaptable resource allocation, i.e. flexible and responsive frequency reuse patterns

and cell sizes, unconstrained by the physical location of base-stations. Such almost real-time adaptation should provide greatly increased overall capacity compared with current fixed terrestrial schemes or satellite systems [162].

- *Rapid deployment (compared to terrestrial networks and satellites):* Emergency or disaster relief communications rely on rapid deployment of a wireless network. With their rapid deployment ability, HAPs can play a key role in emergency or disaster relief applications by restoring the telecommunication services in a matter of hours [163].

- *Favorable HAP-ground channel characteristics:* The under-utilized mmWave frequency spectrum is seen as a promising candidate for future wireless systems. However, the use of the mmWave spectrum in terrestrial networks is challenging because it is sensitive to blockage and requires the LoS propagation between the transmitter and the receiver. With the aid of HAPs, the LoS propagation is available most of the time which allows the realization of using mmWave and other point-to-point communication technologies such as free space optics (FSO) [164].

3) Applications of HAPs: Owing to the above advantages, HAPs have exhibited promising results in many applications and services in civil, public, and military fields. The applications and services that can benefit from HAPs include telecommunications services, surveillance, remote sensing, pollution monitoring, traffic monitoring, and emergency services [165, 166]. The emphasis in this subsection is on the telecommunications services, including broadband internet, multicast/broadcast services, and backhaul/fronthaul.

- *Broadband wireless access:* HAPs can be used to provide broadband services to both mobile and fixed users with data rates of the megabit per second order, at the frequency bands allocated by International Telecommunications Union (ITU) to HAPs. The ITU has allocated several frequency bands for HAPs to provide different broadband multimedia applications in mmWave band and International Mobile Telecommunications (IMT)-2000 services in third generation (3G) frequency bands. The expected services are audio/video streaming, distributed games, distance education, medical applications, web browsing, large files transfer, and Ethernet line bridging [167]. These services can be delivered efficiently by relaying information over hybrid terrestrial/HAPs/satellite networks resulting in wider coverage areas, distribution of services without overloading the terrestrial segments, and the reduced overall costs.

- *Multicast/broadcast services:* Due to increasing demands of users for ubiquitous access to multimedia services, 3GPP has introduced multimedia multicast and broadcast concept in future communications networks. Some of the services (e.g., digital

29

video/audio broadcasting) have already been provided by terrestrial and satellite networks. The provision of these services is highly dependent on the operating environment and hence can have high operational costs. In this respect, HAPs can provide cost-effective solutions to build standardized low-cost receivers [168, 169]. The onboard HAPs base stations (BSs) would be similar in principle, but more complex as compared to conventional terrestrial base stations as they will serve large number of cells. The HAPs technology would implement two types of onboard payloads: one for satellite-HAPs links and the other for HAPs-terrestrial links and hence extra hardware requirements on terrestrial and satellite segments would be reduced. In addition, in integrated scenarios, return channel to satellite can be provided by HAPs which reduces the congestion issues in terrestrial segments.

- *Vertical backhaul/fronthaul interconnection via HAPs:* One of the key use cases for HAPs as an integral part of the future wireless infrastructure is provision of backhaul/fronthaul links for the small and omnipresent pico- and femto-cells in 5G and B5G networks [170], since not all the traffic will be able to be routed through the meshed network foreseen to interconnect corresponding base stations. Moreover, provision of backhaul/fronthaul via HAPs can make noncontiguous deployment of small base stations easier, effectively only aiming at meeting access network capacity demands and not solving the transport network demands with the mesh network of base stations. From the backhaul link perspective, HAPs could be also used in the global wireless infrastructure to relay the increasingly huge amount of data collected by low earth orbit (LEO) observation satellites to the ground centers. HAPs would essentially break the satellite terrestrial link to weather independent high-capacity optical link between satellite and HAP, making it possible to download data in the short time pass of satellite, and the fixed radio frequency (RF) and/or FSO link between HAP and ground station subject to atmospheric weather conditions but with reduced throughput requirements.

4) Challenges of HAPs: Despite the many benefits of HAPs, HAPs-based communication networks pose several challenges. For example, HAPs are more expensive and the deployment time is longer than LAPs. At the same time, they also have to maintain station and the stabilization of the on-board antenna. Besides, since the HAPs operate in the stratosphere for serving communication applications, some environmental conditions such as rain attenuation may interfere with the system performance.

2.2.2   LAP-Based Communication Networks

On the other hand, compared to HAP-based communications, wireless communications with LAPs (typically referred to small fuelled unmanned airplanes, have short mission durations and operate at an altitude not exceeding several kilometers) have been also receiving considerable attention from the research community recently, due to their flexible mobility, preferable link budget and cost-effective maintenance features.

In the rest of this subsection, the classification, characteristics, deployment and constraints of LAP communication networks are provided.

1) Classification of LAPs: Depending on their flying mechanisms, LAPs (e.g., drones) can be mainly classified into two types:

- **Fixed-wing LAPs:** They can glide over the air, which makes them energy efficient and able to carry heavy payload. Gliding also helps fixed-wing LAPs to travel at a faster speed. The downsides of fixed-wing LAPs are that (i) they require a runway to take off and land as vertical take-off and landing are not possible, and (ii) they cannot hover over a fixed location. Fixed-wing LAPs are also more expensive than multi-rotor LAPs.

- **Rotary-wing LAPs:** They allow vertical take-off and landing, and can hover over a fixed location to provide continuous cellular coverage for certain areas. This high manoeuvrability makes them suitable for assisting cellular communications, since they can deploy BSs at the desired locations with high precision, or fly in a designated trajectory while carrying BSs. However, multi-rotor LAPs have limited mobility and consume significant power as they have to fight against gravity all the time.

2) Frequently Changed Topology of LAP Networks: Node mobility may be one of the most apparent differences between LAP networks and other types of ad hoc networks such as vehicular ad hoc networks (VANET) and mobile ad hoc networks (MANET) [171]. In LAP networks, the extent of mobility may be much higher than that in both VANET and MANET. Depending on applications, the speed of a LAP-UAV may be in the range of 0-460 km/h [172]. Trajectories of LAP nodes may also be different. For example, LAP nodes fly in the sky, while MANET nodes move over a particular terrain, and VANET nodes move on roads. Therefore, topologies of LAP networks may change more frequently than those of both VANET and MANET. In addition to the mobility of LAP nodes, the failure of LAP nodes as well as the addition of new LAP nodes may also affect network topologies. In such case, old communication links are removed or new links are established, which may result in frequent update in the network topologies. Moreover, link outages due to airframe blockage and signal interference may further change the network topologies.

3) Deployment of LAPs: LAP deployment can be explained as a dynamic process of determining the appropriate number of LAPs and their spatial locations (i.e., trajectory and hovering points) according to communication requirements of networks. Typically, the LAP deployment problem is modeled as a mathematical optimization problem, and LAP networks can be efficiently deployed by solving this optimization problem. There are two types of optimal deployment problems. The first type is to optimize the network revenue such as maximizing performance (e.g., coverage and achievable rates) due to LAP deployment under certain constraints such as LAP transmission power, LAP hovering time, and the number of LAPs. On the contrary, the second type is to minimize the cost (e.g., transmission power, LAP hovering time, LAP stop points, and the number of LAPs) of deploying LAPs while satisfying specific communication requirements, for example, quality-of-service (QoS) requirements. Existing LAP deployment mechanisms may be classified into two categories: two-dimensional (2-D) optimal deployment and three-dimensional (3-D) optimal deployment [173–176].

4) Constraints of LAPs: All LAPs suffer from size, weight, and power constraints, which would limit the endurance, computation, and communication capabilities of LAPs. For small LAPs, the energy constraint may be significant. This is due to the fact that the energy of a small LAP may support it to fly for only a few minutes, or at most a few tens of minutes. Furthermore, energy-constrained LAPs may shorten the lifetime of a LAP network. Imagine a scenario where some LAPs would be out of services because of lack of energy. The absence of energy-exhausted LAPs may change network configurations. The changed configuration would force LAP networks to self-organize to maintain the network connectivity, which may exacerbate the drainage of the network energy. Therefore, the energy-aware LAP deployment and transmission mechanisms should be investigated to prolong the lifetime of LAP networks. The computing power is also a significant concern of a LAP. The size and weight constraints of a LAP significantly affect its computing power. Besides, a shortage of dedicated licensed spectrum means that LAPs always need to coexist with existing terrestrial systems using shared spectrum.

To sum up, in terms of HAP and LAP, each one has its specific advantages and drawbacks. However, if considering leveraging the strength of both sides, several key issues will arise, such as: 1) how to design an efficient architecture to integrate both HAPs and LAPs into terrestrial cellular systems, forming a heterogeneous air-ground network? 2) what opportunities and challenges will such an architecture bring? and 3) where are the potential and typical application scenarios for the integrated system? The following sections of this chapter will shed light on the aforementioned queries and provide some research insights.

2.3 Integrated Air-Ground Network Architecture via Leveraging HAPs and LAPs

To fully capitalize on the potential benefits of different types of UAVs, in this section, we propose an *integrated air-ground heterogeneous network* architecture, investigating how HAPs and LAPs can collaborate to provide enhanced coverage and capacity for the underserved areas.

2.3.1 Motivation and Feasibility for the Air-Ground Network Integration

Broadband access everywhere constitutes a pillar of 5G and B5G service requirements, however, standalone 5G terrestrial networks have many challenges to meet such a target, as detailed in the following.

- Dense terrestrial network deployment for rural and remote areas is not practical, due to the high cost of infrastructure, leading to a poor coverage for these regions.

- Even though current mobile networks can actually be reconfigured when load and capacity demands change in certain areas (cells), conventional terrestrial networks are still not efficient enough to deal with some temporary emergency or overloaded cases.

- The maximum coverage diameter is another challenge for terrestrial base stations. For instance, mmWave is one of the principle approaches for 5G, however, due to the higher path loss at the mmWave band this inevitably reduces the coverage to smaller areas. Moreover, for a Long-Term Evolution (LTE) macrocell base station, the coverage diameter is just several kilometers, while that is even less than hundreds of meters for a small cell.

Since there is no single one-size-fits-all solution that can effectively satisfy all the needs of universal Internet access, global service provision will likely need the interworking of multiple heterogeneous wireless technologies. In the regions where providing a desirable terrestrial assistance is not efficient, various types of aerial platforms can act as a viable alternative to improve performance, agility, and flexibility of 5G and beyond mobile networks in unprecedented ways [177, 178]. Through integrating HAPs and LAPs into conventional terrestrial networks, the benefits from both air and ground segments can be fully exploited to support multifarious communication services and scenarios.
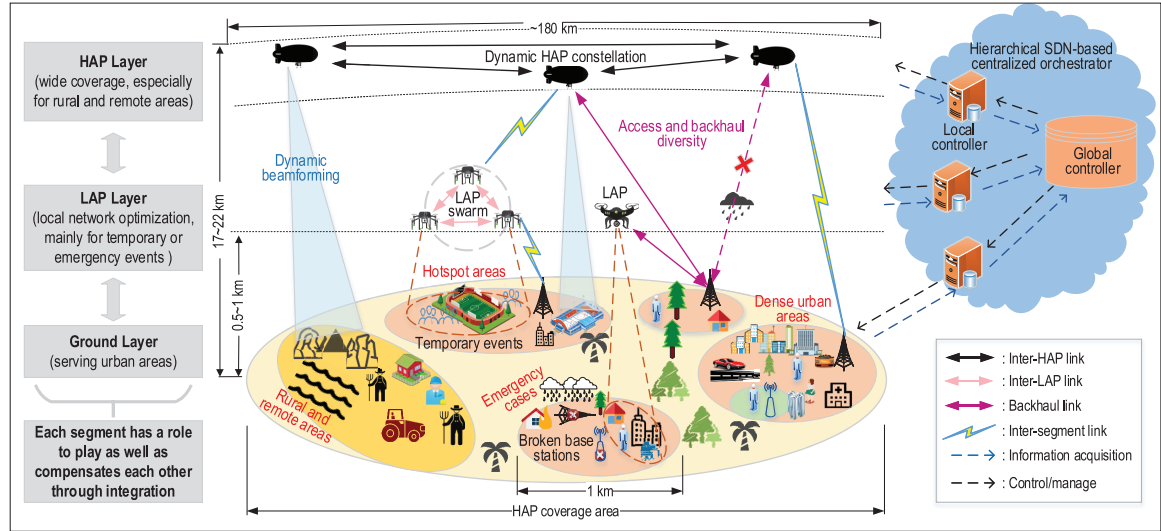
Fig. 2.1 Hierarchical integrated air-ground network architecture.

2.3.2 Integrated HAP-LAP-Terrestrial Hierarchical Network Architecture

Fig. 2.1 shows the proposed hierarchical integrated air-ground system architecture for B5G wireless networks. The integrated network comprises three main segments: *HAP, LAP and ground layers*. A centralized orchestrator based on SDN is also embedded into the system to manage the operation of the whole system at the upper level. The characteristics for each constituent part are summarized as follows:

• **HAP layer:** The HAPs are expected to operate at the stratospheric altitude to deliver LoS connectivity over a large geographical area. They are capable of harvesting and storing solar energy, allowing them to stay aloft for a long period to provide continuous service. A single HAP can establish a wide variety of cells with centralized and flexible capacity provision (the cell sizes may be reduced to provide increased capacity) by using phased array antennas to generate multiple spot beams to simultaneously serve several different areas. This advantage can help HAPs to reduce the end-to-end latency[3] and deliver communication coverage anywhere within the service area without moving their positions. Moreover, a dynamic constellation of HAPs can be formed to provide extended communication cov-

---

[3]Latency is made up of a number of components, dominated by protocol delay and propagation delay. HAPs can provide service to a coverage area up to 200 km radius, resulting in a propagation round trip time of 1.5 ms. In the case of a HAP based system, anywhere in the coverage area can be reached in a single hop. However, the same area served terrestrially will have to rely on the core network and transmission through multiple nodes, each introducing additional protocol delay (protocol delay is generally 1-5 ms per node, mainly caused by the signaling and framing). Thus, the terrestrial system will tend to have a higher delay than the HAP system for end-to-end transmissions of greater than 20 km.

erage and increased capacity density. Besides, with the advantages of high altitude, long endurance and large payloads, HAPs are able to provide localization and environmental information for other wireless systems at lower layers, while performing surveillance to ensure safe and secure operation of the architecture, as well dedicating wireless power transfer to ensure a better quality of charging for low-endurance LAPs.

• **LAP layer:** Unlike the HAPs with their quasi-stationary positions, LAPs can fly with relatively random or optimally distributed locations to offer temporary or localized capacity with low propagation delay. It is possible for LAPs to deliver small cells of hundreds of meters in diameter, creating the possibility of providing ultra-high capacity density communications for temporary events or disaster relief. They are mainly responsible for local network optimization in the integrated architecture through functioning as either aerial users or flying base stations in the sky according to their missions [179]. The LAPs, if needed, can also operate in a swarm through mutual cooperation to form a self-organized networks, linking with mmWave or free space optics. However, flying LAPs have a limited amount of on-board energy (the battery-powered LAPs are generally expected to work from dozens of minutes to several hours, while the solar power enabled LAPs may last longer). Thus, when designing the LAP layer in the system, the improvement of energy efficiency of LAPs requires careful consideration such as exploiting trajectory optimization, energy harvesting, etc. Besides, the optimal altitudes need also to be analyzed when deploying LAPs while considering the impact of both distance and LoS probability.

• **Ground layer:** The terrestrial network system is the main part of the interworking architecture for providing wireless coverage in the conventional core areas such as the metropolis. In these regions, the high performance requirements from massive amount of devices are often supported by rich and complex infrastructures, including macro and small cells, transport networks, and so on. There are three principal enabling technologies for 5G terrestrial networks, i.e., ultra densification, mmWave and massive multiple input multiple output (MIMO). However, to ensure the goal of global access to the Internet for all, several inevitable shortcomings have appeared, such as cost and interference for ultra densification, high path loss at the mmWave band, and the computational burden associated with massive MIMO. Fortunately, in this integrated architecture, the terrestrial networks can leverage the power from the other two aerial layers to relieve the aforementioned issues.

• **Centralized orchestrator:** The central controller, based on SDN [180], will act as the brain of the system at the upper level to manage the whole network and incorporate the cross-tier segments of the architecture. Considering different segments have distinct characteristics, in addition to a global controller in upper layer for the management of the whole system, three separated SDN controllers in lower layer are dedicated to the corresponding
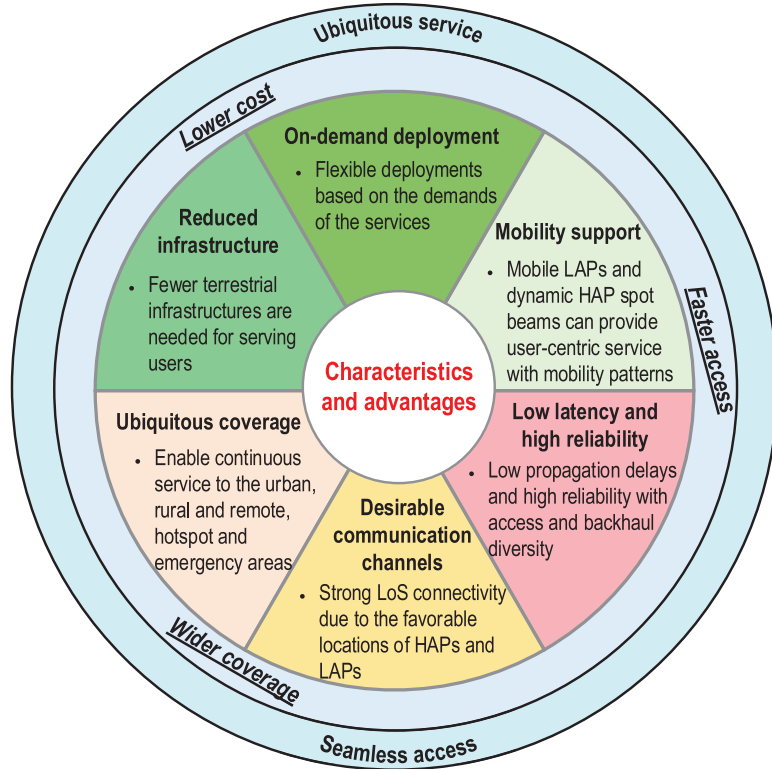
Fig. 2.2 Characteristics and advantages of the integrated air-ground network system.

segment for local network optimization. That is to say, the local SDN controllers perform fine-grained control, while the upper-tier global SDN controller conducts coarse-grained control. In particular, the orchestrator will play an intelligent role from three aspects: infrastructure, control, and application layers. From the perspective of the infrastructure layer, computing, storage and communication resources from different segments will be processed by the controller through a virtualized cloud center. From the perspective of the control layer, the orchestrator will perform distributed decision making and coordination for the abstracted information in the system, such as beam steering of HAPs, movement control and deployment of LAPs, and resource block allocation in terrestrial base stations. Both of HAPs and LAPs are connected to the core network via wireless links and are controlled by the centralized controller. From the perspective of the application layer, a variety of Internet access services and network management functions can be identified according to the instruction from the orchestrator, such as users' request reply, traffic classification, and dynamic route adjustment. In addition, the orchestrator will establish logical connections with the cross-tier segments to send control messages and to receive feedback information.

In summary, each segment has its own role to play in the architecture while each can compensate the others at the same time. Through interworking, the superiorities from both

the sky and ground segments can be exploited. Access and backhaul diversities make the integrated network be capable of delivering a highly reliable connection, achieving ubiquitous coverage and seamless access for users in a real sense. From the holistic system perspective, *the HAP layer is for wide area coverage, and the LAP layer is for local network optimization while the ground layer is for core dense site service.* Moreover, our proposed network architecture will be a highly integrated system due to the fact that HAPs and LAPs have strong compatibility with the current cellular networks. Furthermore, since the cells provided by the three layers form contiguous coverage while the overlap between the cells is limited, the extra overhead with the integrated architecture is relatively small. As shown in Fig. 2.2, with the proposed integrated network architecture, several benefits can be achieved including *wider coverage, faster access and lower cost.*

2.4 Key Enabling Technologies

In this section, we briefly present an overview of several key enabling technologies that are required to efficiently sustain the integrated air-ground networks. These technologies are introduced in four aspects, including *infrastructure design, network connectivity, layers interworking, and traffic identification.*

2.4.1 Aerial Platforms-Infrastructure Design

Since the terrestrial infrastructure has been well studied in existing works, here, we mainly discuss some design considerations for the aerial platforms, with the primary ones being: lightweight material structures, energy supply, and onboard communications payload. To improve the reality and durability of the aerial platforms, especially for the HAPs, the envelope material should have low weight, low permeability to lifting gas, high strength and ability to withstand damage, etc. Fortunately, with the development of advanced materials, these visions have been gradually achieved in recent years, which has resulted in HAPs being actively considered as viable technology again. The choice of energy source is another fundamental issue. Solar power coupled with energy storage has been regarded as primary means of providing energy for HAPs since they have large surfaces suitable to accommodate the solar panel films [135]. For the LAPs, advanced rechargeable batteries such as lithium-sulfur or regenerative fuel cell (RFC) may become the promising enabling technologies in the coming years. In terms of the communications payload, the antenna subsystem is one of the key components, in which phased array antennas are installed for the HAPs to

produce the spot beams while tiny antennas, producing a single cell, are suitable for the size constrained LAPs to save space for other peripherals.

2.4.2 Backhaul Delivery-Network Connectivity

In the integrated air-ground network system, terrestrial infrastructure can utilize wired backhaul links, often fiber optics; whereas the aerial platform communications must exploit the wireless links. For HAP networks, mmWaves are more promising options for supporting long-range HAP-ground links while FSO is a good choice for inter-HAP links, owing to their highly directional beams and LoS paths, thereby providing desirable capacity backhaul in many regions of the world [135]. However, because link outage of mmWaves and FSO are caused primarily by rain attenuation and heavy cloud, such links may not be used in practice in some tropical countries due to the heavy and frequent rainfall. On the other hand, for LAPs with medium range and more limited capacity requirements, one could rely on the more economical sub-6GHz technologies like LTE to provide backhaul connectivity. In addition, satellite communications could be also integrated into the system as a complementary extra segment for situations where aerial and terrestrial communication infrastructures are not available, providing geolocation information and a backhaul alternative. However, it is worth mentioning that such a solution is not suitable for delay-sensitive applications due to the large latency from the satellites.

2.4.3 SDN/NFV-Layers Interworking

SDN and network function virtualization (NFV) have been extensively researched for use in terrestrial cellular networks [137]. In fact, through leveraging the concepts of software and virtualization, they are also being considered as key enabling technologies for more flexible integration and interworking of the air and ground segments. For example, during the operation of the integrated system, UAVs (e.g., LAPs) are required to seamlessly fly into the network during their activity and seamlessly disassociate when their service duration is over, which requires a high degree of network reconfigurability. Since NFV allows a programmable network structure, seamless integration of UAVs into the system will become available. Furthermore, through programming the hardware, NFV allows general UAVs to be used to perform particular network functions such as network gateways, which can reduce the operational expenditure by sharing available network resources [135]. On the other hand, owing to frequent changes of the network configuration, UAV networks need to be more fault tolerant. By abstracting the network and separating the control plane from the data plane, SDN introduces logically centralized control with a global view, which may

be utilized to control and update the network flexibly to enhance the ability of the network fault tolerance and reduce scheduling delay.

2.4.4 Machine Learning-Traffic Identification

To reap the benefits of the integrated air-ground networks for practical telecommunication applications, various traffic requirements of the use cases need to be identified such as latency, efficiency, reliability, interference, etc. In this regard, machine learning enabled schemes are seen as a useful tool for handling these issues. For instance, in a large-scale UAV networks, constantly communicating with a remote node can introduce signaling delays. To reduce such delays, one can rely on on-device machine learning or edge artificial intelligence (AI), such as federated learning, to store a particular task in a distributed fashion across the UAVs and collectively solve the optimization problem [181]. This in turn enables a large number of UAVs to collaboratively allocate their radio resources in a decentralized way, thus reducing wireless congestion and latency. Besides, when cellular-connected UAVs establish LoS connectivity with terrestrial base stations, mutual interference among them as well as to ground users become severe. To address this challenge, deep reinforcement learning algorithms based on echo state network cells can be implemented on each UAV in order to learn the optimal path, transmission power level, and cell association vector at different locations, which enable UAVs to adjust their beamwidth tilt angle and path to minimize the interference on terrestrial networks [182]. In addition, for some multimedia streaming applications, convolutional neural networks (CNNs) can be adopted for allowing cache-enabled UAVs to store common data files since CNNs can extract and store the common features of the data files that are requested by different users [181].

2.5 Potential Applications and Case Studies

In this section, we introduce several potential application scenarios for the proposed integrated air-ground heterogeneous network architecture. Then, a case study is given to demonstrate the performance gain with the integrated architecture.

2.5.1 Potential Scenarios for Enhancing 5G Applications

Since conventional urban/suburban areas are expected to be well served based on the forthcoming 5G deployment, here, we mainly follow with interest the potentially underserved or hard-to-reach districts in which the aerial platforms can be used as an integrated part of
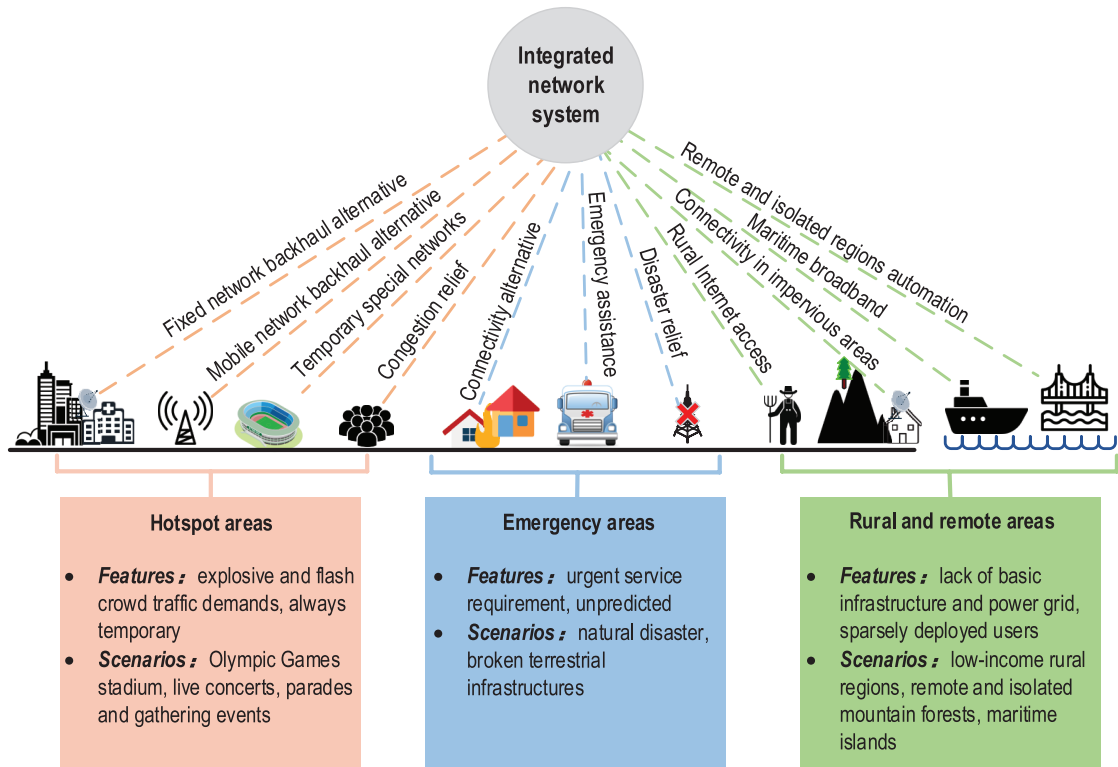
Fig. 2.3 Potential scenarios where the integrated air-ground network system can further enhance the applications of conventional terrestrial networks.

networks to inject additional capacity and expand the coverage. As shown in Fig. 2.3, three typical scenarios are introduced, including *hotspot, emergency, rural and remote areas*.

Specifically, for some hotspot areas, flexible LAP base stations can be fast dispatched in corresponding areas to provide enhanced capacities for users. In terms of those unexpected emergency cases, through leveraging the aerial networks in the integrated system, low-altitude UAVs can be used to deliver emergency response to improve resilience of wireless networks. At the same time, the HAPs can establish new specific spot beams to support additional coverage. For rural and remote areas, if aided by the integrated system, HAPs are capable of bridging the vast digital divide in these regions, since they can stay in the stratosphere to provide wide-area coverage, removing the need for large numbers of terrestrial masts and their associated infrastructures.

2.5.2 Case Study

In this section, we investigate the effectiveness of the proposed integrated air-ground network architecture and evaluate the system performance in terms of user throughput and
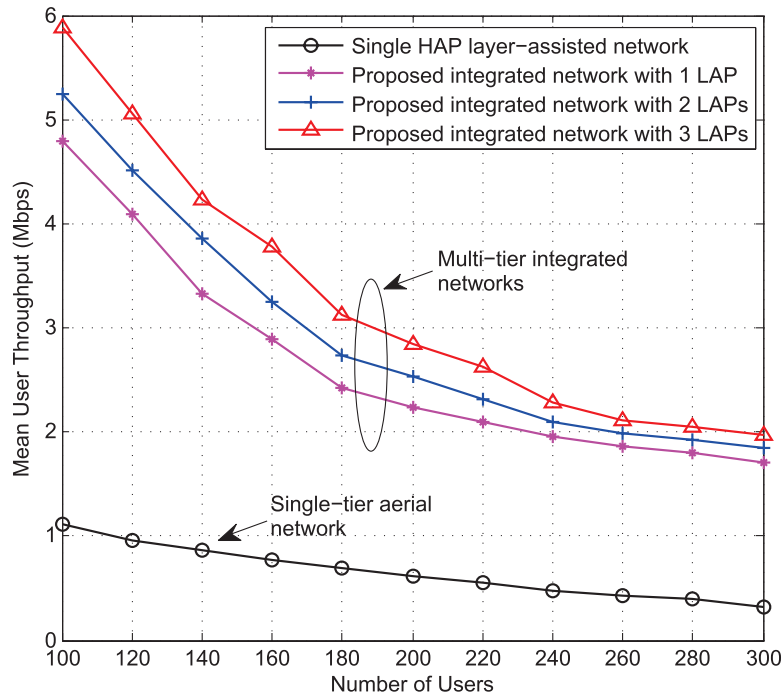
Fig. 2.4 Mean user throughput for standalone HAP-assisted network and multi-tier integrated air-ground networks with variation of the number of users.

outage probability. We consider a HAP located at altitude of $h_{HAP} = 20\,km$ above ground, serving a 30 km radius coverage area. LAPs are located inside the same service area at altitude of $h_{LAP} = 1\,km$ along with a three-sector macro cell placed at the center of the service area using a common frequency band. Users are randomly distributed on the ground. The system uses a carrier frequency of $f_c = 2.6\,GHz$ with $B = 20\,MHz$ bandwidth for a downlink transmission. The path loss of HAP and LAPs is modelled based on the free space path loss model while that is a 3GPP path loss model for the macro cell. The transmit power for HAP, LAPs and terrestrial base station are 37 dBm, 25 dBm and 40 dBm, respectively. The noise power is $N_0 = -130\,dBm$. In order to illustrate the benefits bringing by the flexibility and mobility of LAPs, as in [183], two types of scenarios are considered: 1) static LAP deployment, 2) and dynamic LAP deployment.

Static LAP deployment: At first, we consider the static scenario in which the LAPs do not move or change their positions after deployment inside a HAP cell to serve the downlink users in the presence of one terrestrial base station. Fig. 2.4 illustrates the mean user throughput versus the number of users in the system. The mean user throughput is quantified after several simulation iterations to obtain the consistent results by assuming a user has maximum signal-to-interference-plus-noise ratio (SINR) which is 22 dB in the system. It indicates the possibly achievable performance upper bound with the ideal case given the
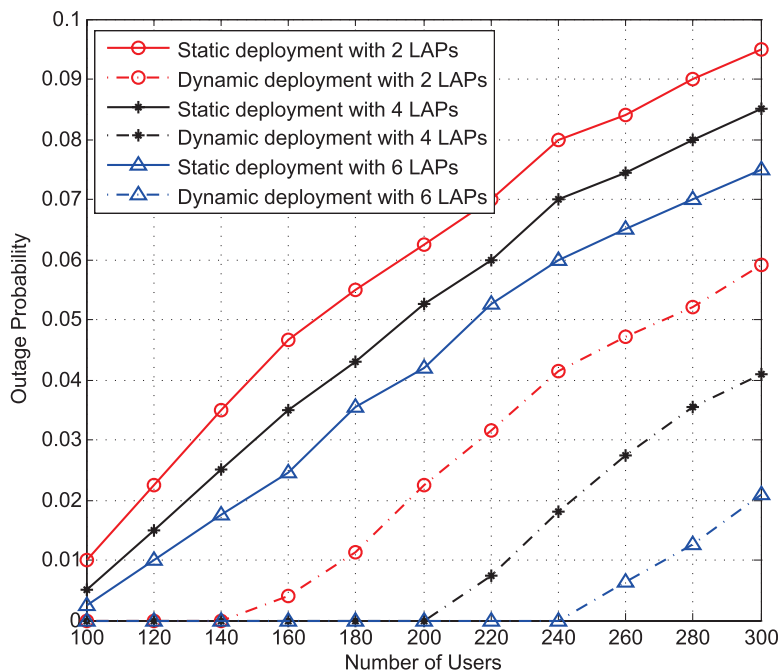
Fig. 2.5 User outage probabilities for dynamic and static usage of LAPs versus different number of users.

efficient interference control mechanism. We assume that the power and spectrum used in the two types of network scenarios are same. As can be observed in the figure, the performances of the proposed integrated HAP-and-LAPs-aided heterogeneous network obviously outperform that of single-tier HAP-assisted cellular network. The reason is that with the incorporation of both HAP and LAPs, the probability for associated users experiencing LoS will be higher than just leveraging standalone HAP layer to assist the terrestrial network. Moreover, increasing the number of LAPs will further improve users' capacity due to the enhanced coverage. This demonstrates a multi-tier UAV-aided cellular network (i.e., integrated HAP-LAP-terrestrial network) exceeds the performance of a single-tier UAV-assisted network (i.e., HAP-terrestrial network).

Dynamic LAP deployment: In dynamic scenarios, we assume that the LAPs can further slightly adjust their positions over the associated service areas without considering the moving time and transmit from a more efficient geographical location which we hereinafter refer to the local center point. Each center point represents the location of mean value of positions for all its previous associated users of a LAP. By moving to the local center point, the system performance of the corresponding service areas for the LAP will be improved due to the decrease in the cumulative communication distance which can increase the coverage probability of the downlink users. In Fig. 2.5, the user outage probability (i.e., the probability that the instantaneous SINR falls below a threshold) versus the number of users

is given. It can be observed that, compared with the static LAP deployment, the dynamic usage of LAPs has better system efficiency with decreasing in the user outage probability.

2.6 Challenges and Open Issues

In spite of the potentials, the research on air-ground integrated heterogenous networks with integrating HAPs and LAPs is still in its infancy, where many key research issues are still open. In this section, some challenges and open issues are discussed.

Resource allocation and interference management: With aerial and terrestrial segments integrated in the hierarchical network system, resource allocation and interference management become more challenging by virtue of the highly dynamic network environment and multi-dimensional heterogeneity in resources and services. Thus, there is a need for designing efficient scheduling techniques to dynamically manage various resources from both aerial and terrestrial networks including energy, bandwidth, transmit power, etc. Besides, in the case of coexistence of multiple communication systems, apart from co-channel interferences between different segments, severe inter-carrier interference at higher transmission frequencies (e.g., mmWave) will be caused by Doppler shift due to mobility of UAVs. Therefore, inherent dynamics of the networks such as time-varying interference, varying traffic patterns, and mobility of the UAVs, should be captured when operating resource management and spectrum sharing. To this end, optimizing the heights and intensities of various tiers of UAVs and coordination among UAVs may be useful [184].

Cross-tier interworking among different segments: Cross-tier networking architecture is supported by various communication protocols, and each layer comprises many devices with different interfaces for configuration and control. Although the SDN is explored to enable unified control of the system, it is still not easy to achieve seamless convergence of multiple radio access technologies and network types. Thus, it is desirable to design some cooperative incentives between aerial and terrestrial segments. Dedicated cross-layer protocols and interworking mechanisms are also needed to ensure link reliability. In addition, in air-ground integrated networks, data packets transmitted from sources to destinations will traverse via various nodes in HAP, LAP and ground networks. Any change of these interconnected networks will affect not only the physical layer channels but also the higher-layer decisions of flow control and routing, thus impacts the performances such as delay, throughput and reliability of the whole integrated system. For example, the network throughput depends on the bandwidth in physical layer, packet switch algorithm in data link layer, and the routing path in the network layer. Therefore, the principle of cross-layer optimization span-

ning from physical layer to the network layer should be considered for HAP-LAP-ground network design.

Energy efficiency: Generally, the energy of the LAPs is quite limited. The whole air-ground integrated system life is determined by the amount of the power in LAPs, in other words, how to efficiently exploit the limited power. In the LAP networks, the communication and motion of the LAPs consume the most part of the energy compared to the sensing and computation. There can be two power supply cases, i.e., the energy for communication equipment and for powering the LAP. In both cases, the energy for communication and control should be tuned well so as to i) respectively prolong the lifespan of communication and flight as much as possible, i.e., improve the energy efficiency for the two parts respectively; ii) jointly extend the whole system life by orchestrating them to achieve a comparable lifetime for the two, since that a power failure for each of the two will deprive the ability of the system to fulfill the mission. There are many researches focusing on improving the energy efficiency of the data transmission to achieve green communication which can be enlightening and applied to the LAPs networks. However, the energy efficiency in the air-ground integrated networks is much more complicated considering the motion characteristic and their tight coupling with the communication of LAPs, which needs to be further studied.

Handover and user/cell association: Handover in the integrated networks will be more frequent due to three factors: 1) movement of the terminal users, 2) flight dynamics of LAPs, and 3) dynamic spot beams of HAPs. Therefore, efficient adaptive algorithms are necessary for a user to achieve fast handover when switching from the aerial networks to the terrestrial networks and vice versa. In this work, we have not considered the handover which would be a future research topic. On the other hand, although the integrated system provides multi-connectivity options, jointly considering the mobility and constraint in flight time of UAVs, user or cell association problems become intractable. In this regard, advanced mathematical tools such as optimal transport theory may be useful for these notoriously difficult optimization problems owing to its much deeper fundamental analysis of network performance optimization [10].

Privacy and public safety: The regulation to exploit aerial platforms for commercial use in cellular networks is still underway. Nonstandard and illegal deployment or utilization of UAVs may lead to serious public safety hazard [185]. Thus, suitable safety and surveillance schemes are urgently needed. Moreover, due to the wireless transmission properties of the aerial networks, they are particularly vulnerable to malicious attacks. Thus, safeguard strategies or protocols are of paramount importance. Besides, SDN controllers are mainly responsible for managing the system, protecting the SDN controllers from different cyber attacks is also needed in integrated networks.

2.7 Conclusion

In this chapter, we have proposed a hierarchical air-ground integrated network architecture to exploit the advantages of integration of HAP, LAP and ground segments, to support ubiquitous communication services in various scenarios efficiently and cost-effectively. The designed system is envisioned to be deployed as a complementary solution to broaden the applications of current terrestrial cellular networks for underserved scenarios and hard-to-reach areas. In order to clearly state the characteristics of different types of UAVs (e.g., HAPs and LAPs), we have presented a comprehensive comparison of HAP communication networks and LAP communication networks. Then, the basic networking architecture and main enabling technologies about the air-ground integrated networks are introduced. Furthermore, the potential advantages, applications and challenges of jointly integrating multi-tier aerial platforms into future wireless networks have been also discussed. Simulation results demonstrate that the proposed multi-tier HAP-LAP-ground network has a better system performance compared with standalone aerial networks. This chapter has been about how an integrated network architecture will work in general terms, with the later chapters investigating specific constraints relevant to the architecture.

Chapter 3

Robust Resource Allocation for Air-Ground Integrated Networks with Reliable Connection

3.1 Introduction

In Chapter 1 and Chapter 2, we have introduced the new paradigm of integrating UAVs into the cellular networks from a high level. It is shown that, on the one hand, UAVs can be considered as aerial users to access the cellular networks for communications, which are referred to as *cellular-connected UAVs* . On the other hand, UAVs can be used as aerial communication platforms, such as base stations (BSs), to assist terrestrial wireless networks by providing data access from the sky, thus called *UAV-assisted wireless communications*. In this chapter, we will firstly study the potentials of cellular-connected UAVs with UAVs acting as flying users to perform sensing and communication task in a cellular network, where each UAV moves along its pre-determined trajectory to collect data, and then uploads these data to a ground BS. In such a scenario, the UAV transmissions can be supported by two basic modes, namely UAV-to-infrastructure (U2I) transmissions via air-to-ground links and UAV-to-UAV (U2U) transmissions via air-to-air links. Specifically, U2U transmissions can be realized by leveraging the available device-to-device (D2D) communications in LTE and 5G systems [9]. Similarly to ground D2D communications [186–189], U2U communications may also have implications in terms of spectral and energy efficiencies, extended cellular coverage, and reduced backhaul demands [190].

Generally, D2D-enabled U2U communications can work in two different modes: the reuse mode and the dedicated mode, where U2U transmissions share the same resources as

the cellular networks and occupy dedicated resources, respectively. Although the dedicated mode is easy to implement since exclusive spectrum is assigned to the U2U links, the reuse mode is often preferred, where the proximity, hop, and reuse gains can be largely exploited and spectral efficiency can be further improved. However, in the air-ground integrated networks, considering the limited communication resource, high mobility and transmission links heterogeneity of the UAVs, it is not trivial to address the following issues. Firstly, since the U2U transmissions underlay the spectrum resources of the U2I transmissions, the U2I transmissions may be interfered by the U2U transmissions when sharing the same channels. Thus, the mutual interference between them needs to be properly coordinated. Secondly, due to the high-speed moving of UAVs, link disconnections of U2U communications may easily occur which can adversely affect the network robustness. In addition, wireless channels change rapidly over time, traditional methods of radio resource management strategies under full channel state information (CSI) assumption are no longer applicable since it would be quite challenging to track channel variations on such a short time scale. Thirdly, different types of UAV communication links usually have different service requirements. For example, the U2I links always concern more on data throughput due to the considerable amount of data delivery between the aerial and terrestrial networks. Meanwhile, the U2U links have stringent demand on the reliability and timeliness since they often exchange the environment related information, e.g., common awareness messages and decentralized environmental notification messages, among surrounding UAVs either in a periodic or event triggered way. Therefore, link transmission difference should be also taken into account. In the literature, some works on the cellular-connected UAV communication network have been studied [191–195]. Nevertheless, the majority of the existing works focused on instantaneous resource allocation. In realistic UAV-aided sensing scenarios, however, what UAVs care about is the total amount of data transmitted during the access to the BS. Thus, it is practical to maximize the throughput during one access period, or the average capacity equivalently.

Motivated by the above observations, in this chapter, we study robust resource allocation in a cellular network deployment where U2U transmit-receive pairs share the same spectrum with the uplink U2I communication links. Both types of UAV connections, i.e., U2I and U2U links, are supported under the D2D-enabled cellular architecture where the U2I link is performed by the cellular uplink connectivity and the U2U link is supported through localized D2D communications. Since the fast varying CSI is quite difficult to obtain, we will design spectrum and power allocation based on large-scale slowly fading channel information. To incorporate and meet different quality-of-service (QoS) requirements of the applications hosted by different kinds of UAV connections, we aim to maximize the sum

ergodic capacity (long-term average over fast fading) of the U2I links during one access period while guaranteeing the reliable connectivity of the U2U links, where the U2U link reliability is ensured by maintaining the outage probability of received SINR below a small threshold. We will show that the primal resource allocation issue can be decomposed into a pure power allocation subproblem and a pure channel allocation subproblem, both of which can be efficiently solved. Through our analysis and design, we propose a robust resource allocation algorithm. Moreover, simulation results demonstrate the desired throughput performance and reliability.

The main contributions of the chapter are summarized as follows.

- In view of the distinguishing QoS requirements of different UAV connections, we formulate a resource allocation problem of maximizing the sum ergodic capacity of the U2I links in a given time period subject to the reliability constraint for the U2U links based on slow fading parameters and statistical information of the channels, which addresses the challenge of fast channel variation in a UAV communication environment.

- Since interference exists only between each U2U-U2I spectrum reusing pair, we propose to decompose the original optimization problem into two subproblems, i.e., power control and spectrum allocation, which can be addressed in sequence with satisfactory results.

- A low-complexity algorithm is developed to deal with the resource optimization problem. Then, by building the simulation of an air-ground integrated network, we illustrate that our proposed robust resource allocation scheme satisfies the various link connection requirements and effectively improves the overall throughput.

The rest of this chapter is organized as follows. Section 3.2 introduces the system model and formulates the sum U2I capacity maximization problem with minimum QoS guarantee for U2I and U2U connections. Then, by transforming the optimization problem, a spectrum and power allocation strategy is developed in Section 3.3. Afterwards, simulation results are given in Section 3.4. Finally, Section 3.5 concludes this chapter.

3.2 System Model and Problem Formulation

In this section, we will at first introduce the scenario and channel model, and then present a resource allocation problem aiming to optimize the capacity of the U2I links subject to the constraints on the U2U links' reliability.
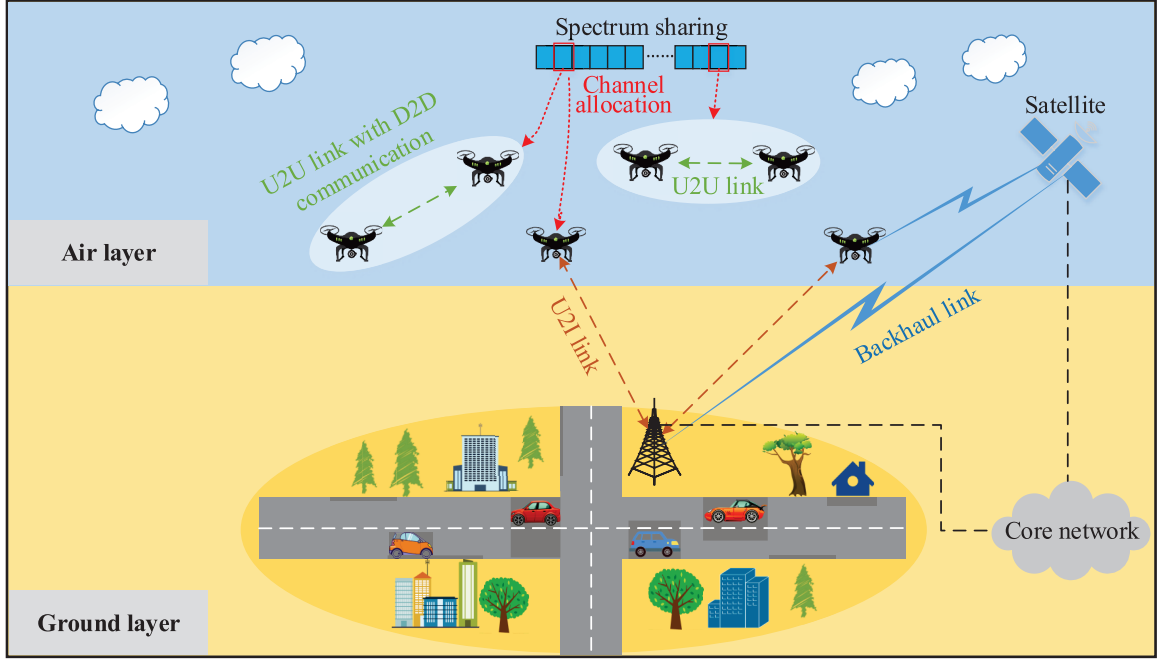
Fig. 3.1 An air-ground integrated network with U2U links sharing uplink resources of the U2I links.

3.2.1 System Model

Consider a UAV-aided air-ground integrated communication network as shown in Fig. 3.1, where the BS is located at the cell center, where M UAVs desire high-capacity uplink U2I connections to BS for sensing data delivery, denoted as cellular users (CUEs), and K pairs of UAVs carry out local U2U information exchange in the form of D2D communications, called aerial D2D users (DUEs). The UAVs are connected to the core network through the base station on the ground. It is assumed that the orthogonally allocated uplink spectrum of CUEs is reused by the DUEs to improve spectrum utilization efficiency. All UAVs are capable of performing U2I and U2U communications at the same time and thus one physical UAV equipped with multiple radios might act as a CUE and a DUE simultaneously. Assume that all communicating parties are equipped with a single antenna. The sets of the CUEs and the DUEs are denoted by $\mathcal{M} = \{1, \ldots, M\}$ and $\mathcal{K} = \{1, \ldots, K\}$, respectively.

The channel power gain from the mth CUE to the BS, denoted by $h_{m,B}$, is formulated as

$$h_{m,B} = A_{m,B} d_{m,B}^{-2} \beta_{m,B} g_{m,B} \overset{\Delta}{=} \alpha_{m,B} g_{m,B}, \tag{3.1}$$

where $A_{m,B}$ is the path loss coefficient, $d_{m,B}$ is the distance between the mth CUE and the BS, $\beta_{m,B}$ is a log-normal shadow fading random variable, $\alpha_{m,B}$ accounts for the slowly varying

large-scale fading power component and $g_{m,B}$ represents the fast varying small-scale fading power component and assumed to be exponentially distributed with unit mean. The channel between the kth DUE pair, the interfering channel from the transmitter (Tx) of the kth DUE pair to the BS, and the interfering channel from the mth CUE to the receiver (Rx) of the kth DUE pair are similarly expressed as $h_k = \alpha_k g_k$, $h_{k,B} = \alpha_{k,B} g_{k,B}$, and $h_{m,k} = \alpha_{m,k} g_{m,k}$, respectively. It is assumed that the BS has the knowledge of the large-scale fading components of all channels, i.e., the path loss and shadowing of all links, since they are usually dependent on users' locations and vary on a slow scale. Such information can be estimated at the BS for links between CUEs/DUEs and BS, i.e., $\alpha_{m,B}$ and $\alpha_{k,B}$, while for links between UAVs, i.e., α_k and $\alpha_{m,k}$, the parameters will be measured at the DUE receiver and reported to the BS periodically. As for small-scale fading components, only their distributions instead of their realizations are available at the BS since it is impractical to feed full CSI back to the BS in a UAV communication environment with high mobility.

Let P_m^c, P_k^d, and $\rho_{m,k} \in \{0,1\}$ denote the transmit power of the mth CUE, the transmit power of the kth DUE, and the spectrum allocation indicator, respectively, where $\rho_{m,k} = 1$ indicates that the kth DUE reuses the spectrum of the mth CUE and $\rho_{m,k} = 0$ otherwise. We assume that the spectrum of each CUE can be reused by at most one DUE and each DUE can share the spectrum of at most one CUE, i.e., $\sum_{k=1}^{K} \rho_{m,k} \leq 1$ and $\sum_{m=1}^{M} \rho_{m,k} \leq 1$. The SINR of the link from the mth CUE to the BS is given by

$$\gamma_m^c = \frac{P_m^c h_{m,B}}{\sigma^2 + \sum_{k \in \mathcal{K}} \rho_{m,k} P_k^d h_{k,B}}, \tag{3.2}$$

while the SINR of the link between the kth DUE pair is

$$\gamma_k^d = \frac{P_k^d h_k}{\sigma^2 + \sum_{m \in \mathcal{M}} \rho_{m,k} P_m^c h_{m,k}}, \tag{3.3}$$

where σ^2 is the power of the additive white Gaussian noise. Since it is quite challenging for the BS to acquire the small scale fading information, the ergodic capacity of the mth CUE with the assumption of Gaussian inputs is considered which is given by

$$C_m = \mathbb{E}\left[\log_2\left(1 + \gamma_m^c\right)\right], \tag{3.4}$$

where the expectation $\mathbb{E}[\cdot]$ is taken over the fast fading distribution. The ergodic capacity derives from the Shannon bound which is not achievable in practice.

In order to guarantee the total amount of data transmitted from CUEs to the BS during one access period, we define some motion parameters for the expectation of capacity with
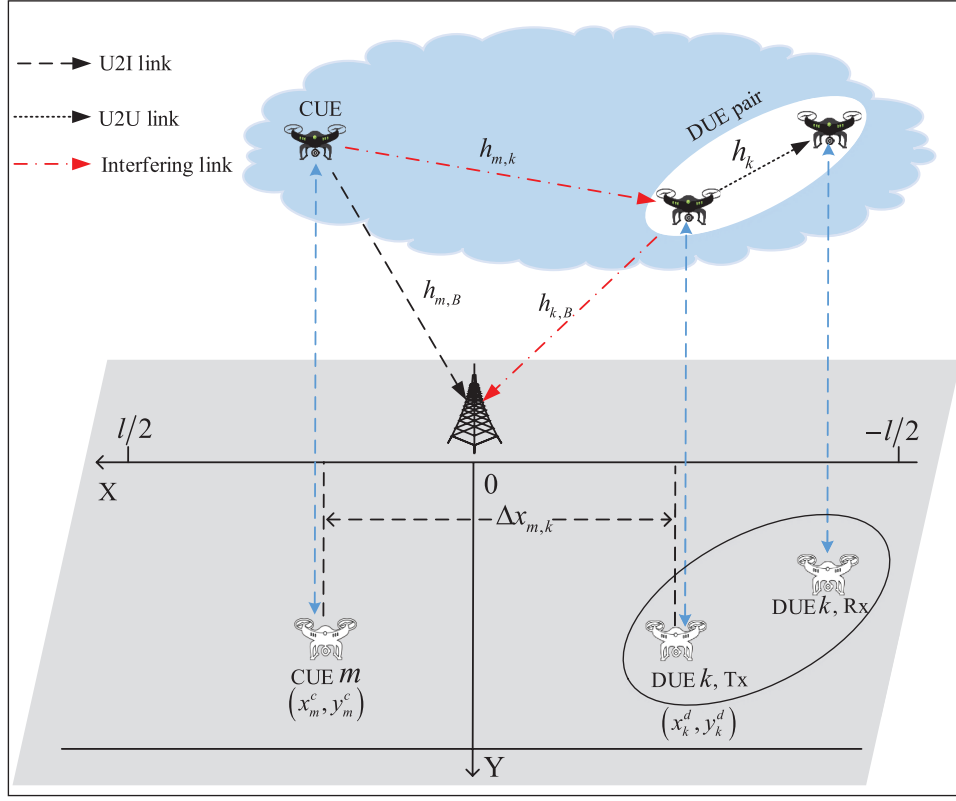
Fig. 3.2 Cartesian coordinate of the U2U underlaying cellular system.

respect to all possible positions. Without loss of generality, we consider a three-dimensional (3D) Cartesian coordinate system such that the BS is located at the origin, as shown in Fig. 3.2. It is assumed that UAVs fly at a fixed altitude of H above ground, which can be considered as the minimum altitude required for safety considerations such as terrain or building avoidance without the need of frequent aircraft ascending and descending. Positive direction of the X axis is defined as the UAVs' sensing task direction (note that only one-way sensing task is considered here). The coordinate of the mth CUE on the horizontal is denoted by (x_m^c, y_m^c), while that of the transmitter of the kth DUE pair denoted by (x_k^d, y_k^d). As is shown in Fig. 3.1, we consider a scenario that each UAV flies above the same line, therefore y_m^c and y_k^d remain constant. Define an access period as the path from $(-l/2, 0)$ to $(0, l/2)$ with an assumption that the CUEs always have data to be delivered. Thus, the expectation of the sum ergodic capacity for such an access period, called position ergodic capacity, can be expressed as

$$\bar{C}_m = \frac{1}{l} \int_{-l/2}^{l/2} C_m(x)\, dx = \frac{2}{l} \int_0^{l/2} C_m(x)\, dx. \tag{3.5}$$

51

3.2.2 Problem Formulation

Recognizing the different QoS requirements of different types of links, i.e., large transmission capacity for U2I connections and high reliability for U2U connections, we aim to maximize the position ergodic capacity (the expectation of the sum ergodic capacity for an access period) of the CUEs while guaranteeing the reliability for the DUEs. In addition, we provide a QoS guarantee for each CUE by setting a minimum achievable capacity constraint. The reliability for the link connection of the kth DUE pair is achieved through controlling the outage probability, where the received SINR γ_k^d is below a predetermined threshold γ_0^d. The ergodic capacity of the CUEs can be computed through the long-term average over the fast fading, where the codeword length spans several coherence periods over the time scale of slow fading [196]. Moreover, the ergodic capacity can be approached ultimately as UAVs move faster since the induced faster variation of channels produces more channel states within a given period, which allows the codeword to traverse most, if not all, of the channel states to average out the effects of fast fading [197, 198]. To this end, the resource allocation problem is formulated as

$$(P): \max_{\left\{\rho_{m,k}\right\},\left\{P_m^c\right\},\left\{P_k^d\right\}} \sum_{m\in\mathscr{M}} \bar{C}_m\left(P_m^c, P_k^d\right)$$

$$\text{s.t. } \mathbb{E}\left[\log_2\left(1+\gamma_m^c\right)\right] \geq r_0^c, \ \forall m \in \mathscr{M} \tag{3.6}$$

$$\Pr\left\{\gamma_k^d \leq \gamma_0^d\right\} \leq p_0, \ \forall k \in \mathscr{K} \tag{3.7}$$

$$0 \leq P_m^c \leq P_{\max}^c, \ \forall m \in \mathscr{M} \tag{3.8}$$

$$0 \leq P_k^d \leq P_{\max}^d, \ \forall k \in \mathscr{K} \tag{3.9}$$

$$\sum_{m\in\mathscr{M}} \rho_{m,k} \leq 1, \ \rho_{m,k} \in \{0,1\}, \ \forall k \in \mathscr{K} \tag{3.10}$$

$$\sum_{k\in\mathscr{K}} \rho_{m,k} \leq 1, \ \rho_{m,k} \in \{0,1\}, \ \forall m \in \mathscr{M}, \tag{3.11}$$

where r_0^c is the minimum capacity requirement of the CUEs for data transmission and γ_0^d is the minimum SINR needed by the DUEs to establish a reliable link. $\Pr\{\cdot\}$ denotes the input probability and p_0 is the tolerable outage probability of the U2U links at the physical layer. $P_{\max}^c$ and $P_{\max}^d$ are the maximum transmit powers of the CUE and DUE, respectively. Constraints (3.6) and (3.7) represent the minimum capacity and reliability requirements for each CUE and DUE, respectively. (3.8) and (3.9) ensure that the transmit powers of CUEs and DUEs are non-negative and within their maximum limit. (3.10) and (3.11) characterize our assumption that the spectrum of one CUE can be shared with at most one DUE and, conversely, one DUE can only reuse the spectrum of at most one CUE. Such an assump-

tion moderates the complexity of the interference management and serves as a reasonable starting point to study the challenging resource allocation problem in air-ground integrated networks.

The formulated optimization problem (P) captures different requirements for different types of UAV connection links as well as the factors in the unique features of time varying channels of UAV communications. However, this is a mixed-integer and non-convex optimization problem with complicated constraints, which cannot be effectively solved via existing methods. Therefore, more efficient resource allocation schemes are needed.

3.3   Robust Resource Allocation Scheme Design

In this section, we will solve the overall throughput optimization problem by dividing the original one into two subproblems. First, we exploit the separability of power allocation and spectrum reuse pattern design by observing that interference exists only within each CUE-DUE spectrum reusing pair as dictated by the constraints (3.10) and (3.11). Focusing on each possible CUE-DUE spectrum reusing pair, we study the optimal power allocation to maximize the CUE's position ergodic capacity while guaranteeing the DUE's connection reliability. Second, taking into account the minimum required capacity of the CUEs, we rule out the infeasible pairs and find the optimal spectrum sharing pattern between the sets of CUEs and DUEs by addressing a bipartite matching problem. Finally, by combining the above two steps, we propose a robust resource allocation algorithm to achieve a globally optimal solution to the optimization problem (P) fully considering the dynamic characteristics and the different requirements for different transmission links of the air-ground integrated networks, i.e., maximizing the sum ergodic capacity (long-term average over fast fading) of the U2I links during one access period while guaranteeing the reliable connectivity of the U2U links, where the U2U link reliability is ensured by maintaining the outage probability of received SINR below a small threshold.

3.3.1   Power Allocation for Each CUE-DUE Pair

In this part, we concentrate upon the optimal power allocation for all possible spectrum reusing pairs. Considering an arbitrary spectrum reusing pattern, e.g., the kth DUE sharing the band of the mth CUE, the power allocation problem for such a single CUE-DUE pair

turns out to be

$$(P1): \max_{P_m^c, P_k^d} \bar{C}_m \left(P_k^d, P_m^c \right)$$

$$\text{s.t. } \Pr\left\{ \gamma_k^d \leq \gamma_0^d \right\} \leq p_0 \tag{3.12}$$

$$0 \leq P_m^c \leq P_{\max}^c \tag{3.13}$$

$$0 \leq P_k^d \leq P_{\max}^d, \tag{3.14}$$

where the constraint on the ergodic capacity of the mth CUE, i.e., $C_m \geq r_0^c$, is temporarily left out which will be reconsidered after deriving the optimal solution to the problem $(P1)$. If the optimal objective value of the problem satisfies $C_m \geq r_0^c$, then the spectrum reusing pair is feasible. Otherwise, the reusing pair is infeasible. Before deriving the optimal solution to the problem $(P1)$, a transformed problem is firstly studied which is given by

$$\left(P1'\right): \max_{P_m^c, P_k^d} \mathbb{E}\left[\log_2\left(1 + \gamma_m^c\right)\right]$$

$$\text{s.t. } \Pr\left\{ \gamma_k^d \leq \gamma_0^d \right\} \leq p_0 \tag{3.15}$$

$$0 \leq P_m^c \leq P_{\max}^c \tag{3.16}$$

$$0 \leq P_k^d \leq P_{\max}^d. \tag{3.17}$$

In order to further process the problem $(P1')$, we present the following lemma to evaluate the reliability constraint.

Lemma 3.1. *The reliability constraint for the kth DUE, i.e., (3.15) in the formulated problem $(P1')$, can be expressed as*

$$P_m^c \leq \frac{\alpha_k P_k^d}{\gamma_0^d \alpha_{m,k}} \left[\frac{1}{1 - p_0} \exp\left(\frac{-\gamma_0^d \sigma^2}{\alpha_k P_k^d} \right) - 1 \right]. \tag{3.18}$$

Proof. Given a particular spectrum reusing pair consisting of the mth CUE and the kth DUE, i.e., $\rho_{m,k} = 1$, and substituting the channel model (3.1) in (3.15), we can get

$$\Pr\left\{ \gamma_k^d \leq \gamma_0^d \right\}$$

$$= \Pr\left\{ \frac{P_k^d h_k}{\sigma^2 + P_m^c h_{m,k}} \leq \gamma_0^d \right\}$$

$$= \Pr\left\{ \frac{P_k^d \alpha_k g_k}{\sigma^2 + P_m^c \alpha_{m,k} g_{m,k}} \leq \gamma_0^d \right\}. \tag{3.19}$$

Based on the closed form of the outage probability in [199] and the assumption that g_k and $g_{m,k}$ are independent and identically distributed (i.i.d.) exponential random variable with unit mean, we can further have

$$
\begin{aligned}
\Pr & \left\{ \frac{P_k^d \alpha_k g_k}{\sigma^2 + P_m^c \alpha_{m,k} g_{m,k}} \le \gamma_0^d \right\} \\
& = \int_0^\infty \mathrm{d}g_{m,k} \int_0^{\frac{\gamma_0^d \left(\sigma^2 + P_m^c \alpha_{m,k} g_{m,k} \right)}{P_k^d \alpha_k}} \exp\left[-\left(g_k + g_{m,k} \right) \right] \mathrm{d}g_k \\
& = 1 - \left(1 + \frac{\gamma_0^d P_m^c \alpha_{m,k}}{P_k^d \alpha_k} \right)^{-1} \exp\left(-\frac{\gamma_0^d \sigma^2}{P_k^d \alpha_k} \right) \le p_0.
\end{aligned}
\tag{3.20}
$$

Subsequently, (3.18) can be easily acquired by rearranging the terms of the inequality in the last line of (3.20). Therefore, Lemma 3.1 can be proved. ∎

Define the function of P_k^d on the right side of (3.18) as $\Phi\left(P_k^d \right)$, i.e.,

$$
\Phi\left(P_k^d \right) = \frac{\alpha_k P_k^d}{\gamma_0^d \alpha_{m,k}} \left[\frac{1}{1 - p_0} \exp\left(\frac{-\gamma_0^d \sigma^2}{\alpha_k P_k^d} \right) - 1 \right].
\tag{3.21}
$$

To distinguish the monotonicity of the function $\Phi\left(P_k^d \right)$, we present its first derivative as

$$
\begin{aligned}
\frac{\mathrm{d}\Phi\left(P_k^d \right)}{\mathrm{d}P_k^d} & = \frac{\mathrm{d}\left\{ \frac{\alpha_k P_k^d}{\gamma_0^d \alpha_{m,k}} \left[\frac{1}{1-p_0} \exp\left(\frac{-\gamma_0^d \sigma^2}{\alpha_k P_k^d} \right) - 1 \right] \right\}}{\mathrm{d}P_k^d} \\
& = \frac{\alpha_k}{\gamma_0^d \alpha_{m,k}} \left\{ \left[\frac{1}{1 - p_0} \exp\left(\frac{-\gamma_0^d \sigma^2}{\alpha_k P_k^d} \right) - 1 \right] \right. \\
& \quad \left. + \frac{\gamma_0^d \sigma^2}{\alpha_k P_k^d \left(1 - p_0 \right)} \exp\left(\frac{-\gamma_0^d \sigma^2}{\alpha_k P_k^d} \right) \right\}
\end{aligned}
\tag{3.22}
$$

For ease of exposition, we set

$$
\chi = \frac{\alpha_k}{\gamma_0^d \alpha_{m,k}},
\tag{3.23}
$$

$$
\psi = \frac{1}{1 - p_0} \exp\left(\frac{-\gamma_0^d \sigma^2}{\alpha_k P_k^d} \right) - 1,
\tag{3.24}
$$

and

$$
\omega = \frac{\gamma_0^d \sigma^2}{\alpha_k P_k^d \left(1 - p_0 \right)} \exp\left(\frac{-\gamma_0^d \sigma^2}{\alpha_k P_k^d} \right),
\tag{3.25}
$$

then the above equation (3.22) can be rewritten as

$$\frac{d\Phi\left(P_k^d\right)}{dP_k^d} = \chi \times (\psi + \omega). \tag{3.26}$$

It is obvious that $\chi > 0$ and $\omega > 0$. Since the transmission power is non-negative, based on (3.18) and (3.24), we have $\psi \geq 0$. Thus, the first derivative of the function $\Phi\left(P_k^d\right)$ is greater that zero. On this basis, $\Phi\left(P_k^d\right)$ is a monotonically increasing function of P_k^d. Subsequently, considering the constraint of $P_m^c \geq 0$, the minimum transmission power $P_{k,\min}^d$ of the kth DUE is the value of P_k^d at the the zero-crossing point, which can be obtained by setting $\Phi\left(P_k^d\right) = 0$. Then, we have

$$P_{k,\min}^d = \frac{-\gamma_0^d \sigma^2}{\alpha_k \ln\left(1 - p_0\right)}. \tag{3.27}$$

Therefore, in the range of $\left(P_{k,\min}^d, +\infty\right)$, $\Phi\left(P_k^d\right)$ is monotonically increasing with regard to the DUE power P_k^d. This is intuitive as an increase of the DUE power would lead to a higher interference margin, implying the DUE is more tolerable to the interference from the CUE.

Based on the above discussions, we can characterize the optimal solution to problem $(P1')$ in the following theorem.

Theorem 3.1. *The optimal power allocation solution to optimization problem $(P1')$ is given by*

$$P_m^{c*} = \min\left\{P_{\max}^c, \Phi\left(P_{\max}^d\right)\right\}, \tag{3.28}$$

and

$$P_k^{d*} = \min\left\{P_{\max}^d, \Phi^{-1}\left(P_{\max}^c\right)\right\}. \tag{3.29}$$

Proof. Please refer to Appendix A.1. ∎

Note that $\Phi^{-1}\left(P_{\max}^c\right)$ can be found by bisection search since the function $\Phi(\cdot)$ is monotonically increasing in the range of interest. Theorem 3.1 yields the optimal power allocation for a single CUE-DUE pair that maximizes ergodic capacity of the specific CUE and guarantees link reliability for its reusing DUE. Now we can solve the problem $(P1)$ that considers the maximization of the expectation of sum ergodic capacity during a given access period by the following lemma.

Lemma 3.2. *Problem $(P1)$ is equivalent to problem $(P1')$.*

Proof. First, problem $(P1)$ and problem $(P1')$ have the same constraints, so the upper bound of P_m^c determined by the constraints are both characterized by Lemma 3.1, which

means that their feasible regions are the same. Second, the solution to $(P1')$ is given in Theorem 3.1 where $P_m^{c\,*}$ and P_k^{d*} are the optimal transmission power of the corresponding CUE and DUE, respectively. It can be observed that $P_m^{c\,*}$ and P_k^{d*} are irrelevant with CUE's position, so if $\left(P_m^{c\,*}, P_k^{d*}\right)$ is the optimal power allocation that maximizes $\mathbb{E}\left[\log_2\left(1 + \gamma_m^c\right)\right]$, then it will also maximize the position ergodic capacity $\bar{C}_m\left(P_k^d, P_m^c\right)$. Therefore, Lemma 3.2 is proved. ∎

According to Theorem 3.1 and Lemma 3.2, the solution to problem $(P1)$ can be directly obtained by (3.28) and (3.29). As mentioned earlier, the original resource allocation problem (P) to maximize the position ergodic capacity of all CUEs has been divided into two major steps by observing that interference exists only within each spectrum reusing pair. The first step deals with the optimal power allocation for each single pair, which has been studied by the above discussions. The rest is to perform optimal spectrum reusing pair matching to maximize the position ergodic capacity of CUEs while considering all QoS requirements.

3.3.2 Spectrum Allocation with Reusing Pair Matching

By now, we have obtained the optimal power allocation for all possible CUE-DUE spectrum reusing pairs. However, the capacity requirement of the CUE has not taken into account in the problem $(P1)$, implying that the obtained optimal capacity might be less than its minimum QoS demand. In this case, the spectrum reusing pair of the mth CUE and the kth DUE is infeasible since the highest capacity that the CUE can achieve still fails to satisfy the QoS requirement. Thus, we need to eliminate those CUE-DUE pairs that do not satisfy the minimum capacity requirement for the CUE, even when applying the optimal allocation scheme obtained from Theorem 3.1.

For a paired CUE m, assuming its spectrum is reused by the kth DUE, based on the channel model in (3.1) and the definition of the position ergodic capacity in (3.5), position ergodic capacity of this CUE is given by the following lemma.

Lemma 3.3. *The position ergodic capacity, $\bar{C}_m\left(P_m^c, P_k^d\right)$, of the mth CUE when sharing spectrum with the kth DUE is given by*

$$
\begin{aligned}
&\bar{C}_m\left(P_m^c, P_k^d\right) \\
&= \frac{2}{l\ln 2}\int_0^{\frac{l}{2}} \frac{a(x)\left\{e^{1/a(x)}E_1\left[1/a(x)\right] - e^{1/b(x)}E_1\left[1/b(x)\right]\right\}}{a(x) - b(x)}\mathrm{d}x,
\end{aligned} \qquad (3.30)
$$

where

$$a(x) = \frac{P_m^c A \beta_{m,B} (x^2 + y^2 + H^2)^{\frac{-\gamma}{2}}}{\sigma^2}, \tag{3.31}$$

$$b(x) = \frac{P_m^c A \beta_{k,B} \left[(x - \Delta x_{m,k})^2 + (y_k^d)^2 + H^2 \right]^{\frac{-\gamma}{2}}}{\sigma^2}, \tag{3.32}$$

$x \triangleq x_m^c$, $y \triangleq y_m^c$, $\Delta x_{m,k} \triangleq x_m^c - x_k^d$, and $E_1(z) = \int_z^\infty \frac{e^{-t}}{t} \mathrm{d}t$ *is the exponential integral function of the first order.*

Proof. Define $C_m(x)$ as the capacity of a paired CUE m at a given position (x, y). Here $C_m(x)$ is assumed to only depend on x since one DUE's y-coordinate remains constant by keeping on the same lane during the sensing process. Note that γ_m^c can be derived by letting $d_{m,B} = \sqrt{x^2 + y^2 + H^2}$ and $d_{k,B} = \sqrt{(x + \Delta x_{m,k})^2 + (y_k^d)^2 + H^2}$ in $h_{m,B}$ and $h_{k,B}$, respectively. Here $\Delta x_{m,k}$ is the difference between CUE m and the transmitter of the kth DUE pair in x-coordinate, which is assumed to be constant during the moving period. Based on the expression of the ergodic capacity C_m in (3.4), we have

$$
\begin{aligned}
C_m(x) &= \mathbb{E}\left[\log_2 \left(1 + \frac{P_m^c \alpha_{m,B} g_{m,B}}{\sigma^2 + P_k^d \alpha_{k,B} g_{k,B}} \right) \right] \\
&\triangleq \mathbb{E}\left[\log_2 \left(1 + \frac{a(x) X}{b(x) Y} \right) \right],
\end{aligned}
\tag{3.33}
$$

where $a(x)$ and $b(x)$ are defined in (3.31) and (3.32), respectively, $X \triangleq g_{m,B}$, and $Y \triangleq g_{k,B}$.

Defining $Z = a(x) X / [1 + b(x) Y]$ and assuming $g_{m,B}$ and $g_{k,B}$ are i.i.d. exponential random variables with unit mean, then the cumulative distribution function (CDF) of Z can be calculated as

$$
\begin{aligned}
F_Z(z) &= \Pr\left\{ \frac{a(x) X}{1 + b(x) Y} \leq z \right\} \\
&= \int_0^\infty \mathrm{d}y \int_0^{\frac{z[1+b(x)y]}{a(x)}} e^{-(x+y)} \mathrm{d}x \\
&= 1 - e^{-\frac{z}{a(x)}} \frac{a(x)}{a(x) + b(x) z}.
\end{aligned}
\tag{3.34}
$$

Then, the ergodic capacity of the mth CUE can be calculated by

$$
\begin{aligned}
C_m &(x) \\
&= \frac{1}{\ln 2} \int_0^\infty \ln(1+z) f_Z(z)\, dz \\
&= \frac{1}{\ln 2} \int_0^\infty \frac{1 - F_Z(z)}{1+z}\, dz \\
&= \frac{a(x)}{[a(x) - b(x)]\ln 2} \left[e^{\frac{1}{a(x)}} E_1\left(\frac{1}{a(x)}\right) - e^{\frac{1}{b(x)}} E_1\left(\frac{1}{b(x)}\right) \right].
\end{aligned}
\tag{3.35}
$$

According to he definition of position ergodic capacity, we have

$$
\bar{C}_m = \frac{2}{l} \int_0^{\frac{l}{2}} C_m(x)\, dx.
\tag{3.36}
$$

Substituting (3.35) into (3.36) leads to (3.30). Therefore, Lemma 3.3 is proved. ∎

Let $\bar{C}_m^*$ denote the optimal position ergodic capacity of the mth CUE if the kth DUE reuses its spectrum. For the spectrum reusing pair of the mth CUE and the kth DUE, we can obtain the optimal power allocation $\left(P_m^{c\,*}, P_k^{d*} \right)$. Substituting $\left(P_m^{c\,*}, P_k^{d*} \right)$ in (3.30) yields the maximum capacity of the mth CUE, denoted by $\bar{C}_m\left(P_m^{c\,*}, P_k^{d*} \right)$, while guaranteeing the reliability of the DUE. Although $\bar{C}_m\left(P_m^{c\,*}, P_k^{d*} \right)$ is the maximum capacity, it might be still less than the CUE's minimum required throughput r_0^c as the constraint of the CUE's capacity is not explicitly considered in the proposed power allocation in Section 3.3.1. In this case, the reusing pattern is infeasible. To this end, we modify the optimal position ergodic capacity of the CUE for the pair of the mth CUE ($m \in \mathcal{M}$) and the kth DUE ($k \in \mathcal{K}$) as

$$
\bar{C}_m^* = \begin{cases} \bar{C}_m\left(P_m^{c\,*}, P_k^{d*} \right), & \text{if } \bar{C}_m\left(P_m^{c\,*}, P_k^{d*} \right) \geq r_0^c \\ -\infty, & \text{otherwise,} \end{cases}
\tag{3.37}
$$

where the setting of $\bar{C}_m^* = -\infty$ will prevent the spectrum reusing pair in case of infeasibility.

After evaluating all possible combinations of the CUE-DUE pairs, the rest is to find the optimal spectrum reusing pattern by determining $\rho_{m,k}$ for all $m \in \mathcal{M}$ and $k \in \mathcal{K}$, which can

be formulated as a linear assignment problem given by

$$(P2): \max_{\{\rho_{m,k}\}} \sum_{m \in \mathcal{M}} \sum_{k \in \mathcal{K}} \rho_{m,k} \bar{C}_m^*$$

$$\text{s.t.} \sum_{m \in \mathcal{M}} \rho_{m,k} \le 1, \ \forall k \tag{3.38}$$

$$\sum_{k \in \mathcal{K}} \rho_{m,k} \le 1, \ \forall m \tag{3.39}$$

$$\rho_{m,k} \in \{0,1\}, \ \forall k, \ m. \tag{3.40}$$

The problem $(P2)$ can also be regarded as a bipartite matching problem in graph theory [200]. In the next, we will first present the definition of a bipartite graph.

Definition 3.1 (Bipartite graph [201]). *Denote a graph as $G = (V, E)$, where V is the vertex set and E is the edge set of the graph. If the vertex set V can be partitioned into two disjoint subsets V_1 and V_2, in addition, any two vertices v_1 and v_2, which are connected by an edge e_{v_1,v_2} ($e_{v_1,v_2} \in E$), belong to different subsets, $v_1 \in V_1$ and $v_2 \in V_2$. Then, G is referred to as a bipartite graph.*

For problem $(P2)$, we can construct a graph model with the CUEs and DUEs acting as vertexes, i.e., $G = (\mathcal{M} \cup \mathcal{K}, E)$. Under the one-to-one channel reusing constraint, a vertex is only allowed to connect with one edge, and the edges of the graph G only exist between different kinds of vertices, which corresponds to the definition of the bipartite graph. Therefore, problem $(P2)$ can be regarded as a maximum weight bipartite graph matching problem, which can be efficiently solved by the Hungarian algorithm [201, 202]. By combining the graph theory and duality theory of linear programming, the Hungarian algorithm is a sequential combinatorial optimization algorithm that leads to the global optimum of a bipartite matching problem in polynomial time, e.g., $\mathcal{O}\left([\max\{M, K\}]^3\right)$ for the problem $(P2)$.

3.3.3 Robust Resource Allocation Algorithm

Based on the above two-step decomposition, in this subsection, we propose a robust resource allocation algorithm to find the optimal solution to the formulated problem in (P) for the dynamic and heterogenous air-ground integrated communication network with different link transmission requirements , which is summarized in Algorithm 1. The computational complexity of the proposed algorithm contains two parts, i.e., the power allocation for single CUE-DUE pair and the Hungarian method [201, 202] for spectrum reusing pair matching. First, supposing an accuracy of ε, the bisection search for the optimal power allocation of a single CUE-DUE pair as given in Theorem 3.1 requires $\log\left(1/\varepsilon\right)$ iterations. Then, the total

---

Algorithm 1 Robust Resource Allocation Algorithm

1: **for** $m = 1, 2, \ldots, M$ **do**
2:     **for** $k = 1, 2, \ldots, K$ **do**
3:         Obtain the optimal power allocation $\left(P_m^{c\,*}, P_k^{d\,*} \right)$ from Theorem 3.1 for the single CUE-DUE pair;
4:         Substitute $\left(P_m^{c\,*}, P_k^{d\,*} \right)$ into (3.30) to obtain $\bar{C}_m^*$;
5:         **if** $\bar{C}_m \left(P_m^{c\,*}, P_k^{d\,*} \right) \geq r_0^c$ **then**
6:             $\bar{C}_m^* = \bar{C}_m \left(P_m^{c\,*}, P_k^{d\,*} \right)$
7:         **else**
8:             $\bar{C}_m^* = -\infty$
9:         **end if**
10:     **end for**
11: **end for**
12: Obtain the optimal reuse pattern $\left\{ \rho_{m,k}^* \right\}$ of problem $(P2)$ by using the Hungarian method;
13: Return the optimal spectrum reuse pattern $\left\{ \rho_{m,k}^* \right\}$ and the corresponding power allocation $\left\{ \left(P_m^{c\,*}, P_k^{d\,*} \right) \right\}$.

---

complexity for determining the power allocations for all possible spectrum reusing pairs is $\mathcal{O}\left(MK \log \left(1/\varepsilon \right) \right)$. Second, the spectrum reusing pattern optimization problem can be solved by the Hungarian method with complexity $\mathcal{O}\left(\left[\max \{M, K\} \right]^3 \right)$. Therefore, the total complexity of the proposed algorithm is $\mathcal{O}\left(MK \log \left(1/\varepsilon \right) + \left[\max \{M, K\} \right]^3 \right)$.

It should be highlighted that the advantages of our proposed robust resource allocation scheme lie in the following three aspects. First, for the robustness, it eliminates the dependence on the precise and full CSI, and only adopts the slow fading factor of the channel to implement the optimization process. Second, for efficiency, the computational complexity of the proposed algorithm is relatively low. Third, for optimality, the proposed method leads to the globally optimal solution since the derived spectrum reusing pattern is optimally chosen from all possible reusing patterns based on their optimal power allocation.

3.4 Simulation Results

In this section, numerical simulations are provided to demonstrate the performance of our proposed joint resource allocation algorithm for dynamic cellular-enabled UAV communica-

Table 3.1 Simulation Parameters

Parameters	Value
Carrier frequency	2 GHz
Bandwidth	10 MHz
BS antenna gain	8 dBi
UAV antenna gain	4 dBi
Height of UAVs	100 m
Number of DUEs	20
Number of CUEs	20
Minimum capacity requirement r_0^c	0.5 bps/Hz
SINR threshold for DUE γ_0^d	5dB
Tolerable outage probability p_0	0.001
Maximum transmit power of CUEs	15, 20 dBm
Maximum transmit power of DUEs	15, 20 dBm
Absolute UAV speed	16 m/s
Noise power	-114 dBm
Bisection search accuracy	10^{-5}

tion networks. If not otherwise specified, the configurations of simulation parameters follow the existing work and 3GPP specifications [203], which are listed in Table 3.1 specifically.

Fig. 3.3 demonstrates the sum ergodic capacities of CUEs achieved by our proposed algorithm (denoted as Algorithm 1) and minimum CUE ergodic capacity maximization scheme (denoted as Algorithm 2) with respect to a genie-aided benchmark based on a modified traditional D2D resource allocation scheme developed in [204] where accurate knowledge of instantaneous CSI for all links is assumed to be perfectly known at the BS. We note that in high speed UAV environments, such full CSI assumption is by no means realistic, but it serves as an ideal reference to benchmark our proposed algorithms. It is observed that the sum ergodic capacities of CUEs achieved by both Algorithms 1 and 2 get larger if higher outage probability of DUEs is allowed. This is due to the fact that higher acceptable outage of DUEs renders them more tolerable to interference from CUEs, thus encouraging CUEs to increase their transmit powers. As a result, the CUE capacity grows larger. From Fig. 3.3, the performance of Algorithm 1 is well close to the ideal benchmark scheme in terms of sum
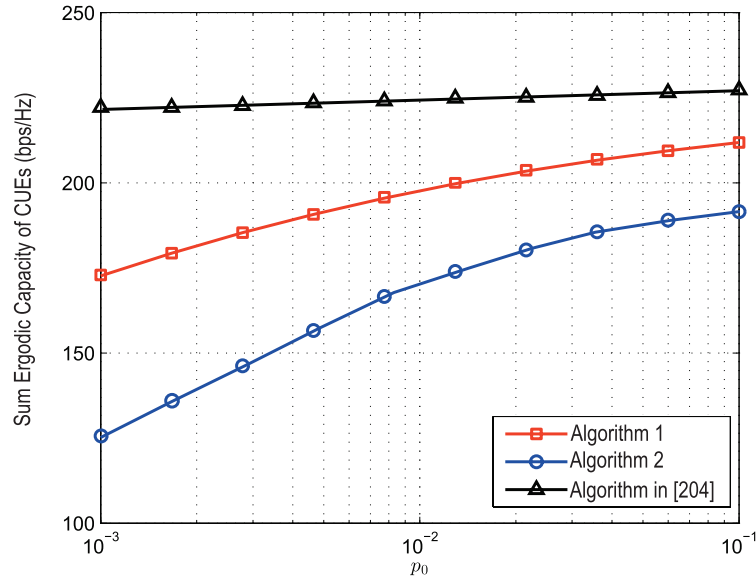
Fig. 3.3 Capacity performance of cellular users (CUEs) with varying aerial D2D user (DUE) outage probability.

capacity at fairly low outage probability. These are encouraging findings as the proposed resource allocation scheme makes use of slowly varying large-scale fading parameters only and update every few hundred milliseconds. Nonetheless, they can achieve performance measurably close to the genie-aided benchmark scheme, which requires accurate real-time CSI of all links and is inapplicable in a UAV communication environment featuring high mobility.

Fig. 3.4 shows the sum ergodic capacities of all CUEs with an increasing UAV speed. From the figure, the sum CUE capacities decrease as the UAVs move faster. This is because the distance between adjacent UAVs tends to be longer as UAV speed increases and give rise to less reliable U2U links with lower received power. As such, less interference from CUEs can be tolerated given the maximum transmit power constraints of DUEs, which leads to less power being allocated to CUEs and decreases their sum ergodic capacities. It also reveals that Algorithm 1 achieves higher sum ergodic capacity than Algorithm 2. This makes sense since Algorithm 1 aims to maximize the sum ergodic capacity while Algorithm 2 takes the minimum ergodic capacity as its design objective.

Fig. 3.5 demonstrates the sum ergodic capacities of CUEs with respect to increasing SINR threshold for DUEs. We observe that the investigated ergodic capacity will decrease when the minimum QoS requirement for DUEs grows large. Such performance degradation results from the reduced interference tolerability of DUEs due to an increase in their required SINR threshold, which will impose stricter constraints on the allowable transmit power of
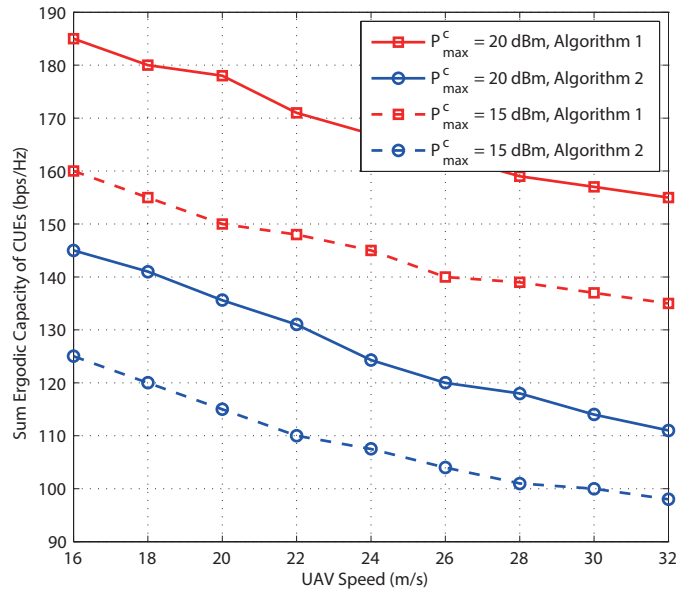
Fig. 3.4 Capacity performance of cellular users (CUEs) with varying UAV speed.
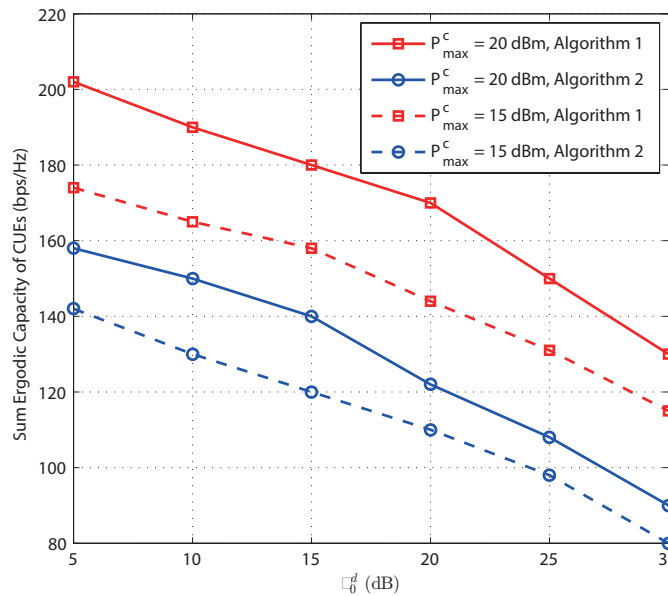
Fig. 3.5 Capacity performance of cellular users (CUEs) with varying aerial D2D user (DUE) SINR threshold.

the pairing CUEs. Reduced transmit power of CUEs directly translates into a decrease of the sum ergodic capacities they are capable of achieving given all QoS constraints satisfied.

3.5 Conclusion

In this chapter, we have investigated the spectrum sharing and power allocation design for air-ground integrated networks in which U2U links reuses spectrum of the U2I links. Due to fast channel variations arising from high UAV mobility, instantaneous CSI is hard to track in practice, rendering traditional resource allocation schemes requiring full CSI inapplicable. In addition, link disconnection for U2U transmissions often occurs in a dynamic UAV communication environment. To address these issues, we have taken into account the differentiated QoS requirements of UAV communications, i.e., high capacity for U2I links while high reliability for U2U links, and formulated optimization problems aiming to design a resource allocation scheme based on slowly varying large-scale fading information only. A robust algorithm has been proposed to maximize the sum ergodic capacity of U2I links during an access period, while ensuring reliability for all U2U links. Simulation results demonstrate the desirable performance of the proposed method.

Chapter 4

Blockchain-Based Secure Spectrum Trading for UAV-Assisted Cellular Networks

4.1 Introduction

In Chapter 3, we investigated the robust resource allocation for air-ground integrated networks. However, to fully reap the benefits of deploying UAVs for communication purposes, some core technical challenges still need to be faced. On the one hand, most UAVs in the market operate on the unlicensed spectrum (e.g., the industrial, scientific and medical bands), which is usually of limited data rate, unreliable and vulnerable to interference, thus severely restricting the potential performance of UAVs [205]. On the other hand, there always exist significant security and privacy threats for UAV-assisted wireless communications due to the untrusted broadcast features and wireless transmission of UAV networks. However, these problems have not been well studied in existing works. These observations motivate us to focus on investigating the spectrum usage for UAV-assisted cellular networks while considering the security and privacy issues in this chapter.

Due to the scarcity of wireless spectrum, UAVs always need to share spectrum with existing communication systems (e.g., cellular networks with licensed spectrum). However, traditional spectrum sharing mechanisms through spectrum sensing [206, 207] or spectrum databases [208] are actually not efficient for UAV-assisted cellular networks, because spectrum sensing is generally imperfect and subject to sensing errors while spectrum databases are based on centralized management. It is challenging to apply these methods into UAV networks to achieve distributed and reliable communications. To deal with these challenges,

some researchers attempt to exploit the property-right spectrum sharing techniques operating based on an agreement where the spectrum owners lease or share their spectrum to the unlicensed ones in exchange for some certain services [209, 210]. However, these works do not take into account the practical challenges of UAV deployments for cellular services from the perspective of operators. In fact, UAVs and ground base stations often belong to multiple different operators, each selfishly seeking to maximize their individual benefit. In general, the cellular network operators will be not willing to share their own spectrum to the UAV networks, since the total usable bandwidth of the cellular networks is limited, and sharing part of the total bandwidth with UAVs may harm the capacity of the cellular base stations. Thus, to promote the adoption of spectrum sharing, some incentive mechanisms should be developed to motivate the mutual cooperation between the operators.

Incentive mechanism design has been extensively studied for networking problems, such as caching [211, 212], traffic/computation offloading [213, 214], cooperative communications [215], etc. However, none of them consider the UAV-assisted application scenarios. Besides, existing incentive mechanisms with high complexity and centralized control may not be suitable for UAV networks when considering the energy constraint and distributed features of UAV networks. Recently, Hu *et al.* in [216] investigated the use of contract theory to formulate the spectrum trading problem between the macro base station manager and the UAV operators to encourage the macro base station manager to lease its owned bandwidth to the UAVs. However, there are significant security and privacy challenges for such peer-to-peer (P2P) spectrum trading in UAV-assisted cellular networks for the following reasons. i) It is insecure for mobile network operators (MNOs) to carry out large-scale spectrum trading in an untrusted and nontransparent trading environment, where malicious UAV operators could heavily threaten cellular network's security through malicious exploitation, e.g., falsification, advertising fraudulent spectrum demands, etc. ii) In traditional centralized spectrum trading, there is an intermediary managing the trading among the operators, which may suffer from problems such as single point of failure and privacy leakage.

In recent years, *blockchain technology* [217–219] has attracted growing attention of researchers, which may provide possible solutions addressing the above challenges because of its advantages of decentralization, anonymity and trust. Blockchain is a decentralized ledger-based storage method, which provides a unique tool for secure transactions in a distributed manner without trusted agents [220]. Moreover, in blockchain-based networks, each node manages a copy of whole or part of a database from the system. These advantages enable spectrum trading to be executed in a decentralized, transparent, and secure market environment. Some recent works have explored blockchain to address the transaction security issues for local P2P networks, such as the blockchain-based anonymous rewarding scheme

for vehicle-to-grid networks in [221], and utilizing blockchain for crowdsourcing to preserve the privacy of the participants in [222, 223]. However, these methods can not be directly employed in localized spectrum trading for energy-limited UAV networks due to the challenges of the high computation cost associated with establishing a blockchain. Recently, there are several works attempting to apply blockchain into UAV networks. For example, Zhu *et al.* in [224] used blockchain to construct a decentralized information storage platform for air-to-ground industrial networks. In [225], a neural-blockchain based drone-caching approach was designed to ensure ultra-reliable communications. However, spectrum sharing or trading is not considered in these works. Moreover, they also do not propose efficient solutions to deal with the high cost for building a blockchain.

Motivated by the aforementioned observations, in this chapter, we exploit the consortium blockchain technology to develop a secure spectrum trading system named *spectrum blockchain* for UAV-assisted cellular networks. A consortium blockchain is a special blockchain with multiple pre-selected nodes to establish the distributed shared database with moderate cost [226, 227]. To deal with the computation-intensive blockchain creation and verification process, mobile edge computing is applied to help to offload the computation task to proximate authorized edge computing nodes. Under the mobile edge computing aided consortium blockchain framework, secure spectrum trading between the MNO and the UAV operators with privacy protection can be achieved in a distributed manner. Moreover, since spectrum pricing along with the amount of traded spectrum need to be optimized in the spectrum blockchain, a Stackelberg game is formulated to jointly maximize the profits of the MNO and the UAV operators.

Specifically, the contributions of this chapter are summarized as follows:

- A pricing-based incentive mechanism is firstly presented to motivate the MNO to open its owned spectrum for UAV networks, in which the MNO acts as a spectrum seller and leases the idle spectrum to a secondary UAV network in exchange for some revenue from the UAV operators.

- To address the potential security and privacy issues caused by malicious attacks in the spectrum trading process, a spectrum blockchain framework is proposed to illustrate the detailed operations of how the blockchain can help to improve the transaction security without relying on a third party.

- Under the blockchain framework, a Stackelberg game is formulated to obtain the optimal spectrum pricing and purchasing strategies, which can jointly maximize the revenues of the MNO and the UAV operators.

- Two pricing schemes are investigated, including *non-uniform pricing* in which different spectrum prices are assigned to different UAV operators, and *uniform pricing* in which the same price applies to all the UAV operators. In addition, we develop a non-uniform pricing algorithm and a distributed spectrum price bargaining algorithm respectively for the two different pricing cases to achieve the optimal solutions.

The rest of this chapter is organized as follows. The system model for spectrum trading is introduced in Section 4.2. Detailed operations of the spectrum blockchain are illustrated in Section 4.3. In Section 4.4, a Stackelberg game is formulated to obtain the optimal pricing and purchasing strategies, considering two different pricing schemes. Security assessment and numerical results are shown in Section 4.5 before the chapter is concluded in Section 4.6.

4.2 System Model for Spectrum Trading

4.2.1 Network Model

We consider a heterogeneous network, in which one cellular base station owned by the MNO is overlaid with a number of UAVs possessed by different UAV operators. The set of UAV operators is denoted by $\mathcal{N}$, $\mathcal{N} = [1, 2, \cdots, N]$. Since UAVs always operate on unlicensed spectrum with limited capacity that restricts their performances to provide better services for local mobile users, UAV operators have a strong wish to be allowed to share spectrum with the MNO. Nevertheless, the quality of experience (QoE) of cellular users may diminish if UAVs take up some spectrum owned by cellular base station for serving cellular users. Thus, it is difficult for a MNO to be so altruistic to allow UAV users to access licensed spectrum without any remuneration.

To deal with the above issues, an incentive mechanism can be designed to motivate the cooperation between the MNO and the UAV operators in which the MNO can lease some idle bandwidth to UAVs in exchange for a certain level of profit (e.g., revenue) from the UAV networks while the UAVs will benefit from enhanced quality of service with licensed spectrum. In this way, both systems can increase their own interest and a *win-win situation* can be achieved. Therefore, in this section, a pricing-based incentive mechanism is introduced to promote spectrum sharing between the cellular and UAV networks. In particular, we investigate the spectrum leasing problem and design an incentive mechanism at the data (message) level from a network operator's perspective, in which each UAV operator can temporally buy some licensed spectrum from the MNO to provide better services for its local mobile users. Detailed design considerations are given as follows.

4.2.2 Utility Function for the Incentive Mechanism

For the MNO, we define μ_i as the price for each unit of bandwidth provided to the UAV operator i. Let b_i denote the spectrum that UAV operator i intends to purchase. Under the pricing-based incentive mechanism, the MNO's objective is to maximize its revenue obtained from selling the spectrum to the UAV operators. Mathematically, the utility function of the MNO can be modelled as

$$U_{MNO}(\boldsymbol{\mu}, \boldsymbol{b}) = \sum_{i=1}^{N} \mu_i b_i, \tag{4.1}$$

where $\boldsymbol{\mu}$ is the spectrum price vector with $\boldsymbol{\mu} = [\mu_1, \mu_2, \cdots, \mu_N]^T$, and $\boldsymbol{b}$ is a vector of bandwidth purchased by UAV operators with $\boldsymbol{b} = [b_1, b_2, \cdots, b_N]^T$. Note that $\forall i$, b_i is actually a function of μ_i, i.e., $b_i \triangleq f_i(\mu_i)$, which indicates that the amount of the spectrum that each UAV operator is willing to buy is dependent on its assigned bandwidth price. Besides, it is assumed that the total available idle bandwidth of the MNO is Q, i.e., the aggregate allocated spectrum for all the UAV operators should not be larger than Q, which can be expressed as $\sum_{i=1}^{N} b_i \leq Q$.

From the spectrum purchaser's perspective, each UAV operator i requests spectrum from the MNO according to the real requirement for serving its own users for a specific application. Without loss of generality, the utility function of an arbitrary UAV operator is defined as

$$U_i(b_i, \mu_i) \triangleq \mathscr{R}(b_i, d_i) - \mathscr{C}(b_i, \mu_i), \tag{4.2}$$

where $\mathscr{R}(b_i, d_i)$ is the payoff/benefit gained from allocated spectrum, with d_i denoting the basic bandwidth demand of the UAV which reflects the service type, and $\mathscr{C}(b_i, \mu_i)$ is the cost incurred due to buying the spectrum. Note that each UAV operator's utility function consists of two parts: payoff and cost. In the following, we present how to model them under the proposed incentive mechanism.

Payoff: The payoff of a UAV operator i is the benefit or reward gained from the allocated spectrum. Specifically, the payoff is modeled as

$$\mathscr{R}(b_i, d_i) = g_i \mathscr{H}(b_i, d_i), \tag{4.3}$$

where $\mathscr{H}(b_i, d_i)$ is the spectrum obtainment gain, and g_i is a positive coefficient converting the spectrum obtainment gain into monetary reward. Here, we define g_i as the spectrum coins that the UAV operator i possesses to pay for the spectrum received from the MNO. The spectrum coin is one kind of digital cryptocurrency which is employed to facilitate

the spectrum trading between the MNO and the UAV operators. More details about the spectrum coins will be given in Section 4.3. Intuitively, the more spectrum you are allocated, the more gain you should receive. Thus, $\mathscr{H}(b_i, d_i)$ should be an increasing function of b_i. Besides, UAV operators should also take into account the real demands of serving users when purchasing bandwidth due to considering the cost of buying spectrum. Here, a log function is used to model the spectrum obtainment gain, i.e.,

$$\mathscr{H}(b_i, d_i) = \log_2\left(1 + \frac{b_i}{d_i}\right). \tag{4.4}$$

Though other functions (such as linear or exponential functions) can also be used to model the spectrum obtainment gain, log functions are shown in literature to be more suitable to representing the relationship between the network performance and a large class of elastic data traffic [228, 229]. It is observed from (4.4) that when the amount of received spectrum is zero ($b_i = 0$), the obtained gain $\mathscr{H}$ is also equal to zero, while the gain increases with the increasing of allocated spectrum. Moreover, $\mathscr{H}(b_i, d_i)$ can also reflect the degree of "happiness" of the UAV operator if receiving bandwidth b_i under the demand d_i. These indicate that (4.4) is able to capture the relationship between the UAV operators' benefit and the received bandwidth.

Cost: $\mathscr{C}(b_i, \mu_i)$ denotes the cost incurred when UAV operator i purchases spectrum from the MNO. In general, the cost increases with the increasing of the amount of obtained spectrum. Thus, it can be easily modeled as

$$\mathscr{C}(b_i, \mu_i) = \mu_i b_i. \tag{4.5}$$

Therefore, the utility function of an arbitrary UAV operator can be written as

$$U_i(b_i, \mu_i) = g_i \log_2\left(1 + \frac{b_i}{d_i}\right) - \mu_i b_i. \tag{4.6}$$

Obviously, with a larger bandwidth b_i, UAV operator i can obtain a more satisfactory system performance, however, this also increases the cost. Therefore, optimal strategies are needed for a rational operator to balance the cost and achieved benefit in order to maximize its utility.

4.2.3 Security Threats

In the above subsection, we focus on designing a pricing-based incentive mechanism for spectrum trading between the cellular and UAV networks. However, this monetary approach

always needs to rely on trusted centers that may not only leak operators' privacy, but also be vulnerable to attack. In addition, due to the untrusted broadcast features and wireless transmission of the UAV networks, there also exist significant trust issues which may threaten system security and privacy. Typically, three kinds of attackers or adversaries may appear:

1) Malicious spectrum provider: A malicious cellular operator who advertises fraudulent spectrum leasing services without enough available spectrum.

2) Malicious spectrum buyer: A malicious UAV operator who pretends that it has not received any spectrum from the cellular operator and refuses to pay.

3) Malicious trusted third party: The malicious trust center may not only disclose the MNO's privacy but tamper the UAV operators' credit value (e.g., spectrum coins) for profit.

To deal with these security threats, distributed and trusted management schemes are needed to identify and defend against malicious peers. To this end, we exploit blockchain technology to provide a trusted environment to enhance secure spectrum trading among the operators.

4.3   Spectrum Blockchain

Blockchain is a P2P decentralized ledger, which is designed to efficiently record transactions among participants in a verifiable and permanent way, without relying on a trusted center. Blockchain technology enables spectrum trading to be executed in a distributed, transparent and secure market environment. Thus, in this section, a blockchain-enabled *spectrum blockchain* framework is proposed to support secure spectrum trading between the cellular and UAV operators.

4.3.1   Overview of Spectrum Blockchain

The core issue of the blockchain is a computational processing called "*mining*" (consensus), in which a set of participants called "*miners*" need to solve a complex computation problem, i.e., proof-of-work puzzle, to confirm and secure the integrity and validity of transactions before adding the records into the blockchain. The security and privacy of the blockchain depend on the distributed consensus mechanism managed by these miners. However, in a traditional public/permissionless blockchain (such as Bitcoin and Ethereum), the consensus stage is executed by all nodes (miners) which leads to high cost. To relieve the computation-intensive challenge of establishing a blockchain, unlike existing works, in this chapter, we use consortium blockchain technology to perform distributed spectrum trading. A consortium blockchain is a special permissioned blockchain in which the consensus process is
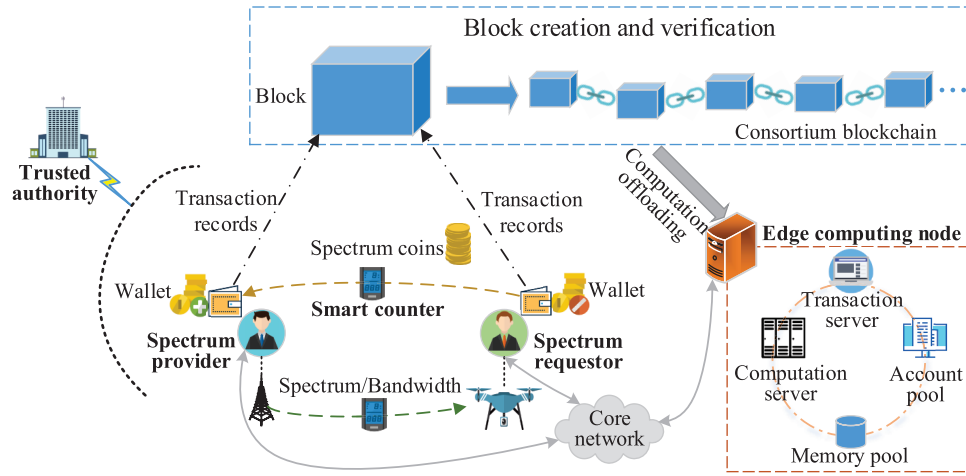
Fig. 4.1 Framework of spectrum blockchain.

executed on pre-selected nodes with moderate cost[1]. Thus, it is more suitable and feasible for energy-constraint UAV networks. Moreover, to further solve the high computing power needed in blockchain creation, we leverage edge computing as a network enabler to offload the computation-intensive proof-of-work puzzles to proximate edge computing nodes. Compared to traditional cloud computing [231–234], edge computing brings network resources (e.g., computation or storage resources) closer to the users which can effectively shorten the transmissions delay and reduce the energy consumption [235–237]. The practicality of integrating edge computing and blockchain comes from both the same decentralized infrastructure and the same functions of storage and computation [238].

The consortium blockchain-based secure spectrum trading framework is shown in Fig. 4.1, which consists of the following major entities.

- *Trusted authority (TA)*: The TA is responsible for initializing the whole spectrum trading system, generating public parameters and cryptographic keys, and managing the operators' identities. Note that the TA only serves as a parameter initializer to provide identity authorization and certificate issuance of entities before running spectrum blockchain. It will remain offline for most of the time. That is to say, this role does not conflict with the decentralization of the blockchain.

- *Spectrum provider and requestors*: The UAV operators act as the spectrum requestors to purchase bandwidth from the spectrum provider. The MNO acts as the spectrum provider and leases its own idle licensed spectrum to the UAV operators in return for reward.

---

[1]As for consortium blockchain, Hyperledger is one of the most famous application platforms [230].

- *Edge computing nodes*: It is assumed that there are edge devices (nodes) in the system which can provide computing and storage services. As shown in Fig. 4.1, each edge computing node consists of four components: a transaction server, an account pool, a memory pool and a computation server. The transaction server collects the real-time spectrum requests from the UAV operators and the price announcements from the MNO, and transmits the trading-related information among the MNO and the UAV operators via the core network. Here, a digital cryptocurrency named spectrum coin works as UAV operators' digital assets to purchase spectrum from the MNO. Each UAV operator has a virtual wallet to manage personal spectrum coins. The account pool in the edge computing nodes records and stores spectrum coins in the personal wallet of the UAV operators, and the numerical value of the amount of the MNO's spectrum. The memory pool stores all the transaction records of local operators. The computation server provides computing power for the process of block generation and validation.

- *Smart counters*: A built-in smart counter in each entity records the amount of traded spectrum in real time. The UAV operators pay the MNO according to the records of smart counters.

In the framework, the spectrum trading between the UAV operators and the MNO are forwarded based on blockchain technology, in which all the transactions should be announced to the audit edge computing nodes for verification through broadcasting, instead of direct transactions among them. In this way, a secure spectrum trading environment can be established, which guarantees transaction security and privacy protection. The detailed mechanism of operation is given in Section 4.3.3.

4.3.2 Design Goals

Based on the proposed blockchain-enabled spectrum trading scheme, the following properties are expected to be achieved:

- **Operator authentication**. Operators should be authenticated in an anonymous way so that no adversary can impersonate a registered operator.

- **Privacy**. The requests, announcements and transactions do not leak any personal information about their sources (i.e., anonymity).

- **Traceability**. The TA can track the identity of a operator in case of a dispute or something unexpected occurs.
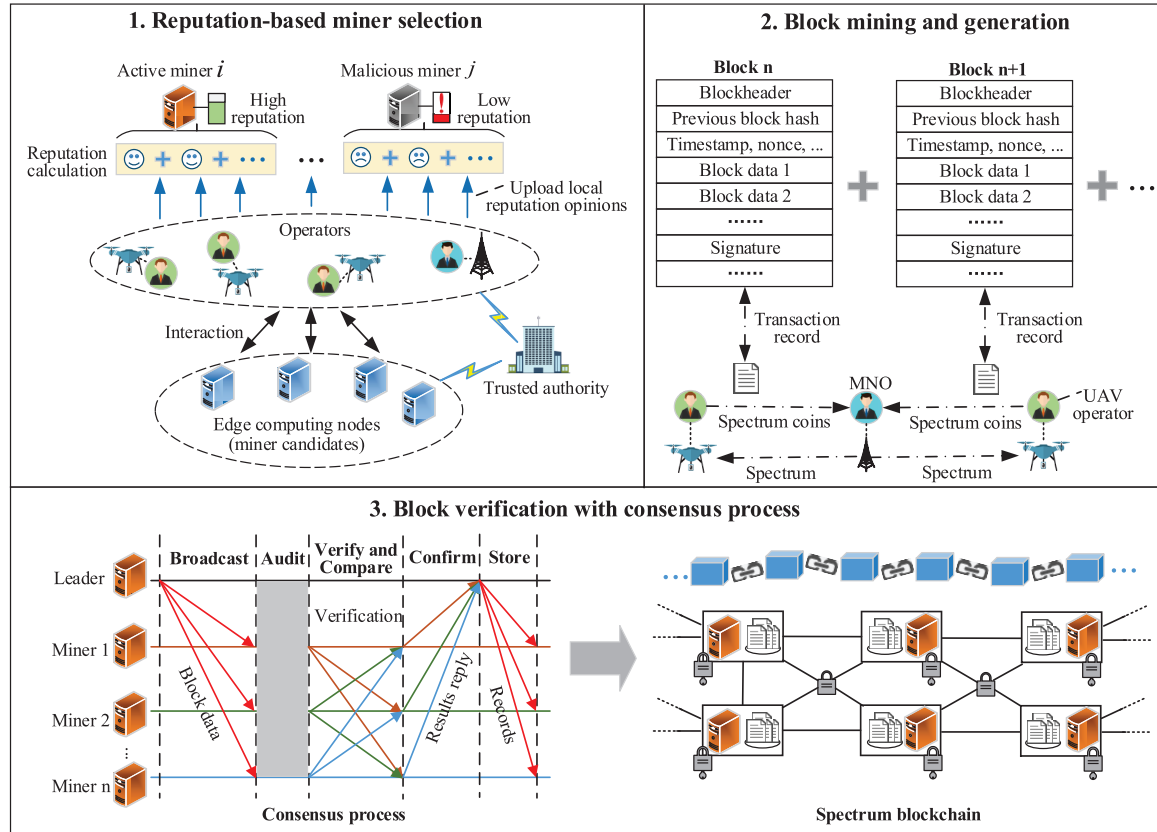
Fig. 4.2 Operation procedure of the blockchain-based secure spectrum trading.

- **Reliability**. According to the design idea of blockchain, every operator can manage a copy of the whole block chains of transactions, and each transaction is related to the phases of spectrum trading. Thus, an entity is unable to modify the transactions without authorization.

- **Data confidentiality and integrity**. The contents of any trading messages should be protected from the operators, edge computing nodes, and other entities. All accepted messages should be transmitted without being altered.

4.3.3 Operation Details of the Blockchain-based Secure Spectrum Trading

As depicted in Fig. 4.2, there are mainly three parts for the operation of the spectrum blockchain for secure spectrum trading. (i) *Reputation-based miner selection*. Since not all the edge nodes are trusted in the system, those malicious edge nodes may falsely modify or discard transaction records during their mining process. Thus, it is necessary to design a

secure and efficient reputation management scheme for the edge computing nodes and select the candidates with high reputation acting as active miners to ensure a reliable consensus process. (ii) *Block mining and generation.* The selected edge computing nodes then act as miners to collect the transaction records from the MNO and the UAV operators, and perform block generation. (iii) *Block verification with consensus process.* A new generated block needs to be audited by the miners via the consensus mechanism before storing it. As long as most miners agree on the block data, this block can be added into the spectrum blockchain. More details are given in the subsequent discussions.

1) System initialization: In the spectrum blockchain, to guarantee the data integrity and unforgeability, an elliptic curve digital signature algorithm and asymmetric cryptography [239] are utilized for system initialization. Every operator becomes a legitimate entity with proprietary registration information after passing identity authentication by a TA, such as a government department. A UAV operator i can firstly get its certificate $Cert_i$ from the TA and the $Cert_i$ is used to uniquely identify itself through binding its registration information, e.g., identity ID_i and license plate number. Then UAV operator i joins the spectrum blockchain network with its $Cert_i$ and obtains its public/private key pair (PK_i, SK_i) and wallet address add_i. Here, each UAV operator's account includes its account balance Bal_i, certificate $Cert_i$, current spectrum coin value g_i, public/private key pair (PK_i, SK_i) and wallet address add_i. The MNO's account contains its account balance Bal_{MNO}, available spectrum, public/pricate key pair (PK_{MNO}, SK_{MNO}) and wallet address add_{MNO}. The asymmetric cryptography scheme for ensuring the authenticity and integrity of information transmission is expressed as

$$Dec_{PK_i}\left(Sig_{SK_i}\left(H\left(m\right)\right)\right) = H\left(m\right), \tag{4.7}$$

where Sig_{SK_i} is the digital signature of sender i with private key, Dec_{PK_i} is to decode the signed data with sender i's public key, $H\left(m\right)$ is the hash digest of message m [240]. When executing system initialization, each operator uploads its wallet addresses being used to the account pool of its nearest edge computing node. Operators check the integrity of their account and download data about their account from a memory pool in the edge computing nodes. The memory pool stores all transaction records in the spectrum blockchain.

2) Reputation-based miner selection: Since not all edge devices/nodes are trusted, an edge node that wants to be a miner candidate needs to firstly submit its identity-related information to the TA. The TA verifies the validity of the edge node by estimating its average reputation according to the feedback information about the reputation opinions from the operators. Only if its average reputation is higher than a trust threshold or ranked at the forefront, the edge node can be issued a legitimate certificate and act as a miner to perform mining task. Here, to calculate edge nodes' reputation, a subjective logic model

based on historical interactions between the edge nodes and the operators is utilized, which is a framework for probabilistic information fusion operated on subjective beliefs about the world [241]. The subjective logic uses the term "opinion" to indicate the representation of a subjective belief, and models positive statements, negative statements and uncertainty. It also provides a broad range of logical operators to combine and relate different opinions [242]. Thus, the subjective logic model is a suitable mechanism to quantify the edge computing nodes' reputation. The basic procedure of using a subjective logic model for reputation calculation is given as follows.

Considering an operator ope_i and an edge node e_j, the operator may interact with the edge node during the spectrum trading. The trustworthiness (i.e., local opinion) of ope_i to e_j in the subjective logic can be formally expressed as a local opinion vector $\omega_{i \to j}$, i.e., $\omega_{i \to j} := \{bel_{i \to j}, dis_{i \to j}, uncer_{i \to j}\}$, where $bel_{i \to j}$, $dis_{i \to j}$ and $uncer_{i \to j}$ represent the belief, distrust, and uncertainty, respectively. Here, $bel_{i \to j}, dis_{i \to j}, uncer_{i \to j} \in [0, 1]$ and $bel_{i \to j} + dis_{i \to j} + uncer_{i \to j} = 1$. According to the subjective logic model, we have

$$\begin{cases} bel_{i \to j} = \left(1 - uncer_{i \to j}\right) \frac{N_{PI}}{N_{PI} + N_{NI}}, \\ dis_{i \to j} = \left(1 - uncer_{i \to j}\right) \frac{N_{NI}}{N_{PI} + N_{NI}}, \\ uncer_{i \to j} = 1 - succe_{i \to j}, \end{cases} \tag{4.8}$$

where N_{PI} is the number of positive interactions, while N_{NI} is the number of negative interactions. The positive interaction means that the operators believe that the services provided by edge computing nodes are relevant and useful. The communication quality $succe_{i \to j}$ of a link between ope_i and e_j, i.e., the successful transmission probability of data packets, determines the uncertainty of local opinion vector $uncer_{i \to j}$. According to $\omega_{i \to j}$, the reputation value $rep_{i \to j}$ represents the expected belief of operator ope_i that edge node e_j is trusted and behaves in the spectrum blockchain network, which can be expressed as

$$rep_{i \to j} = bel_{i \to j} + \phi uncer_{i \to j}, \tag{4.9}$$

where $\phi \in [0, 1]$ is the given constant indicating an effect level of the uncertainty for reputation. Operators can calculate all edge nodes' reputation based on (4.8) and (4.9). Moreover, to achieve higher credibility and accuracy, a multi-weight subjective logic model can be exploited to characterize the local opinions, considering different influencing factors such as interaction frequency, interaction timeliness and interaction effects, while taking into account the recommended opinions from other operators. Further studies about the multi-weight subjective logical model can refer to the literature [241, 242].

After calculating the reputation opinions, each operator votes for y candidates from the edge nodes as the potential miners according to its local ranking of reputation opinions for edge nodes. Then, the top k candidates with the highest reputation are selected to be active miners. These active miners will be authorized by the TA and join in the spectrum blockchain to carry out trading-related tasks.

3) Trading spectrum between MNO and UAV operators: UAV operators send spectrum requests to the transaction server of a nearby miner (i.e., selected edge node). The transaction server in the edge node counts the total spectrum demands and broadcasts these demands to the MNO. The edge node works as a spectrum broker and sets a pricing-based incentive mechanism (as shown in Section 4.2) to attract MNO for participation in the spectrum trading. Motivated by the incentive mechanism, the MNO determines its initial spectrum to be leased and the corresponding price and gives responses to the transaction server. The transaction server then coordinates and matches the spectrum supply and demand among the operators. According to the pricing-based incentive mechanism in Section 4.2, it can be seen that both the MNO and the UAV operators are rational and selfish in the process of spectrum trading, in which all of the them attempt to maximize their own benefits. Thus, to balance spectrum demand and supply in our spectrum blockchain, a solution for analyzing and determining the optimal spectrum price for the MNO and the optimal spectrum requests for the UAV operators is necessary. Here, a game theoretic method is used to execute spectrum negotiations and transactions between the seller and the buyers. More details about the optimal spectrum trading strategies based on game theory will be given in Section 4.4.

After spectrum trading, a UAV operator transfers spectrum coins from its wallet to the wallet address given by the MNO. The MNO obtains the latest blockchain data from the memory pool of edge nodes to verify this payment activity. The UAV operators generate new transaction records, and the MNO verifies and digitally signs the transaction records and thus uploads the records to blockchain miners for audit.

4) Block mining and generation: Edge nodes collect all local transaction records between spectrum seller and buyers during a certain period, and then encrypt and digitally sign these records to guarantee authenticity and accuracy. As shown in part 2 of Fig. 4.2, all the transaction records are packaged into blocks. A block consists of a transaction set, a timestamp, a hash value of pre-block and other information that are significant to record. For traceability and verification, each block has a unique and cryptographic hash to prior blocks in the spectrum blockchain. Similar to that in Bitcoin, the edge nodes try to find their own valid proof-of-work about data audit (i.e., a hash value meeting a certain level of difficulty) [243]. Each edge node calculates the hash value of its block based on a random

nonce value φ, timestamp, transactions' Merkle root, and historical block hash value and so on (denoted as *previous$_{data}$*), which is written as:

$$Hash\left(\varphi + previous_{data}\right) < N_{difficulty}, \tag{4.10}$$

where $N_{difficulty}$ is a number that can be adjusted by the system to control the speed of finding out the specific nonce value φ [244]. Each authorized edge node (miner) in the spectrum blockchain competes to create a block by finding a valid proof-of work (i.e., nonce value φ). After a valid proof-of-work is found, the fastest miner works as a leader and broadcasts the block and the specific nonce value to other edge nodes in the spectrum blockchain for audit and verification. If other edge nodes agree on the block, data information in this new block will be added to the spectrum blockchain in a linear and chronological order, and the fastest miner is awarded by spectrum coins.

5) Block verification with consensus process: To ensure that each authorized node in the system has a copy of the recognized version of the whole blockchain, the audit stage, i.e., the block verification with consensus process should be carried out. To this end, a distributed consensus algorithm is proposed in Algorithm 2 to reach consensus efficiently in the spectrum blockchain. More details are given as follows.

As shown in part 3 of Fig. 4.2, the miner leader firstly broadcasts block data *Block_data*, timestamp, and the specific φ to other authorized edge nodes for audit. In order to achieve mutual supervision and verification, these edge nodes check the block data and broadcast their audit results with signatures to each other. After receiving the audit results, each edge node compares its result with others and sends a reply back to the miner leader. The reply is made up of the edge node's signatures, audit result, comparison result, and the records of received audit results. The leader performs statistics analysis of received replies from edge nodes. If the block data is approved by all the edge nodes, i.e., reaching consensus, the leader will broadcast records including current audited block data and a corresponding signature to all authorized edge nodes for storage. Then, the new block is added into the consortium blockchain in a linear and chronological order, which contains a cryptographic hash to the prior block. At the same time, every node synchronizes its local copy of the blockchain with the new block. However, if some edge nodes do not agree on the block data, the leader needs to check the audit results and send the ledger update requests to these edge nodes once again for audit if necessary. At last, the block that fails to pass the verification will be discarded, and the implementation phase goes back to the step of block mining and generation for next round of consensus process.

Algorithm 2 Distributed consensus algorithm

1: The miner leader broadcasts the *Block_data* to all edge nodes;
2: **for** all edge computing nodes **do**
3:     **if** its own data do not contain the block information **then**
4:         Compare its own data with data in the block;
5:         **if** all the data are identical **then**
6:             Set $verify(Block\_data) = True$;
7:         **else**
8:             Set $verify(Block\_data) = False$;
9:         **end if**
10:         Broadcast its audit result to other edge nodes for mutual supervision and verification;
11:         Each edge node compares its result with others and sends a reply back to the leader;
12:     **else if** its own data contain the block data **then**
13:         No action;
14:     **end if**
15: **end for**
16: The leader analyzes the received replies from edge nodes;
17: **if** all the edge nodes approve the block **then**
18:     The leader will send records including current audited block data and a corresponding signature to all authorized edge nodes for storage;
19: **else if** some edge nodes do not agree on the block **then**
20:     The leader checks the audit results and sends the block data to these edge nodes once again for audit;
21: **end if**
22: Discard the block that fails to pass the verification;
23: Go back to the step of block generation for next round of audit.

4.4 Optimal Spectrum Trading Strategies

In this section, we present the problem definition for the spectrum pricing and the amount of traded spectrum between the MNO and the UAV operators, and analyze the optimal strategies that are made in Section 4.3.3 to maximize the utilities of both sides during the spectrum blockchain management process.

4.4.1 Problem Formulation

In Section 4.2, a pricing-based incentive mechanism is introduced to motivate the spectrum trading between the cellular networks and the UAV networks. Since both MNO and UAV operators are selfish and rational entities who try to pursue personal utility maximization in

a distributed manner, it is obvious that game theory is the most suitable tool to analyze the problem. The game should involve two phases, in which the MNO firstly announces the initial price of the spectrum to be leased and the UAV operators then request the spectrum according to the price. Thus, it is reasonable to formulate the process as a Stackelberg game [245, 246].

A Stackelberg game is a strategic game that consists of a leader and several followers competing with each other on certain resources. In this chapter, we formulate the MNO as the leader, and the UAV operators as the followers. The leader (i.e., MNO) needs to finally find the optimal spectrum price $\boldsymbol{\mu}$ to maximize its revenue within its limited available spectrum. Every follower (i.e., UAV operator) will respond with the best amount of spectrum request (i.e., b_i) based on the price given by the leader. The optimization problems can be formulated as follows.

Leader's spectrum pricing:

$$\max_{\boldsymbol{\mu} \succcurlyeq 0} U_{MNO}(\boldsymbol{\mu}, \boldsymbol{b}), \tag{4.11}$$

$$\text{s.t.} \sum_{i=1}^{N} b_i \leq Q. \tag{4.12}$$

Follower's spectrum purchasing:

$$\max_{b_i \geq 0} U_i(b_i, \mu_i), \tag{4.13}$$

where $U_{MNO}(\boldsymbol{\mu}, \boldsymbol{b})$ and $U_i(b_i, \mu_i)$ are defined in (4.1) and (4.6), respectively.

The above problems together form a Stackelberg game. The objective is to find the Stackelberg Equilibrium point(s) from which neither the leader (MNO) nor the followers (UAV operators) have incentives to deviate. For the proposed Stackelberg game, the SE is defined as follows.

Definition 4.1 (Stackelberg Equilibrium). *Let $\boldsymbol{\mu}^*$ be a solution for the spectrum pricing problem and b_i^* be a solution for the spectrum purchasing problem of the ith UAV operator. Then the point $(\boldsymbol{\mu}^*, \boldsymbol{b}^*)$ is a SE for the proposed Stackelberg game if for any $(\boldsymbol{\mu}, \boldsymbol{b})$ with $\boldsymbol{\mu} \succcurlyeq 0$ and $\boldsymbol{b} \succcurlyeq 0$, the following conditions are satisfied:*

$$U_{MNO}(\boldsymbol{\mu}^*, \boldsymbol{b}^*) \geq U_{MNO}(\boldsymbol{\mu}, \boldsymbol{b}^*), \tag{4.14}$$

$$U_i(b_i^*, \boldsymbol{\mu}^*) \geq U_i(b_i, \boldsymbol{\mu}^*). \tag{4.15}$$

Note that the same or different prices can be charged to the UAV operators, which here are referred to as the *uniform and non-uniform* pricing schemes, respectively. In the following, we use the backward induction method to analyze the Stackelberg game under these two pricing schemes.

4.4.2 Non-Uniform Pricing Scheme

The non-uniform pricing scheme is firstly considered, in which the MNO can set different unit prices for leasing spectrum to different UAV operators. If the spectrum price for a UAV operator i is donated as μ_i, the optimal spectrum purchasing problem can be written as

$$\underline{\textit{Problem 4.1:}} \max_{b_i \geq 0} g_i \log_2 \left(1 + \frac{b_i}{d_i} \right) - \mu_i b_i. \tag{4.16}$$

It is observed that the objective function is a concave function over b_i, and the constraint is affine. Thus Problem 4.1 is a convex optimization problem. For a convex optimization problem, the optimal solution must satisfy the Karush-Kuhn-Tucker (KKT) conditions. Therefore, by solving the KKT conditions, the optimal solution for Problem 4.1 can be obtained in the following theorem.

Theorem 4.1. *For a given bandwidth price μ_i, the optimal solution for Problem 4.1 is given by*

$$b_i^* = \begin{cases} \frac{g_i}{\mu_i \ln 2} - d_i, & \text{if } \mu_i < \frac{g_i}{d_i \ln 2}, \\ 0, & \text{if } \mu_i \geq \frac{g_i}{d_i \ln 2}. \end{cases} \tag{4.17}$$

Proof. Please refer to Appendix B.1. ∎

From the Theorem 4.1, it is observed that if the bandwidth price is too high, i.e., $\mu_i \geq \frac{g_i}{d_i \ln 2}$, UAV operator i will not buy any bandwidth, which indicates that operator i will not participate in the game. Besides, under the same spectrum price, more bandwidth is allocated to the UAV operator with higher spectrum coins for the same demand type. Substituting (4.17) into MNO's optimal pricing strategies, i.e., combining (4.11) and (4.12), the optimization problem at the MNO side can be written as

$$\underline{\textit{Problem 4.2:}} \max_{\boldsymbol{\mu} \succcurlyeq 0} \sum_{i=1}^{N} \left(\frac{g_i}{\ln 2} - \mu_i d_i \right)^+, \tag{4.18}$$

$$\text{s.t.} \sum_{i=1}^{N} \left(\frac{g_i}{\mu_i \ln 2} - d_i \right)^+ \leq Q, \tag{4.19}$$

where $(\cdot)^+ \overset{\Delta}{=} \max(\cdot, 0)$. Note that the objection function is a convex function of $\boldsymbol{\mu}$, while the maximization of a convex function is generally non-convex which is difficult to solve. However, it is shown in the following that the above problem can be converted to a series of convex subproblems.

For UAV operator i ($i = 1, 2, \cdots, N$), we introduce the following indicator function

$$\chi_i = \begin{cases} 1, & \text{if } \mu_i < \frac{g_i}{d_i \ln 2}, \\ 0, & \text{otherwise.} \end{cases} \tag{4.20}$$

Then, the Problem 4.2 can be reformulated as

$$\underline{Problem\ 4.3:}\ \max_{\boldsymbol{\chi}, \boldsymbol{\mu} \succcurlyeq 0} \sum_{i=1}^{N} \chi_i \left(\frac{g_i}{\ln 2} - \mu_i d_i \right), \tag{4.21}$$

$$\text{s.t.} \sum_{i=1}^{N} \chi_i \left(\frac{g_i}{\mu_i \ln 2} - d_i \right) \leq Q, \tag{4.22}$$

$$\chi_i \in \{0, 1\}, \ \forall i, \tag{4.23}$$

where $\boldsymbol{\chi} \overset{\Delta}{=} [\chi_1, \chi_2, \cdots, \chi_N]^T$. It is observed that the above problem is still non-convex due to $\boldsymbol{\chi}$. Nevertheless, for a given indicator vector $\boldsymbol{\chi}$, it is easy to verify that Problem 4.3 is convex. Under this observation, we consider a special case of Problem 4.3 by assuming that the total available bandwidth of MNO is sufficient large (i.e., Q is large enough) such that all the requests from the UAV operators are admitted. As a result, the indicators for all UAV operators are equal to 1, i.e., $\mu_i < \frac{g_i}{d_i \ln 2}$, $\forall i$. Then, Problem 4.3 can be further converted to a minimization problem as

$$\underline{Problem\ 4.4:}\ \min_{\boldsymbol{\mu} \succcurlyeq 0} \sum_{i=1}^{N} \mu_i d_i, \tag{4.24}$$

$$\text{s.t.} \sum_{i=1}^{N} \frac{g_i}{\mu_i \ln 2} \leq Q + \sum_{i=1}^{N} d_i. \tag{4.25}$$

It is not difficult to see that the above objective function now becomes convex, and minimization of convex function is a convex optimization problem. The optimal solution is given by the following proposition.

Proposition 4.1. *The optimal solution to Problem 4.4 is given by*

$$\mu_i^* = \frac{1}{\ln 2} \sqrt{\frac{g_i}{d_i}} \frac{\sum_{i=1}^{N} \sqrt{g_i d_i}}{Q + \sum_{i=1}^{N} d_i}, \ \forall i \in \{1, 2, \cdots, N\}. \tag{4.26}$$

Proof. Please refer to Appendix B.2. ∎

The optimal solution of Problem 4.4 can be related to the original problem, i.e., Problem 4.2, in the following proposition.

Proposition 4.2. *The bandwidth prices given by (4.26) are the optimal solutions of Problem 4.2 if and only if the following condition holds:*

$$Q > \frac{\sum_{i=1}^{N} \sqrt{g_i d_i}}{\min_i \sqrt{\frac{g_i}{d_i}}} - \sum_{i=1}^{N} d_i. \tag{4.27}$$

Proof. Please refer to Appendix B.3. ∎

With the above results obtained from a number of subproblems, the original problem can now be addressed. The optimal solution of Problem 4.2 is given by the following theorem.

Theorem 4.2. *Assuming that all the UAV operators are sorted in the order $\frac{g_1}{d_1} > \frac{g_2}{d_2} \cdots \frac{g_{N-1}}{d_{N-1}} > \frac{g_N}{d_N}$, the optimal solution for Problem 4.2 can be expressed as*

$$\boldsymbol{\mu}^* = \begin{cases} \frac{q_N}{\ln 2} \left[\sqrt{\frac{g_1}{d_1}}, \sqrt{\frac{g_2}{d_2}}, \cdots, \sqrt{\frac{g_N}{d_N}} \right]^T, & \text{if } Q > Y_N \\ \frac{q_{N-1}}{\ln 2} \left[\sqrt{\frac{g_1}{d_1}}, \cdots, \sqrt{\frac{g_{N-1}}{d_{N-1}}}, \infty \right]^T, & \text{if } Y_N \geq Q > Y_{N-1} \\ \quad \vdots & \quad \vdots \\ \frac{q_1}{\ln 2} \left[\sqrt{\frac{g_1}{d_1}}, \infty, \cdots, \infty \right]^T, & \text{if } Y_2 \geq Q > Y_1 \end{cases}, \tag{4.28}$$

where $q_K = \frac{\sum_{i=1}^{K} \sqrt{g_i d_i}}{Q + \sum_{i=1}^{K} d_i}$, and $Y_K = \frac{\sum_{i=1}^{K} \sqrt{g_i d_i}}{\sqrt{\frac{g_K}{d_K}}} - \sum_{i=1}^{K} d_i, \forall K \in \{1, 2, \cdots, N\}$.

Proof. From the Proposition 4.2, it is observed that the UAV operators which cannot fulfill the condition (4.27), are removed from the game and the bandwidth price for these operators will be set to ∞. If $Q > Y_N$, the optimal bandwidth price for each UAV operator is already obtained by Proposition 4.2. For the other intervals of Q, e.g., $Y_{N-1} < Q \leq Y_N$, the proof of the optimality for the corresponding $\boldsymbol{\mu}^*$ can be obtained similarly as Proposition 4.2, and is thus omitted. The proof of Theorem 4.2 thus follows. ∎

Now, the Stackelberg game for the non-uniform pricing scheme is completely solved. With the optimal solutions obtained in Theorem 4.1 and Theorem 4.2, the SE for the proposed Stackelberg game is given as follows.

Theorem 4.3. *The SE for the Stackelberg game formulated in the Problems 4.1 and 4.2 is $(\boldsymbol{\mu}^*, \boldsymbol{b}^*)$, where $\boldsymbol{\mu}^*$ is given by (4.28), and $\boldsymbol{b}^*$ is given by (4.17).*

Algorithm 3 Non-uniform spectrum pricing and purchasing algorithm

---

Input: the number of UAV operators N, basic bandwidth demand d_i ($i \in \mathcal{N}$) for each UAV operator, total amount of available idle spectrum Q, and g_i;

Output: Non-uniform spectrum price vector $\boldsymbol{\mu}$ and bandwidth purchasing vector $\boldsymbol{b}$;

    Spectrum Pricing

1: Based on the spectrum blockchain network, an authorized miner acts as a trusted coordinator and local computation center, and sets $K = N$.

2: **for** $K = N \rightarrow 1$ **do**

3:     Sort the K operators such that $\frac{g_1}{d_1} \geq \cdots \geq \frac{g_{K-1}}{d_{K-1}} \geq \frac{g_K}{d_K}$.

4:     Compute $q_K = \frac{\sum_{i=1}^{K} \sqrt{g_i d_i}}{Q + \sum_{i=1}^{K} d_i}$ and compare q_K with $\sqrt{\frac{g_K}{d_K}}$.

5:     **if** $q_K > \sqrt{g_K/d_K}$ **then**

6:         Remove the operator K from the game, set $K = K - 1$, and go to step 4.

7:     **else**

8:         Go to step 9.

9:         With q_K and K, the spectrum price μ_i for operator i is given by

$$\mu_i = \begin{cases} \frac{q_K}{\ln 2} \sqrt{\frac{g_i}{d_i}}, & \text{if } i \leq K \\ \infty, & \text{otherwise.} \end{cases}$$

10:     **end if**

11: **end for**

12: A miner broadcasts the price vector to the UAV operators in the spectrum blockchain.

    Spectrum Purchasing

13: After receiving the spectrum prices, the UAV operators decide the amount of their spectrum request according to (4.17).

14: The miner collects the spectrum demand information from the UAV operators and provides feedback to the MNO.

15: The MNO finally leases the spectrum bandwidth to the UAV operators while the UAV operators transfer the corresponding spectrum coins to the MNO through the blockchain network with security and privacy protection.

In practice, the unique Stackelberg equilibrium can be achieved in a centralized manner as in [246]. However, it is observed from the Theorem 4.2 that, to obtain the optimal spectrum price vector $\boldsymbol{\mu}^*$, the MNO has to collect and measure the network state information to compute and compare $\sqrt{g_i/d_i}$ for each individual UAV operator i. This will lead to high computation complexity and communication overhead for the MNO and the UAV operators. Fortunately, owning to the distributed ledger benefit of blockchain, such information can be safely collected and processed by the edge computing nodes and then shared in the whole network. Moreover, based on the special structure of (4.28), to further relieve the burden,

we propose an optimal non-uniform pricing scheme for the MNO and the corresponding spectrum purchasing scheme for each UAV operator by Algorithm 3. Through leveraging the blockchain and exploiting miners acting as local coordinators and trusted computation center, an efficient implementation solution can be available.

4.4.3   Uniform Pricing Scheme

In this subsection, the uniform pricing scheme is considered, in which the MNO charges all the UAV operators the same unit price for their bandwidth requests, i.e., $\mu_i = \mu, \forall i$. With a uniform price μ, the optimal bandwidth request for UAV operators can be easily obtained from (4.17) by replacing μ_i with μ, which is given by the following theorem.

Theorem 4.4. *For a given uniform bandwidth price μ, the optimal bandwidth request solution for UAV operators is given by*

$$b_i^* = \begin{cases} \frac{g_i}{\mu \ln 2} - d_i, & \text{if } \mu < \frac{g_i}{d_i \ln 2}, \\ 0, & \text{if } \mu \geq \frac{g_i}{d_i \ln 2}. \end{cases} \tag{4.29}$$

Then, at the MNO's side, similar to Problem 4.2, the optimal pricing problem can be expressed as

$$\underline{Problem\ 4.5:}\ \max_{\mu > 0} \sum_{i=1}^{N} \left(\frac{g_i}{\ln 2} - \mu d_i \right)^+, \tag{4.30}$$

$$\text{s.t.} \sum_{i=1}^{N} \left(\frac{g_i}{\mu \ln 2} - d_i \right) \leq Q. \tag{4.31}$$

It is observed that Problem 4.5 has similar formation as Problem 4.2, and its solution can be found in the same way. Details are thus omitted here for brevity.

Theorem 4.5. *Assuming that all the UAV operators are sorted in the order $\frac{g_1}{d_1} > \frac{g_2}{d_2} \cdots \frac{g_{N-1}}{d_{N-1}} > \frac{g_N}{d_N}$, the optimal solution for Problem 4.5 is given by*

$$\mu^* = \begin{cases} \tilde{\mu}_N, & \text{if } Q > \tilde{Y}_N \\ \tilde{\mu}_{N-1}, & \text{if } \tilde{Y}_N \geq Q > \tilde{Y}_{N-1} \\ \vdots & \vdots \\ \tilde{\mu}_1, & \text{if } \tilde{Y}_2 \geq Q > \tilde{Y}_1 \end{cases}, \tag{4.32}$$

where $\tilde{\mu}_K = \frac{\sum_{i=1}^{K} g_i}{\left(Q + \sum_{i=1}^{K} d_i\right) \ln 2}$ and $\tilde{Y}_K = \frac{d_K \sum_{i=1}^{K} g_i}{g_K} - \sum_{i=1}^{K} d_i, \forall K \in \{1, 2, \cdots, N\}$.

Algorithm 4 Distributed spectrum price bargaining algorithm

- *Step 1:* The MNO sets the initial spectrum price μ, and sends the μ to a nearby miner in the blockchain network. The miner records the information and broadcasts the price to all the UAV operators.
- *Step 2:* Each UAV operator computes its optimal bandwidth request b_i^* based on (4.29) for the given μ, and gives responses back to the miner.
- *Step 3:* The miner records the feedback from the UAV operators and measures the total bandwidth requests $\sum_{i \in \mathcal{N}} b_i$, and then transmits the related data to the MNO. The MNO compares the total demand with its available spectrum Q. Assume that τ is a small positive constant that controls the algorithm accuracy, and $\Delta\mu > 0$ is a small step size.

if $\sum_{i \in \mathcal{N}} b_i > Q + \tau$ **then**
  The MNO increases the price by $\Delta\mu$;
else if $\sum_{i \in \mathcal{N}} b_i < Q - \tau$ **then**
  The MNO decreases the price by $\Delta\mu$;
end if
After that, the MNO sends the new spectrum price to the miner. Then, the miner updates the price and broadcasts it to UAV operators. The corresponding transactions are recorded and verified in the spectrum blockchain to guarantee the security.
- *Step 4:* Step 2 and Step 3 are repeated until $|\sum_{i \in \mathcal{N}} b_i - Q| \leq \tau$.

From Theorem 4.5, it is not difficult to observe that when the total available bandwidth margin Q is given, the optimal price strategy is unique. Thus, the Stackelberg equilibrium for this Stackelberg game is also unique and given as follows.

Theorem 4.6. *The Stackelberg equilibrium for the Stackelberg game formulated with the uniform pricing scheme is $(\mu^*, \boldsymbol{b}^*)$, where μ^* is given by (4.32), and $\boldsymbol{b}^*$ is given by (4.29).*

For the uniform pricing scheme, to obtain the Stackelberg equilibrium of the proposed Stackelberg game, some insights about the optimization problem are introduced at first. It can be observed from Problem 4.5 that both the objective function and the left hand side of the constraint condition (4.31) are monotonically decreasing functions of μ. Thus, when the constraint condition is satisfied with equality, the objective function can be maximized. Based on this fact, a distributed spectrum price bargaining algorithm is proposed in Algorithm 4 to implement the proposed game.

It can be seen that Algorithm 4 is a distributed algorithm which greatly reduces the amount of information that needs to be exchanged in the network, as compared to centralized approach. The convergence of the spectrum price bargaining algorithm is guaranteed by the following facts: (i) the optimal spectrum price is always obtained when the total idle

bandwidth of the MNO is fully allocated; (ii) the left hand side of (4.31) is a decreasing function of μ; and (iii) the SE for the proposed Stackelberg game is unique for a given Q.

4.5 Security Discussion and Numerical Results

In this section, a security assessment of our proposed spectrum blockchain is firstly given. After that, several numerical examples are provided to evaluate the performances of the spectrum trading strategies based on the approach of spectrum pricing.

4.5.1 Discussion of Security

Unlike traditional communication security and privacy protection, our proposed method can ensure spectrum trading security by leveraging consortium blockchain technology which can provide a defensive ability against many potential security attacks. More details about the security assessment for the spectrum blockchain are listed as follows.

- *Without reliance on a trusted intermediary*: In our spectrum blockchain, operators trade spectrum in a distributed manner, unlike conventional trading schemes that have to rely on a globally trusted center. This can efficiently solve the security threats caused by the centralized mechanisms such as single point of failure, privacy leakage, and denial of service attacks.

- *Privacy protection*: This feature is guaranteed by the fact that the trading information is sent in the encrypted format among the operators and the edge computing nodes. Without knowledge of the secret key of the sender, it is impossible to derive the original private message from the operators.

- *Wallet security*: As each operator has a unique wallet corresponding to its spectrum coin account, without authorized keys and certificates, no adversary can open an operator's wallet, stealing or distorting spectrum coins from the wallet.

- *Prevention of replay attack*: Each transaction is digitally signed with a unique identifier. Therefore, transactions with the same identifier will be rejected by the consensus servers (i.e., pre-selected edge computing nodes), and thus replay attacks are prevented.

- *Transaction authentication*: All transactions recorded in the blockchain have been publicly audited and authenticated by high-reputation authorized edge computing nodes. Moreover, each block has a unique and fixed hash value, which can be used to

protect the order and the information of blocks. Since modifying any contents of any block will cause a change to the hash values of the other blocks, it is impossible for an adversary to tamper or forge a transaction due to overwhelming cost.

- *Traceability*: When a dispute happens in the spectrum blockchain network, the TA will check one public ledger to find out the corresponding real identity of the illegal or misbehaved operator from the anonymous certificate *Cert* and registered *ID*, and revoke its public key. Thus, the traceability can be guaranteed.

4.5.2 Numerical Results
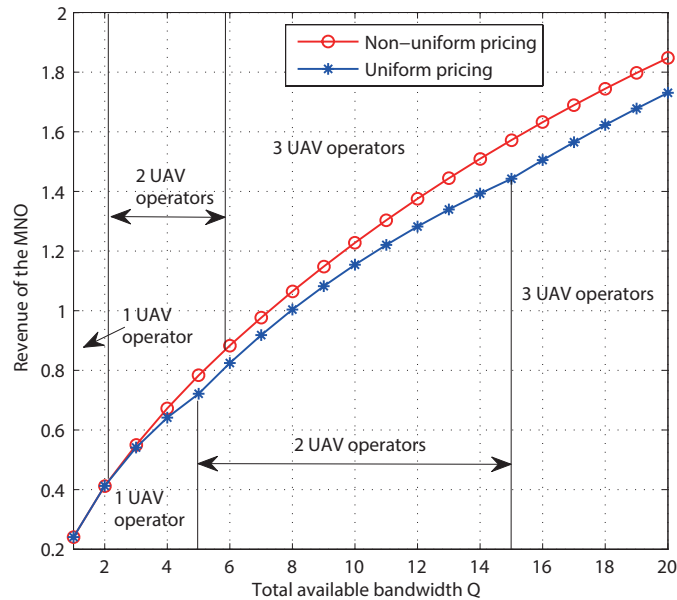
Fig. 4.3 Revenue of the MNO vs. Q.

In this subsection, the simulation results are presented to demonstrate the performances of the proposed pricing-based spectrum trading scheme. An air-ground spectrum sharing for UAV-assisted cellular network with one MNO and three UAV operators is considered. In order to illustrate the impact of spectrum coins and spectrum demands of UAV operators on the system performance, two different cases are investigated. In the first case (i.e., the first three examples), it is assumed that the spectrum coins of all the UAV operators are the same while their basic spectrum demands for serving users (i.e., application types) are different. Without loss of generality, the spectrum coins of all the UAV operators are assumed to be the same with $g_1 = g_2 = g_3 = 1$. The bandwidth demands of these UAV operators at the
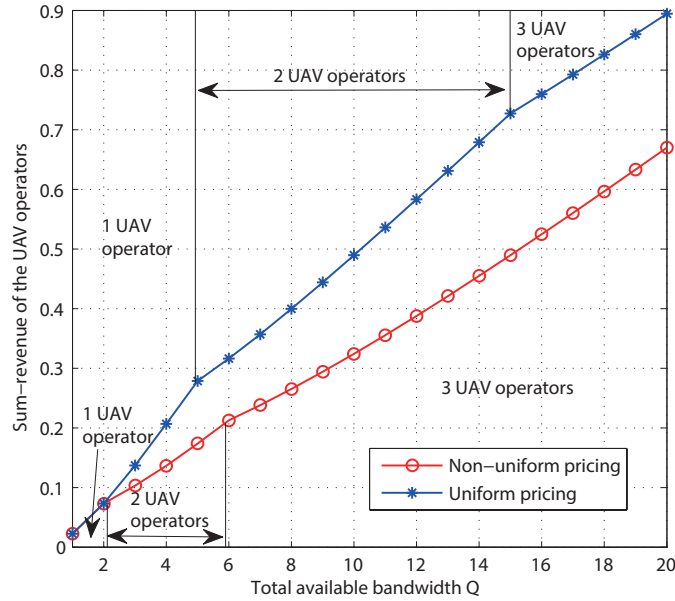
Fig. 4.4 Sum-revenue of the UAV operators vs. Q.

current time are different with $[d_1, d_2, d_3] = [5, 10, 15]$ units[2]. In the second case (i.e., the last example), the UAV operators have the same spectrum demands with different spectrum coins.

Example 1. *Uniform Pricing vs. Non-Uniform Pricing:* In this example, the performance comparison between the two schemes of uniform pricing and non-uniform pricing is examined. Fig. 4.3 and Fig. 4.4 show the MNO revenue and the sum-revenue of UAV operators, respectively, versus the total available bandwidth Q at the MNO, with uniform or non-uniform pricing. It is observed that for the same Q, the revenue of the MNO under the non-uniform pricing scheme is in general larger than that under the uniform pricing scheme, while the reverse is generally true for the sum-revenue of UAV operators. These observations indicate that, from the perspective of revenue maximization for the MNO, the non-uniform pricing is preferable compared to uniform pricing. On the other hand, the uniform pricing scheme is indeed optimal for the sum-revenue maximization of the UAV operators.

In addition, it is worth noting that when Q is sufficiently small, the revenues of the MNO become equal for the two pricing schemes, so are the sum-revenue of UAV operators. This is because when Q is very small, there is only one UAV operator active in the network, and thus by comparing (4.28) and (4.32), the non-uniform pricing scheme is the same as

---

[2]Since we consider spectrum trading purely from the data level, there is no specific unit for the bandwidth, which can be a general parameter.

90
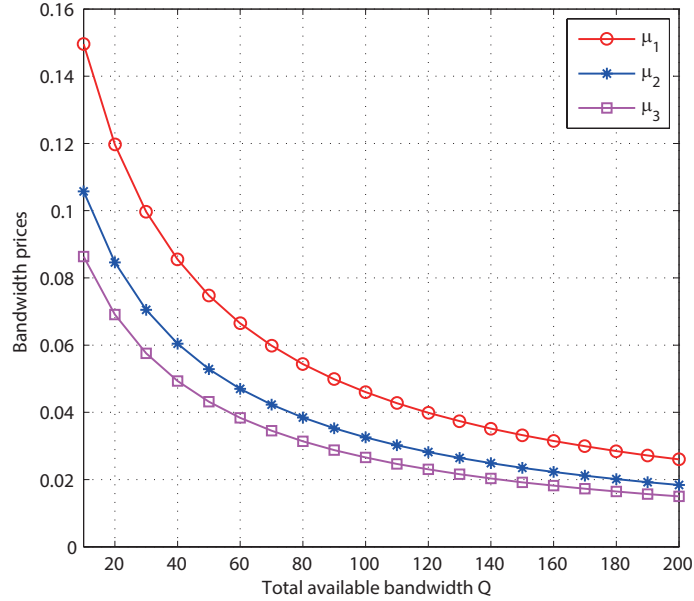
Fig. 4.5 Bandwidth prices vs. Q under non-uniform pricing.

the uniform pricing counterpart in the single-UAV operator case. Besides, it is expected that when Q is sufficiently large, the revenues of the MNO converge to the same value for the two pricing schemes. This can be explained as follows. For the non-uniform pricing scheme, it is observed from (4.28) that arbitrary spectrum price μ_i becomes very small with very large Q, and thus the objective function of Problem 4.2 converges to $\sum_{i=1}^{N} \frac{g_i}{\ln 2}$ as $Q \to \infty$. On the other hand, for the uniform pricing scheme, when Q approaches infinity, the revenue of the MNO will also converge to $\sum_{i=1}^{N} \frac{g_i}{\ln 2}$. Thus, there exists a same upper bound for the two different pricing schemes.

Example 2. *Comparison of Bandwidth Prices for UAV Operators under Non-Uniform Pricing:* In this example, we examine the optimal bandwidth prices for the UAV operators with the variation of Q under non-uniform pricing. First, it is observed from Fig. 4.5 that, for the same Q, the bandwidth price for UAV operator 1 is the highest, while that for UAV operator 3 is the lowest. This is true due to the fact that $\frac{g_1}{d_1} > \frac{g_2}{d_2} > \frac{g_3}{d_3}$, where a larger $\frac{g_i}{d_i}$ indicates that the corresponding UAV operator can achieve a higher profit with the same amount bandwidth allocated. Therefore, the operator with a larger $\frac{g_i}{d_i}$ has a willingness to pay a higher price to buy the spectrum. Secondly, it is observed that the differences between the bandwidth prices decrease with the increasing of Q. The reason is that when Q increases, it can be seen from (4.28) that $\frac{\sum_{i=1}^{N} \sqrt{g_i d_i}}{Q + \sum_{i=1}^{N} d_i}$ decreases. Last, it is observed that the prices for all UAV operators decrease with the increasing of Q, which can be easily inferred from (4.28).
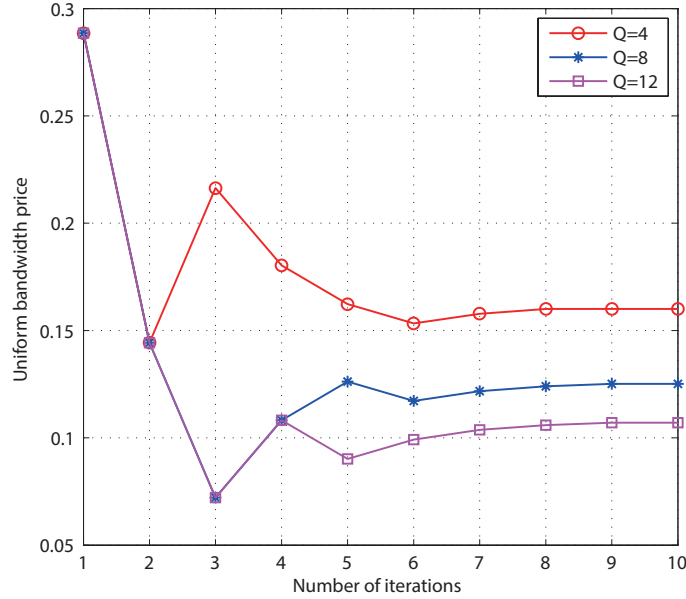
Fig. 4.6 Convergence performance of the distributed spectrum price bargaining algorithm.

Intuitively, this can be explained by the practical rule of thumb that if a seller has a large amount of goods to sell, it would like to price lower to stimulate consumption.

Example 3. *Convergence Performance of Distributed Bandwidth Price Bargaining Algorithm:* In this example, the convergence performance of the distributed bandwidth price bargaining algorithm (i.e., Algorithm 4) is investigated. Actually, the distributed bargaining algorithm can be implemented though the bisection method, for which the implementation procedure is given as follows. First, the MNO initializes a lower bound μ_L and an upper bound μ_H of the bandwidth price. Then, the MNO computes $\mu_M = (\mu_H + \mu_L)/2$ and sends the μ_M to a nearby miner (i.e., authorized edge computing node) through the blockchain network. The miner records the information and broadcasts it to all the UAV operators. After receiving μ_M, UAV operators compute their optimal bandwidth requests and give responses back to the miner. The miner measures the total bandwidth requests $\sum_{i \in \mathcal{N}} b_i$ and transmits the feedback information to the MNO. If $\sum_{i=1}^N b_i < Q$, the MNO sets $\mu_H = \mu_M$; otherwise, the MNO sets $\mu_L = \mu_M$. Then, μ_M is recomputed based on the new lower and upper bounds. The algorithm stops when $\left| \sum_{i=1}^N b_i - Q \right|$ is within the desired accuracy. It is observed from Fig. 4.6 that the distributed bargaining algorithm can converge within 9 iterations for all values of Q.

Example 4. *Relationship between Bandwidth Allocation and Available Idle Spectrum:* In this example, the spectrum demands of all the UAV operators are assumed to be the same
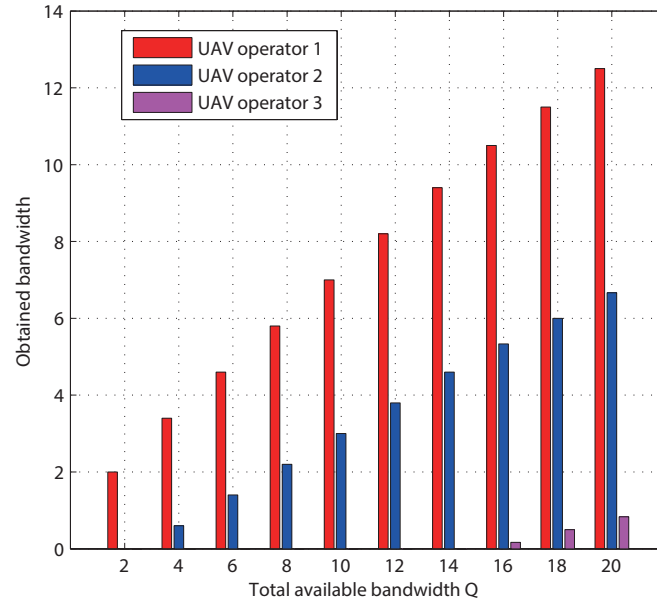
Fig. 4.7 Bandwidth allocation vs. Q.

with $d_1 = d_2 = d_3 = 5$ units while the spectrum coins are different with $[g_1, g_2, g_3] = [3, 2, 1]$. The bandwidth assignments for the three UAV operators with variation of Q are shown in Fig. 4.7. It is observed from Fig. 4.7 that the UAV operators with more spectrum coins have a higher priority in bandwidth obtainment. When the available bandwidth Q is small, the MNO will reject the request from the operators with low spectrum coins, and provide the limited resource to the operators with high spectrum coins. When the available bandwidth Q is large, the MNO will try to meet every operator's request. However, operators with more spectrum coins are given a higher priority in obtaining the bandwidth. It is also observed that with the increasing of Q, the bandwidth assigned for each operators increases. This is due to the fact that the MNO's utility is maximized only when it leases all its available idle spectrum to the UAV operators.

4.6 Conclusion

In this chapter, a consortium blockchain enabled secure spectrum trading framework is exploited for UAV-assisted cellular networks, where MNO and UAV operators are able to trade spectrum in a credible environment without relying on a trusted third party. Under this framework, a Stackelberg game model is adopted to jointly study the utility optimization for the MNO and UAV operators. Non-uniform spectrum pricing and uniform spectrum pricing

schemes are discussed. Additionally, a non-uniform pricing algorithm with low complexity and a distributed uniform pricing bargaining algorithm are respectively designed to obtain the optimal solutions under the two pricing schemes. A security assessment shows that our proposed spectrum blockchain improves transaction security and privacy protection. Numerical results illustrate that the pricing-based incentive mechanisms are effective and efficient for spectrum trading.

Chapter 5

Energy Efficiency Optimization for UAV-Assisted Emergency Communication Coverage with Wireless Laser Charging

5.1 Introduction

In Chapter 2, we introduced that UAVs could be deployed either as mobile user equipment to carry out delivery or surveillance tasks in the sky, or as aerial base stations to enhance the network capacity and expand the coverage for existing terrestrial networks. Then, resource allocation and spectrum trading for air-ground integrated networks from an aerial user's point of view and an operator's perspective were studied in Chapter 3 and Chapter 4, respectively. In this chapter, we will investigate the potential advantages of applying UAVs as *flying base stations* with flexible mobility. In fact, employing UAVs as aerial base stations is envisioned as a promising solution to enhance the performance of the existing cellular systems. For example, in case of a catastrophic event with terrestrial communications infrastructure failure caused by natural disasters, UAV-mounted base stations can temporarily support service recovery and local interim communication facilities for devices without infrastructure coverage. However, the feasibility and reliability of such applications still face some common and crucial challenges, especially for long-duration missions, due to the limited onboard battery and power supply availability of UAVs. In fact, the majority of the commercially available UAVs in the market can only stay in the air for less than several hours, which dramatically restricts the wide utilization of UAVs in large scale.

To overcome the aforementioned problem, many works in the literature focused on investigating energy-saving issues for UAV-assisted wireless communication systems. For instance, in [247], the authors proposed a low-complexity method based on the rotation transformation technique to maximize the flight time of UAV in an air-to-ground free space optical communication network. Zhang *et al.* [248] studied a computation offloading problem that aimed to minimize the total energy consumption for UAV-aided mobile edge computing system. Besides, an optimal UAV location deployment algorithm was designed in [249] to minimize the transmit power of the UAV while satisfying the rate requirements of all users. Moreover, Ghorbel *et al.* [250] further presented a joint position and travel path optimization scheme to reduce the energy consumption of the UAV for data gathering in wireless sensor networks. Despite these research efforts, the energy supply for the battery-powered UAVs is still fundamentally unsustainable in virtue of the finite battery capacity. In order to increase UAVs' flight time to complete some long time-consuming tasks, some researchers have also attempted to leverage energy harvesting for UAV networks, such as [251, 252]. Nevertheless, traditional wireless power transfer technologies are always restricted by short charging distances or low charging efficiency, resulting in that it is challenging to offer sufficient power over long distance for safely charging UAVs in the sky.

In this context, a novel technology to prolong mission duration is laser beaming [253]. This technology proves the ability to enable much longer UAV flight time and is currently being developed by a number of companies [254]. Implementing a high power laser device is proven to be possible using an appropriate power beaming system, in which an energy-rich laser array can be oriented through a complex optical system (set of mirrors or diamonds) and then shines on the target UAV. As compared to other wireless power transfer techniques enabled by radio frequency signals, the laser-beamed power transfer is able to deliver much larger energy amounts to the receivers with narrower energy beam divergence. It is regarded as an important technique for emergency responses, military operations, and also to accelerate the pace of implementing 5G-oriented UAV networks [255].

Motivated by the above observations, in this chapter, we study a laser-powered UAV wireless communication system, where a laser transmitter delivers laser energy to charge a UAV in flight, and the UAV uses the harvested energy from the laser power link to support its flight and downlink information transmission to multiple ground users in a disaster area. Our objective is to maximize the energy efficiency of the UAV in the system via jointly optimizing UAV's transmission power, flight trajectory as well as the user scheduling. However, such a joint trajectory and adaptive communication design problem is non-trivial to solve. This is because the user scheduling and association, UAV trajectory optimization, and trans-

mit power control are closely coupled with each other in our considered problem, which makes it challenging to solve in general.

To tackle the above challenges, we first relax the binary variables for user scheduling and association into continuous variables and solve the resulting problem with an efficient iterative algorithm by leveraging the block coordinate descent method. Specifically, the entire optimization variables are partitioned into three blocks for the user scheduling and association, UAV trajectory, and transmit power control, respectively. Then, these three blocks of variables are alternately optimized in each iteration, i.e., one block is optimized at each time while keeping the other two blocks fixed. However, even with fixed user scheduling and association, the UAV trajectory optimization problem with fixed power control and the UAV power control problem with fixed trajectory are still difficult to solve due to their non-convexity. We thus apply the successive convex optimization technique to solve them approximately. Numerical results show that energy efficiency gains are achieved by our proposed joint design, as compared to other benchmark schemes with heuristic UAV trajectories.

The main contributions of the chapter are summarized as follows.

- A general optimization framework for joint user scheduling, UAV power allocation and trajectory design in a UAV-assisted emergency communication system with laser charging is proposed.

- To address the formulated problem, the block coordinate descent method and the successive convex optimization technique are applied to divide the original problem into three subproblems to solve iteratively.

- Computer simulations are conducted to validate the effectiveness of the proposed scheme. Performance comparisons demonstrate that the proposed joint design algorithms are able to outperform baseline methods.

The rest of this chapter is organized as follows. Section 5.2 introduces the system model and the problem formulation for a UAV-enabled wireless network. In Section 5.3, we propose an efficient iterative algorithm by applying the block coordinate descent and the successive convex optimization techniques. Section 5.4 presents the numerical results to demonstrate the performance of the proposed design scheme. Finally, we conclude the chapter in Section 5.5.
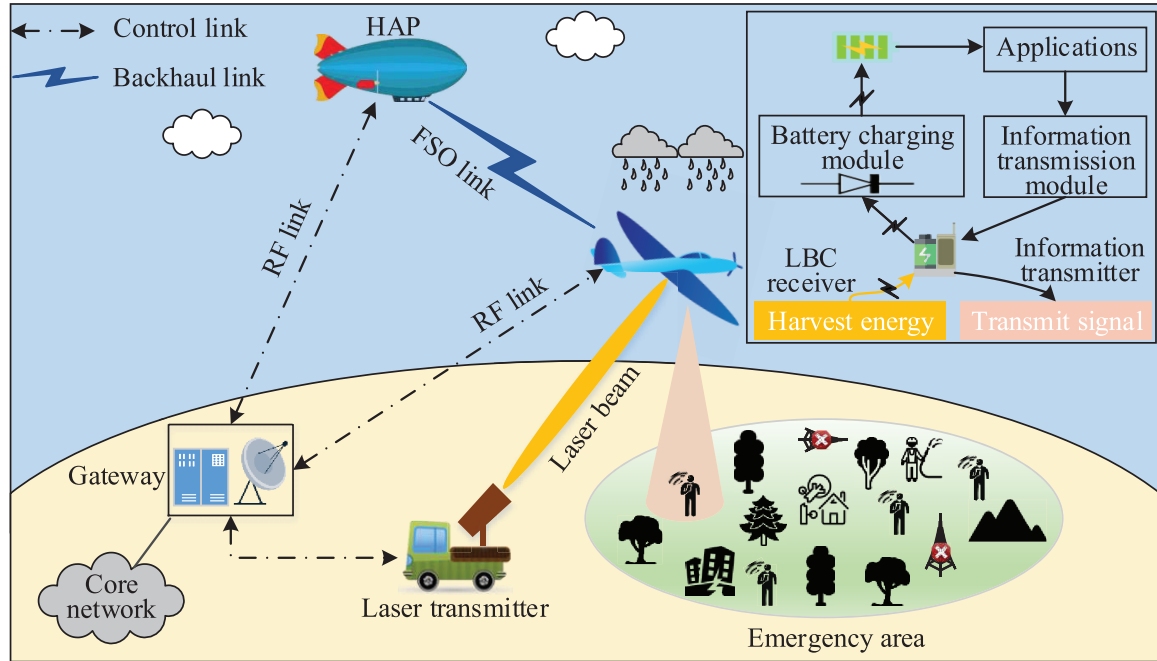
Fig. 5.1 UAV-assisted emergency communication coverage with laser charging.

5.2 System Model and Problem Formulation

5.2.1 System Model

As shown in Fig. 5.1, we consider a disaster area where terrestrial communication infrastructures have been destroyed due to some natural causes such as earthquake, flood, etc. The fast communication recovery is urgent for the mobile users to establish connection and send rescue massages to the outside world. In this case, a UAV mounted with a transceiver is swiftly dispatched as a flying base station to deliver emergency coverage in the area. Since most commercial UAVs are energy-constrained due to their limited power capacity of batteries, excessive power consumption for high-performance transmission will undoubtedly drain their batteries and further shorten the operation lifetime. To tackle such an issue, a laser transmitter carried by a lorry is exploited to charge the UAV through emitting laser beams. This can be practically implemented by installing two individual modules on the UAV, i.e., one laser beam charging (LBC) receiver which helps the UAV to harvest laser power from the laser transmitter, and one information transmitter enabling the UAV to serve the ground users. The backhaul connectivity and local geographical information can be supported by a HAP via FSO links [256]. The aerial platforms and ground laser transmitter are connected to the core network through the RF links.

A group of ground users are expressed as $\mathscr{K}$, where $|\mathscr{K}| = K$, with $|\cdot|$ denotes the cardinality. Without loss of generality, a 3D Cartesian coordinate system is considered where the laser transmitter is assumed to be located at the origin $(0,0,0)$, and the horizontal location of the kth user is $\mathbf{w}_k = [x_k, y_k]^T \in \mathbb{R}^{2 \times 1}$, $k \in \mathscr{K}$. We focus on a particular time period with finite duration $T > 0$, during which the UAV is deployed to fly horizontally at a constant altitude H from a given initial location to a final position and serves the ground users via periodic time-division multiple access (TDMA). In practice, H could correspond to the minimum altitude required for safe operation according to certain terrain. At any instant time $t \in [0, T]$, the time-varying coordinate of the UAV can be denoted by $[x(t), y(t), H]$, and the corresponding horizontal coordinate is express as $\mathbf{q}(t) = [x(t), y(t)]^T$. For ease of exposition, the period T is discretized into $N = |\mathscr{N}|$ equal-time slots, indexed by $n = 1, \dots, N$. The elemental time interval $\delta_t = T/N$ is chosen to be sufficiently small such that the UAV's location is considered as approximately unchanged within each time slot. Therefore, the UAV's trajectory $\mathbf{q}(t)$ can be approximated by the sequence $\mathbf{q}[n] = [x(n), y(n)]^T$, where $\mathbf{q}[n] \overset{\Delta}{=} \mathbf{q}(n\delta_t)$ denotes the UAV location at time slot n, with $n \in \mathscr{N}$. Then, the distance from the laser transmitter to the UAV at time slot n is denoted by

$$d_{lu}[n] = \sqrt{\|\mathbf{q}[n]\|^2 + H^2}. \tag{5.1}$$

Similarly, the distance between the UAV and user k can be expressed as

$$d_k[n] = \sqrt{\|\mathbf{q}[n] - \mathbf{w}_k\|^2 + H^2}. \tag{5.2}$$

Different from terrestrial communications, the air-to-ground channel is more likely to be dominated by LoS links. Thus, to illustrate the essential design insights, we adopt the LoS communication model for the UAV-to-ground/ground-to-UAV links. Furthermore, the Doppler effect that arises from the UAV's mobility is assumed to be well compensated. Then, the effective channel gain from user k to the UAV can be derived following the free space path loss model as

$$h_k[n] = \beta_0 d_k^{-2}[n] = \frac{\beta_0}{\|\mathbf{q}[n] - \mathbf{w}_k\|^2 + H^2}, \forall n \in \mathscr{N}, \tag{5.3}$$

where β_0 denotes the channel power gain at the reference distance $d_0 = 1$ m. Define a binary variable $\lambda_k[n]$ indicating the scheduling and association status of user k at time slot n. Specifically, the kth user is served in time slot n if $\lambda_k[n] = 1$, and otherwise $\lambda_k[n] = 0$. We assume that in each time slot, at most one user is served by the UAV, which can be expressed

as

$$\sum_{k=1}^{K} \lambda_k[n] \leq 1, \forall n \in \mathcal{N}. \tag{5.4}$$

Therefore, if user k is scheduled for communicating with the UAV at time slot n, the signal-to-noise ratio (SNR) at the user can be express as

$$\gamma_k[n] = \frac{p[n] h_k[n]}{\sigma^2} = \frac{p[n] \gamma_0}{\|\mathbf{q}[n] - \mathbf{w}_k\|^2 + H^2}, \tag{5.5}$$

where $p[n]$, σ^2 and $\gamma_0 = \beta_0 / \sigma^2$ denote the transmit power of UAV at time slot n, noise power and reference received SNR at 1 m, respectively. As a result, the aggregated communication throughput for user k is given by

$$R_k = \sum_{n=1}^{N} \lambda_k[n] \delta_t B \log_2(1 + \gamma_k[n]), \tag{5.6}$$

where B is the channel bandwidth.

The total power consumption of the UAV in general consists of two parts, i.e., communication related power and propulsion power. Note that the communication-related power consumption is usually much smaller than the UAV's propulsion power in practice, and is thus ignored here. As derived in [257], the propulsion power consumption model of a fixed-wing UAV can be approximately expressed as

$$P_c[n] = c_1 \|\mathbf{v}[n]\|^3 + \frac{c_2}{\|\mathbf{v}[n]\|} \left(1 + \frac{\|\mathbf{a}[n]\|^2}{g^2}\right), \tag{5.7}$$

where c_1 and c_2 aircraft design related parameters, g is the gravitational acceleration with value 9.8 m/s^2, and $\mathbf{v}[n]$ and $\mathbf{a}[n]$ are the velocity and acceleration of the UAV at time slot n, respectively. In addition, the relationship among $\mathbf{q}[n]$, $\mathbf{v}[n]$ and $\mathbf{a}[n]$ can be described as follows

$$\mathbf{v}[n+1] = \mathbf{v}[n] + \mathbf{a}[n] \delta_t, \forall n \in \mathcal{N}, \tag{5.8}$$

$$\mathbf{q}[n+1] = \mathbf{q}[n] + \mathbf{v}[n] \delta_t + \frac{1}{2}\mathbf{a}[n] \delta_t^2, \forall n \in \mathcal{N}. \tag{5.9}$$

Correspondingly, the total consumed energy of the UAV over period T is given by

$$E_c = \delta_t \sum_{n=1}^{N} \left(c_1 \|\mathbf{v}[n]\|^3 + \frac{c_2}{\|\mathbf{v}[n]\|} \left(1 + \frac{\|\mathbf{a}[n]\|^2}{g^2}\right) \right). \tag{5.10}$$

Next, we discuss the UAV's energy harvesting over the laser power link. Considering a linear energy harvesting model with a laser power harvesting efficiency $w \in (0,1)$, the amount of harvested laser energy at the UAV at slot n is represented by

$$
\begin{aligned}
P_h[n] &= \delta_t \frac{p_l w A}{(D + d_{lu}[n]\Delta\theta)^2} \chi e^{-\mu d_{lu}[n]} \\
&= \frac{\delta_t p_l w A \chi e^{-\mu\sqrt{\|\mathbf{q}[n]\|^2 + H^2}}}{\left(D + \sqrt{\|\mathbf{q}[n]\|^2 + H^2}\Delta\theta\right)^2},
\end{aligned}
\tag{5.11}
$$

where p_l is the transmit power of the laser transmitter, A is the area of the receiver telescope or collection lens, χ is the combined transmission receiver optical efficiency, μ is attenuation coefficient of the medium, D is the size of the initial laser beam, and $\Delta\theta$ is the the angular spread of the laser beam [258]. By letting $C = wA\chi$, the total harvested laser energy at the UAV over all N slots is expressed as

$$
E_h = \sum_{n=1}^{N} P_h[n] = \sum_{n=1}^{N} \frac{\delta_t p_l C e^{-\mu d_{lu}[n]}}{(D + d_{lu}[n]\Delta\theta)^2}.
\tag{5.12}
$$

To enable the UAV stay aloft for continuous operation during the task implementation period, the practical energy consumption of the UAV cannot exceed the amount of its harvested laser energy. Thus, the energy-causality constraint needs to be considered, as described in (5.13).

$$
\delta_t \sum_{n=1}^{N} \left(c_1 \|\mathbf{v}[n]\|^3 + \frac{c_2}{\|\mathbf{v}[n]\|} \left(1 + \frac{\|\mathbf{a}[n]\|^2}{g^2}\right) \right) \leq \sum_{n=1}^{N} \frac{\delta_t p_l w A \chi e^{-\mu\sqrt{\|\mathbf{q}[n]\|^2 + H^2}}}{\left(D + \sqrt{\|\mathbf{q}[n]\|^2 + H^2}\Delta\theta\right)^2}.
\tag{5.13}
$$

5.2.2 Problem Formulation

Our objective is to maximize the energy efficiency of the UAV for the emergency communication coverage period by optimizing UAV's trajectory $\{\mathbf{q}[n]\}$ (including UAV velocity $\{\mathbf{v}[n]\}$ and acceleration $\{\mathbf{a}[n]\}$) and transmit power $\{p[n]\}$, joint with transmission scheduling $\{\lambda_k[n]\}$, under the UAV operation energy-causality constraint with wireless laser charging. In addition, to guarantee the serving fairness, common throughput is taken into account, which is given by $\eta \triangleq \min_{k \in \mathcal{K}} R_k$. Then, the energy efficiency is defined as the ratio between the minimum information bits transmitted among the ground users and the total energy consumed at the UAV. For notational convenience, we define $\mathbf{\Lambda} \triangleq \{\lambda_k[n], \forall k, n\}$,

$\mathbf{P} \triangleq \{p[n], \forall n\}$, $\mathbf{Q} \triangleq \{\mathbf{q}[n], \forall n\}$, $\mathbf{V} \triangleq \{\mathbf{v}[n], \forall n\}$, and $\mathbf{A} \triangleq \{\mathbf{a}[n], \forall n\}$. Therefore, the energy efficiency maximization problem is formulated as

$$(P5.1): \max_{\mathbf{\Lambda},\mathbf{P},\mathbf{Q},\mathbf{V},\mathbf{A},\eta} \frac{\eta}{\sum_{n=1}^{N} \delta_t P_c[n]}$$

$$\text{s.t. } R_k \geq \eta, \forall k, \tag{5.14}$$

$$\lambda_k[n] \in \{0,1\}, \forall n, k, \tag{5.15}$$

$$\sum_{k=1}^{K} \lambda_k[n] \leq 1, \forall n, \tag{5.16}$$

$$E_c \leq \sum_{n=1}^{N} \frac{\delta_t p_l C e^{-\mu d_{lu}[n]}}{(D + d_{lu}[n]\Delta\theta)^2}, \tag{5.17}$$

$$\mathbf{v}[n+1] = \mathbf{v}[n] + \mathbf{a}[n]\delta_t, \forall n, \tag{5.18}$$

$$\mathbf{q}[n+1] = \mathbf{q}[n] + \mathbf{v}[n]\delta_t + \frac{1}{2}\mathbf{a}[n]\delta_t^2, \forall n, \tag{5.19}$$

$$\|\mathbf{v}[n]\| \leq v_{\max}, \forall n, \tag{5.20}$$

$$\|\mathbf{v}[n]\| \geq v_{\min}, \forall n, \tag{5.21}$$

$$\|\mathbf{a}[n]\| \leq a_{\max}, \forall n, \tag{5.22}$$

$$\mathbf{q}[0] = \mathbf{q}[n], \tag{5.23}$$

$$0 \leq p[n] \leq p_{\max}, \forall n. \tag{5.24}$$

Note that (5.15) and (5.16) are user scheduling constraints while (5.17) guarantees that the total consumed energy of the UAV should be no larger than the harvested laser energy. The UAV mobility is governed by the velocity and acceleration constraints as specified in (5.18)-(5.22). In addition, according to (5.23), the UAV is dispatched from the base at the first time slot, and flies back to the initial location at the end of the mission period. (5.24) represents the UAV's transmit power constraint.

Problem (P5.1) is challenging to solve due to the following reasons. First, the optimization variables $\mathbf{\Lambda}$ for user scheduling and association are binary and thus (5.15) and (5.16) involve integer constraints. Second, (P5.1) includes a complicated objective function, as well as non-convex constraints in (5.14), (5.17) and (5.21). Therefore, (P5.1) is a mixed-integer non-convex problem, which is difficult to be optimally solved in general.

5.3   Iterative Algorithm Design

As mentioned before, problem (P5.1) is a non-convex problem which cannot be directly solved with standard convex optimization techniques. To address this challenge, in this section, we first reformulate the original problem based on some observations, and then propose an overall iterative algorithm by dividing the optimization problem into several subproblems to obtain a locally optimal solution. Detailed scheme design is given as follows.

It is noted from the wireless laser charging model in (5.12) that μ is always a very small value with 10^{-6}m. Hence, the variations of E_h over the distance $d_{lu}[n]$ is dominated by $(D + d_{lu}[n]\Delta\theta)^{-2}$ in this case. Moreover, the angular spread $\Delta\theta$ is normally very small and the laser transmit power p_l is large, e.g., $\Delta\theta = 3.4 \times 10^{-5}$ and $p_l = 1$ kw [259]. Therefore, combining with the equation (5.12), we can observe that the harvested laser energy generally decreases much slower over the distance between the laser transmitter and the UAV. Based on this fact, the total laser energy received by the UAV during the mission period can be assumed with a upper bound E_{tot}, which means that the consumed energy at the UAV cannot exceed E_{tot}. In addition, to make problem (P5.1) more tractable, we relax the binary variables in (5.15) into continuous variables. Then, the original problem can be reformulated as

$$(P5.2): \max_{\mathbf{\Lambda},\mathbf{P},\mathbf{Q},\mathbf{V},\mathbf{A},\eta} \frac{\eta}{\sum_{n=1}^{N} \delta_t P_c[n]}$$

$$\text{s.t. } (5.14),(5.16),(5.18)-(5.24),$$

$$0 \leq \lambda_k[n] \leq 1, \forall n,k, \tag{5.25}$$

$$\delta_t \sum_{n=1}^{N} \left(c_1 \|\mathbf{v}[n]\|^3 + \frac{c_2}{\|\mathbf{v}[n]\|} \left(1 + \frac{\|\mathbf{a}[n]\|^2}{g^2} \right) \right) \leq E_{tot}. \tag{5.26}$$

However, although relaxed, problem (P5.2) is still non-convex and difficult to solve directly, due to the non-convex constraints in (5.14), (5.21) and (5.26) with coupled variables $\mathbf{\Lambda}$, $\mathbf{P}$ and $\mathbf{Q}$. In the following subsections, an efficient suboptimal solution to (P5.2) is proposed by applying block coordinate descent and successive convex optimization techniques [260]. The key idea is to decompose the problem into three subproblems and alternately optimize the subproblems within each iteration, namely, user scheduling optimization with fixed UAV transmit power and trajectory, and transmit power optimization with fixed user scheduling and UAV trajectory, as well as trajectory optimization with fixed user scheduling and UAV transmit power. Furthermore, we present an overall iterative algorithm to optimize the three sets of variables in an alternating manner until the objective value converges.

5.3.1 User Scheduling and Association Optimization

In this subsection, we consider the first subproblem for optimizing the user scheduling $\mathbf{\Lambda}$ with given UAV transmit power $\mathbf{P}$ and trajectory $\mathbf{Q}$ (including velocity $\mathbf{V}$ and acceleration $\mathbf{A}$). In this case, the energy consumption of the UAV is constant according to (5.10). Therefore, maximizing the energy efficiency can be converted to optimize the common throughput of the users, which is given by

$$(P5.3): \max_{\mathbf{\Lambda},\eta} \; \eta$$

$$\text{s.t.} \; \sum_{n=1}^{N} \lambda_k[n]\, \delta_t B \log_2\left(1+\gamma_k[n]\right) \geq \eta, \forall k, \tag{5.27}$$

$$\sum_{k=1}^{K} \lambda_k[n] \leq 1, \forall n, \tag{5.28}$$

$$0 \leq \lambda_k[n] \leq 1, \forall n, k. \tag{5.29}$$

Note that problem (P5.3) is a standard linear programming problem since the objective function as well as the constraints are linear. Therefore, (P5.3) can be solved efficiently by standard linear programming techniques within polynomial time.

5.3.2 Transmit Power Optimization

In this subsection, with any given user scheduling $\mathbf{\Lambda}$ and UAV trajectory $\mathbf{Q}$, the subproblem of (P5.2) to optimize the UAV transmit power $\mathbf{P}$ is considered, which can be written as

$$(P5.4): \max_{\mathbf{P},\eta} \; \eta$$

$$\text{s.t.} \; \sum_{n=1}^{N} \lambda_k[n]\, \delta_t B \log_2\left(1+\gamma_k[n]\right) \geq \eta, \forall k, \tag{5.30}$$

$$0 \leq p[n] \leq p_{\max}, \forall n. \tag{5.31}$$

It can be observed from (5.6) that R_k is a concave function with respect to $p[n]$, and then the left-hand side of constraint in (5.30) is also concave with regard to $p[n]$. Therefore, problem (P5.4) is a convex optimization problem, which can be solved efficiently by standard convex optimization techniques or tools such as CVX [261].

5.3.3 Trajectory Optimization

In this subsection, for any given user scheduling and association as well as UAV transmit power $\{\mathbf{\Lambda}, \mathbf{P}\}$, the UAV trajectory $\mathbf{Q}$ (including UAV velocity $\mathbf{V}$ and acceleration $\mathbf{A}$) of problem (P5.2) can be optimized by solving the following problem

$$(P5.5): \max_{\mathbf{Q},\mathbf{V},\mathbf{A},\eta} \quad \frac{\eta}{E_c}$$

$$\text{s.t.} \sum_{n=1}^{N} \lambda_k[n]\delta_t B\log_2\left(1+\gamma_k[n]\right) \geq \eta, \forall k, \tag{5.32}$$

$$\delta_t \sum_{n=1}^{N}\left(c_1\|\mathbf{v}[n]\|^3 + \frac{c_2}{\|\mathbf{v}[n]\|}\left(1+\frac{\|\mathbf{a}[n]\|^2}{g^2}\right)\right) \leq E_{tot}, \tag{5.33}$$

$$\|\mathbf{v}[n]\| \geq v_{\min}, \forall n, \tag{5.34}$$

$$\mathbf{v}[n+1] = \mathbf{v}[n] + \mathbf{a}[n]\delta_t, \forall n, \tag{5.35}$$

$$\mathbf{q}[n+1] = \mathbf{q}[n] + \mathbf{v}[n]\delta_t + \frac{1}{2}\mathbf{a}[n]\delta_t^2, \forall n, \tag{5.36}$$

$$\|\mathbf{v}[n]\| \leq v_{\max}, \forall n, \tag{5.37}$$

$$\|\mathbf{a}[n]\| \leq a_{\max}, \forall n, \tag{5.38}$$

$$\mathbf{q}[0] = \mathbf{q}[n]. \tag{5.39}$$

It is noted that problem (P5.5) is neither a convex nor quasi-convex problem due to the non-convex denominator in the objective function and the constraints in (5.32)-(5.34), which thus cannot be directly solved by standard convex optimization techniques. To deal with this issue, we first reformulate (P5.5) by introducing slack variables $\{\tau_n\}$ as

$$(P5.6): \max_{\mathbf{Q},\mathbf{V},\mathbf{A},\eta,\tau_n} \quad \frac{\eta}{\delta_t \sum\limits_{n=1}^{N}\left(c_1\|\mathbf{v}[n]\|^3 + \frac{c_2}{\tau_n} + \frac{c_2\|\mathbf{a}[n]\|^2}{g^2\tau_n}\right)}$$

$$\text{s.t. } (5.35) - (5.39),$$

$$\sum_{n=1}^{N}\lambda_k[n]\delta_t B\log_2\left(1+\gamma_k[n]\right) \geq \eta, \forall k, \tag{5.40}$$

$$\delta_t \sum_{n=1}^{N}\left(c_1\|\mathbf{v}[n]\|^3 + \frac{c_2}{\tau_n} + \frac{c_2\|\mathbf{a}[n]\|^2}{g^2\tau_n}\right) \leq E_{tot}, \tag{5.41}$$

$$\tau_n \geq v_{\min}, \forall n, \tag{5.42}$$

$$\|\mathbf{v}[n]\|^2 \geq \tau_n^2, \forall n. \tag{5.43}$$

Theorem 5.1. *Problem (P5.5) is equivalent to problem (P5.6).*

Proof. It can be observed that without loss of optimality to problem (P5.6), we always have $\tau_n = \|\mathbf{v}[n]\|$ in (5.43). Otherwise, τ_n can be increased with other variables fixed to obtain another feasible solution without changing the objective value of (P5.6). Therefore, there always exists an optimal solution to (P5.6) such that all constraints in (5.43) are satisfied with equality. As a result, problem (P5.5) is equivalent to problem (P5.6), which concludes the proof. ∎

With such a reformulation, the denominator of the objective function in (P5.6) and left-hand side of constraint in (5.41) are now jointly convex with respect to $\mathbf{V}$, $\mathbf{A}$ and $\{\tau_n\}$, whereas introducing a new non-convex constraint in (5.43). Fortunately, it is known that any convex function is globally lower-bounded by its first-order Taylor expansion at any point. Therefore, to tackle the new non-convex constraint, the successive convex optimization technique can be applied to obtain a local optimal solution through approximating the original function by a more tractable function at a given local point in each iteration. Specifically, since the left-hand side of (5.43) is convex and differentiable with respect to $\mathbf{v}[n]$, for any local point $\mathbf{v}_j[n]$ obtained at the jth iteration, we have

$$
\begin{aligned}
\|\mathbf{v}[n]\|^2 &\geq \|\mathbf{v}_j[n]\|^2 + 2\mathbf{v}_j^T[n]\left(\mathbf{v}[n] - \mathbf{v}_j[n]\right) \\
&\overset{\Delta}{=} \psi_{lb}\left(\mathbf{v}[n]\right), \forall n,
\end{aligned}
\tag{5.44}
$$

where the equality holds at the point $\mathbf{v}[n] = \mathbf{v}_j[n]$. It is worth mentioning that both the function $\|\mathbf{v}[n]\|^2$ and its lower bound $\psi_{lb}\left(\mathbf{v}[n]\right)$ have the identical gradient at the local point $\mathbf{v}_j[n]$, which is equal to $2\mathbf{v}_j[n]$. Furthermore, note that $\psi_{lb}\left(\mathbf{v}[n]\right)$ is a linear function with respect to $\mathbf{v}[n]$, and thus convex. Therefore, the constraint (5.43) can be replaced by the following new convex constraint

$$
\psi_{lb}\left(\mathbf{v}[n]\right) \geq \tau_n^2, \forall n.
\tag{5.45}
$$

Similarly, to tackle the non-convex constraint in (5.40), for any given local point $\{\mathbf{q}_j[n]\}$ obtained at the jth iteration, we define the function

$$
\begin{aligned}
R_k^{lb} = \sum_{n=1}^{N} \lambda_k[n]\,\delta_t B \times \\
\left(\alpha_k^j[n] - \beta_k^j[n]\left(\|\mathbf{q}[n] - \mathbf{w}_k\|^2 - \|\mathbf{q}_j[n] - \mathbf{w}_k\|^2\right)\right),
\end{aligned}
\tag{5.46}
$$

where

$$\alpha_k^j[n] = \log_2\left(1 + \frac{p[n]\gamma_0}{H^2 + \left\|\mathbf{q}_j[n] - \mathbf{w}_k\right\|^2}\right), \tag{5.47}$$

$$\beta_k^j[n] =$$

$$\frac{p[n]\gamma_0\log_2 e}{\left(H^2 + \left\|\mathbf{q}_j[n] - \mathbf{w}_k\right\|^2\right)\left(H^2 + \left\|\mathbf{q}_j[n] - \mathbf{w}_k\right\|^2 + p[n]\gamma_0\right)}. \tag{5.48}$$

Note that R_k^{lb} is a concave function with respect to $\{\mathbf{q}[n]\}$. Furthermore, the following theorem can be obtained.

Theorem 5.2. *For any given local point $\left\{\mathbf{q}_j[n]\right\}$, we have*

$$R_k = \delta_t B \sum_{n=1}^{N} \lambda_k[n] \log_2\left(1 + \frac{p[n]\gamma_0}{\left\|\mathbf{q}[n] - \mathbf{w}_k\right\|^2 + H^2}\right)$$

$$\geq R_k^{lb}, \forall k, \tag{5.49}$$

where the equality holds at the point $\mathbf{q}[n] = \mathbf{q}_j[n]$, $\forall n$.

Proof. Please refer to Appendix C.1. ∎

As a result, with any given local points $\left\{\mathbf{q}_j[n], \mathbf{v}_j[n]\right\}$ as well as the lower bounds in (5.44) and (5.49), problem (P5.6) is approximated as the following problem

$$(P5.7): \max_{\mathbf{Q}, \mathbf{V}, \mathbf{A}, \eta, \tau_n} \frac{\eta}{\delta_t \sum_{n=1}^{N}\left(c_1\|\mathbf{v}[n]\|^3 + \frac{c_2}{\tau_n} + \frac{c_2\|\mathbf{a}[n]\|^2}{g^2\tau_n}\right)}$$

$$\text{s.t. } (5.35) - (5.39),$$

$$R_k^{lb} \geq \eta, \tag{5.50}$$

$$\delta_t \sum_{n=1}^{N}\left(c_1\|\mathbf{v}[n]\|^3 + \frac{c_2}{\tau_n} + \frac{c_2\|\mathbf{a}[n]\|^2}{g^2\tau_n}\right) \leq E_{tot}, \tag{5.51}$$

$$\tau_n \geq v_{\min}, \forall n, \tag{5.52}$$

$$\psi_{lb}(\mathbf{v}[n]) \geq \tau_n^2, \forall n. \tag{5.53}$$

It can be seen that problem (P5.7) is a fractional optimization problem with convex denominator and constraints, wherein Dinkelbach method [262] can be employed to solve it. For the analytic simplicity, we define $\mathscr{F}$ as the set of feasible points of optimization problem in (P5.7), and $\tilde{E}_{total} = \delta_t \sum_{n=1}^{N}\left(c_1\|\mathbf{v}[n]\|^3 + \frac{c_2}{\tau_n} + \frac{c_2\|\mathbf{a}[n]\|^2}{g^2\tau_n}\right)$. Without loss of generality, by

defining ζ^* as the maximum energy efficiency of the system, we have

$$\zeta^* = \max_{\mathbf{Q},\mathbf{V},\mathbf{A},\eta,\tau_n} \frac{\eta}{\tilde{E}_{total}}. \tag{5.54}$$

Then, we have the following theorem.

Theorem 5.3. *The optimal solutions of problem (P5.7) achieve the maximum energy efficiency ζ^* if and only if*

$$\max_{\mathbf{Q},\mathbf{V},\mathbf{A},\eta,\tau_n} \eta - \zeta^* \tilde{E}_{total} = 0. \tag{5.55}$$

Proof. Please refer to Appendix C.2. ∎

Theorem 5.3 reveals that for an optimization problem with an objective function in fractional form, there exists an equivalent objective function in subtractive form, e.g., $\eta - \zeta^* \tilde{E}_{total}$ in the considered case. As a result, we can rewrite the problem (P5.7) as

$$(P5.8): \max_{\mathbf{Q},\mathbf{V},\mathbf{A},\eta,\tau_n} \eta - \zeta \tilde{E}_{total}$$
$$\text{s.t. } (5.35) - (5.39),$$
$$R_k^{lb} \geq \eta,$$
$$\delta_t \sum_{n=1}^{N} \left(c_1 \|\mathbf{v}[n]\|^3 + \frac{c_2}{\tau_n} + \frac{c_2 \|\mathbf{a}[n]\|^2}{g^2 \tau_n} \right) \leq E_{tot},$$
$$\tau_n \geq v_{\min}, \forall n,$$
$$\psi_{lb}(\mathbf{v}[n]) \geq \tau_n^2, \forall n.$$

Finally, an efficient algorithm based on Dinkelbach method is proposed for solving problem (P5.8), which is summarized in Algorithm 5. The convergence of Algorithm 5 is verified by the following theorem.

Theorem 5.4. *The convergence of Algorithm 5 based on Dinkelbach method is always guaranteed with local optimality.*

Proof. Please refer to Appendix C.3. ∎

Thus, the problem (P5.7) can be optimally solved by using Algorithm 5, and problem (P5.5) can be approximately solved by successively updating the UAV trajectory based on the optimal solution to problem (P5.7). The details are summarized in Algorithm 6.

Algorithm 5 Dinkelbach Method for Solving Problem (P5.8)

1: Initialize the maximum number of iterations $L_{\max}$ and the maximum tolerance ε.
2: Set maximum energy efficiency $\zeta = 0$ and iteration index $t = 0$.
3: **repeat**
4:     Solve problem (P5.8) with a given ζ and obtain optimal solutions $\{\mathbf{Q}^*, \mathbf{V}^*, \mathbf{A}^*, \eta^*, \tau_n^*\}$.
5:     **if** $\eta^* - \zeta \leq \varepsilon$ **then**
6:         Convergence = **true**.
7:         **return** $\{\mathbf{Q}^*, \mathbf{V}^*, \mathbf{A}^*, \eta^*, \tau_n^*\}$ and $\zeta^* = \frac{\eta^*}{\bar{E}_{total}^*}$.
8:     **else**
9:         Set $\zeta^* = \frac{\eta}{\bar{E}_{total}}$ and $t = t + 1$.
10:        $\zeta = \zeta^*$.
11:        Convergence = **false**.
12:     **end if**
13: **until** Convergence = **false** or $t = L_{\max}$.

Algorithm 6 Successive Optimization Algorithm for (P5.5)

1: Initialize $\mathbf{q}_0[n]$, $\mathbf{v}_0[n]$, $\forall n$. Let $j = 0$.
2: **repeat**
3:     Solve the convex problem (P5.7) for the given local points $\{\mathbf{q}_j[n], \mathbf{v}_j[n]\}$, and denote the optimal solution as $\{\mathbf{q}_j^*[n], \mathbf{v}_j^*[n]\}$.
4:     Update the local points $\mathbf{q}_{j+1}[n] = \mathbf{q}_j^*[n]$ and $\mathbf{v}_{j+1}[n] = \mathbf{v}_j^*[n]$, $\forall n$.
5: **until** the objective value of (P5.7) converges within a prescribed accuracy.

5.3.4 Overall Iterative Algorithm

Based on the results presented in the previous three subsections, we propose an overall iterative algorithm for the joint optimization problem (P5.2) by applying the block coordinate descent method, which is summarized in Algorithm 7.

Specifically, the entire optimization variables in original problem (P5.2) are divided into three blocks, i.e., $\{\mathbf{\Lambda}, \mathbf{P}, \mathbf{Q}\}$. Then, the user scheduling and association $\mathbf{\Lambda}$, UAV transmit power $\mathbf{P}$ and trajectory $\mathbf{Q}$ are alternately optimized, via solving problem (P5.3), (P5.4) and (P5.7) correspondingly, while keeping the other two blocks of variables fixed. Moreover, the obtained results in each iteration is utilized as the input variables of the next iteration. It is worth pointing that for each iteration only convex optimization problems need to be solved, thus the worst-case computational complexity of the proposed Algorithm 7 is polynomial, which is affordable for the UAV-enabled communication networks.

Algorithm 7 The Overall Iterative Optimization Algorithm for Problem (P5.2)

Input: the initial power allocation scheme, the initial UAV trajectory, and the tolerance error ε.

Output: the optimal solution of problem (P5.2).

1: **Initialize:** the iteration index $j = 0$, the initial UAV transmit power $\mathbf{P}_0$, and the initial UAV trajectory $\mathbf{Q}_0$;

2: **repeat**

3:     for given $\mathbf{Q}_j$ and $\mathbf{P}_j$, solve the problem (P5.3) to obtain the optimal solution denoted as $\mathbf{\Lambda}_{j+1}$;

4:     for given $\mathbf{\Lambda}_{j+1}$ and $\mathbf{Q}_j$, solve the problem (P5.4) to obtain the optimal solution denoted as $\mathbf{P}_{j+1}$;

5:     for given $\mathbf{\Lambda}_{j+1}$ and $\mathbf{P}_{j+1}$, solve problem (P5.7) to obtain the optimal solution denoted as $\mathbf{Q}_{j+1}$;

6:     update $j = j + 1$.

7: **until** the fractional increase of objective value is below a threshold $\varepsilon > 0$.

8: **return** the optimal user scheduling scheme $\mathbf{\Lambda}^{opt}$, the optimal transmit power $\mathbf{P}^{opt}$, and the optimal UAV trajectory $\mathbf{Q}^{opt}$.

5.4 Simulation Results

In this section, numerical examples are provided to demonstrate the effectiveness of the proposed method. We consider a system with $K = 5$ ground users that are randomly distributed in a square area of side length 3000m. The flight altitude of the UAV is $H = 100$m with the maximum speed $V_{\max} = 50$m/s, minimum speed $V_{\min} = 3$m/s and maximum acceleration $a_{\max} = 3$m/s^2. The maximum transmit power of the UAV is assumed to be $p_{\max} = 0.1$W, and the total available bandwidth is $B = 1$MHz. The reference channel power at a reference distance $d_0 = 1$m is $\beta_0 = -60$dB and the noise power is $\sigma^2 = -110$dBm. For the UAV's propulsion power consumption model, the constants c_1 and c_2 are set as $c_1 = 9.26 \times 10^{-4}$ and $c_2 = 2250$.

We first show the UAV trajectory and user scheduling with the proposed joint optimization scheme. Then, performance comparisons between the proposed scheme and some benchmark methods are given.

5.4.1 UAV Trajectory and User Scheduling

In Fig. 5.2, we illustrate the optimized trajectories obtained by the proposed Algorithm 6 under different periods T. It is observed that as T increases, the UAV exploits its mobility to adaptively enlarge and adjust its trajectory to move closer to the ground users. In particular, when the given period is big, i.e., $T = 280$s, the UAV will approach each user to maximize
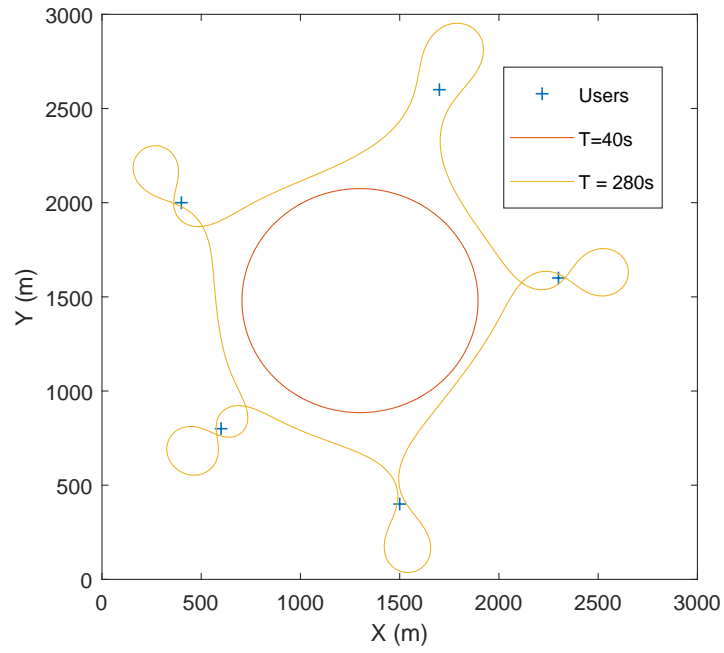
Fig. 5.2 Optimized UAV trajectory.
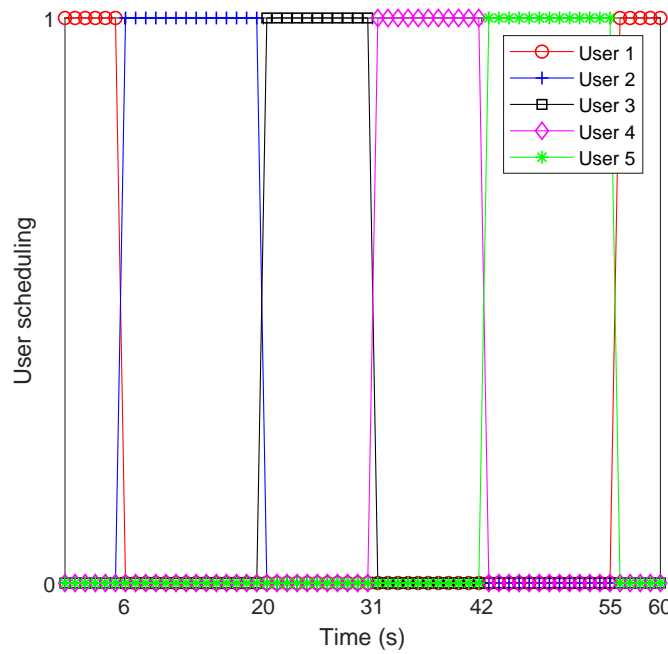
Fig. 5.3 User scheduling.

the throughput and follow an '8' shape path above each user, which is energy-efficient for

111
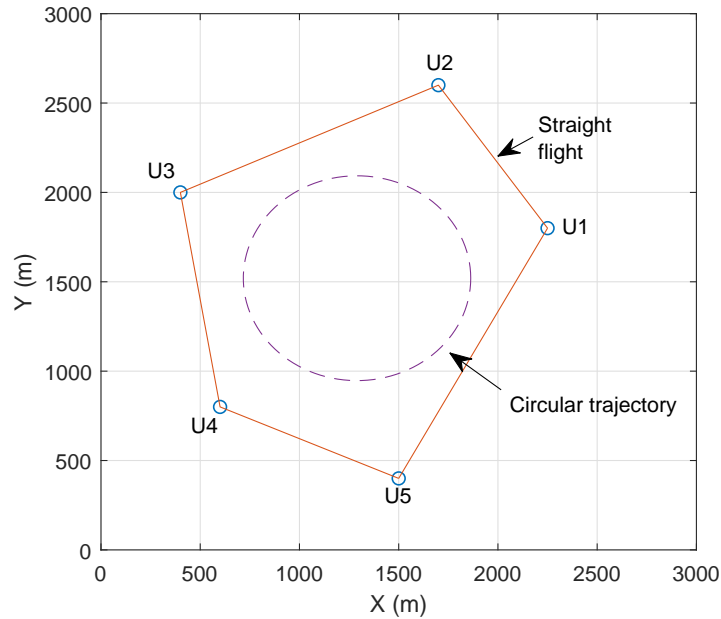
Fig. 5.4 Benchmark UAV trajectories.

fixed-wing UAVs while maintaining good communication channel with the corresponding user being served.

Fig. 5.3 reflects the transmission scheduling among all users with $T = 60$s. It is observed in Fig. 5.3 that the UAV transmits data to only one user at each time slot, and the user is scheduled when the UAV moves closer to the corresponding user.

5.4.2 Performance Comparison

To show the superiority of our proposed scheme in terms of energy efficiency, we consider the following methods:

- **Optimized energy efficiency maximization scheme:** This is our proposed scheme obtained from Algorithm 7 by jointly optimizing the user scheduling, UAV transmission power and trajectory.

- **Circular trajectory scheme:** For this scheme, the UAV flies with a circular path (initial trajectory). The energy efficiency of UAV is obtained by jointly optimizing the UAV transmission power and user scheduling.

- **Straight flight trajectory scheme:** For this scheme, the UAV flies to each user in a straight way with a constant speed.
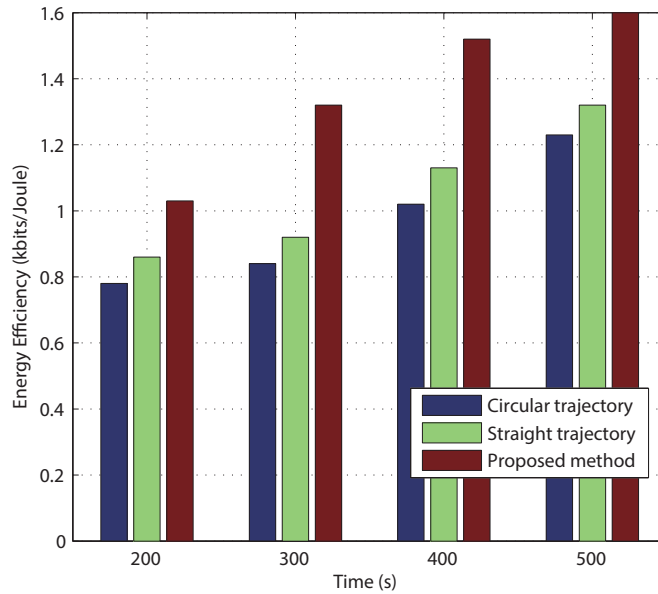
Fig. 5.5 Energy efficiency comparison.

The benchmark trajectories are show in Fig. 5.4. It is observed from Fig. 5.5 that the system energy efficiency for the three schemes increases as the period T grows. This is due to the fact that the UAV can allocate more time to serve the users when T increases. In addition, we can see that our proposed scheme achieves higher energy efficiency as compared with the benchmark methods which demonstrate the superiority of our proposed scheme.

5.5 Conclusion

In this chapter, we study UAV-assisted wireless communication, where a UAV is dispatched serving as an aerial base station to provide emergency communication coverage for multiple ground users in a disaster area. To address the issue of limited flight time of the short-endurance UAV caused by the onboard battery constraint, a laser transmitter is exploited into the system to supply sustainable energy through emitting laser beams to charge the UAV. Under such a laser power-enabled scenario, we maximize the energy efficiency of the UAV by optimizing the multiuser communication scheduling and association jointly with the UAV's power allocation strategy and flight trajectory. The formulated optimization problem is a mixed integer nonlinear problem that is challenging to solve. As such, an iterative algorithm is proposed to obtain a desirable solution which decomposes the original problem into several tractable subproblems by applying the block coordinate decent and

113

successive convex approximation techniques. Specifically, the user scheduling and association, UAV trajectory, and transmit power are alternately optimized within each iteration. Simulation results demonstrate the performance gains of the proposed method as compared to other benchmark schemes.

Chapter 6

Conclusions and Future Work

In this chapter, the main contributions of this thesis are summarized, and some future research directions are also presented.

6.1   Conclusions

This thesis concentrated on the radio resource management for UAV-assisted wireless communications and networking, and aimed to solve the challenges and constraints accompanied with the use of aerial platforms in wireless communication networks. To be brief, the following four aspects have been investigated in this thesis: 1) To fully reap the benefits of diversity of UAVs and address the constraint of network heterogeneity considering the massive devices from aerial and terrestrial layers, a SDN-enabled air-ground heterogeneous network architecture was firstly introduced; 2)To achieve reliable transmission connection of aerial user equipment in performing data sensing and communication task and address the constraint of link disconnection due to UAVs' high mobility, a robust resource allocation scheme was secondly designed; 3) To motivate the spectrum sharing between cellular and UAV operators and address the constraint of privacy and security threat in virtue of UAVs' dynamic transmission environment, a blockchain-based secure spectrum trading method was thirdly proposed; 4) To prolong UAVs' flight time as flying base station for delivering coverage in a disaster area and address the constraint of low endurance because of the limited onboard battery capacity, a laser charging-aided emergency communication system was fourthly presented. A summary of the research topics of this thesis is shown in Fig. 6.1.

Specifically, the main contributions and insights of this thesis are summarized as follows.

In Chapter 2, we proposed a HAP-LAP-ground integrated system architecture, which was envisioned to be deployed as a complementary solution to the terrestrial networks to offer coverage extension and capacity enhancement. In particular, a comprehensive survey on
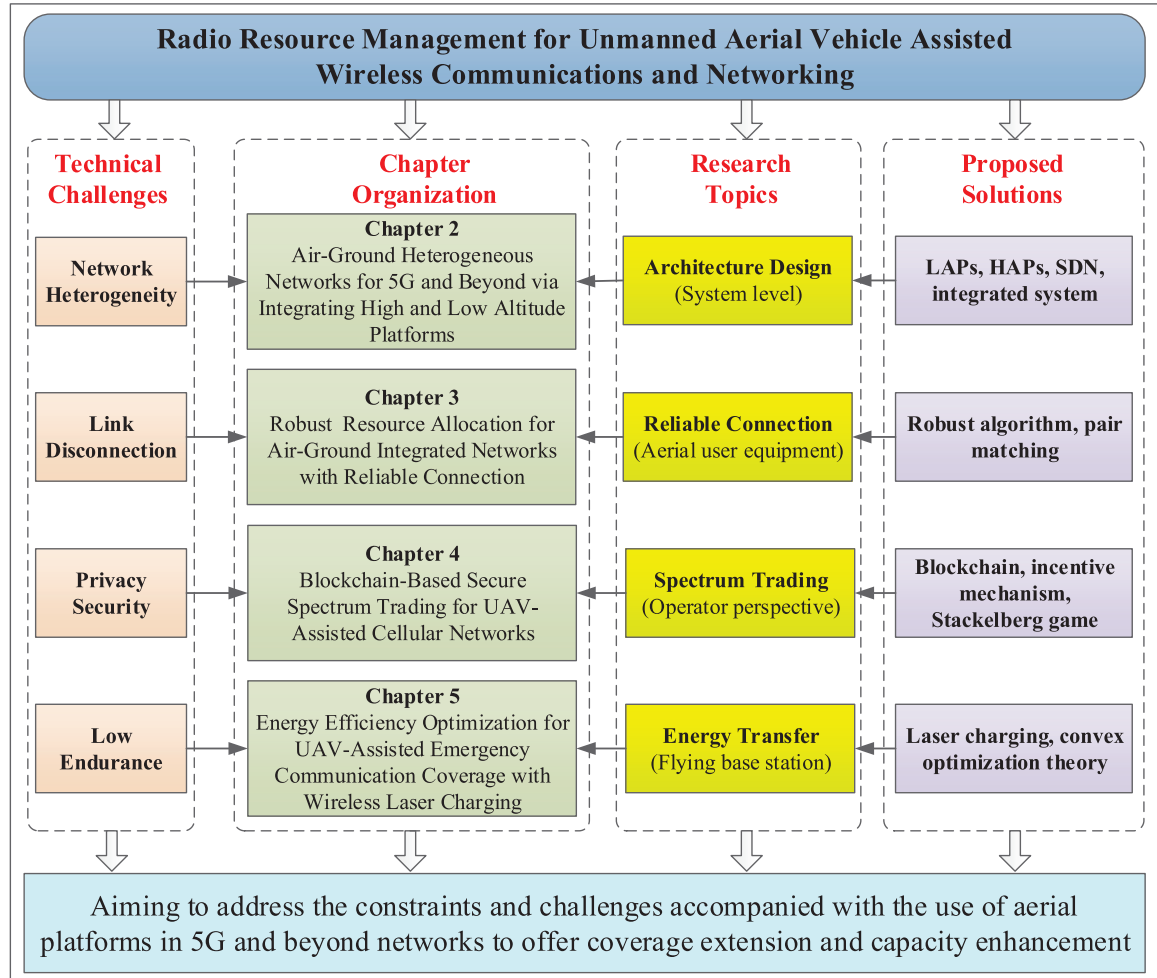
Fig. 6.1 A summary of the research topics in this thesis.

the HAP-based and LAP-based communication networks have been presented with detailed discussions about their types, advantages, applications and constraints for communication services. In order to exploit the advantages of different types of UAVs, an air-ground heterogeneous network architecture coordinated by SDN was proposed which integrated both HAPs and LAPs into terrestrial networks. Such an integrated system was capable of delivering a diverse connection, achieving ubiquitous coverage and seamless access for users in a real sense. The key enabling technologies for the system have been also discussed followed by a case study showing that the proposed multi-tier aerial network system can achieve higher capacity compared with traditional single-tier network architecture. To the best of the authors' knowledge, this is the first work that systematically introduces how HAPs and LAPs can be simultaneously employed into current terrestrial cellular networks to enhance the Internet access for the underserved scenarios and hard-to-reach areas.

In Chapter 3, we designed a robust resource allocation scheme to guarantee the reliable transmission connection for UAV-to-UAV links, in which UAVs served as aerial user equipment to perform data sensing task. In particular, a cellular network deployment scenario where U2U transmit-receive pairs share the same spectrum with the uplink U2I communication links was studied. Considering the different QoS requirements of different UAV connections, i.e., high capacity for U2I links while ultra reliability for U2U links, a power and channel allocation problem with maximizing the sum ergodic capacity of the U2I links in a given time period subject to the reliability constraint for the U2U links was formulated. Since interference existed only between each U2U-U2I spectrum reusing pair, we proposed to decompose the original optimization problem into two subproblems, i.e., power control and spectrum allocation. Then, a low-complexity robust resource allocation algorithm was developed to deal with the optimization problem with globally optimal solution. Simulation results demonstrated that the proposed method satisfied the various link connection requirements as well as effectively improved the overall system throughput. To the best of the authors' knowledge, this is the first work that investigates maximizing the sum ergodic capacity of U2I links taking into account the dynamic features (i.e., channel variation with imperfect CSI) of UAV networks while guaranteeing the reliable connection of U2U links.

In Chapter 4, we presented a blockchain-based secure spectrum trading strategy to protect operators' privacy and data security in the process of spectrum trading between cellular and UAV operators. In particular, in order to address to the scarcity of wireless spectrum for UAV networks, an incentive mechanism model was formulated to motivate the cellular network operators to share their idle spectrum with the UAV operators. However, traditional spectrum trading methods were always centralized with security and privacy threats. To this end, we leveraged blockchain technology to create a distributed and trusted environment where cellular and UAV operators could achieve secure spectrum trading without a third-party authority. Under the blockchain-based spectrum trading framework, we further studied the optimal spectrum pricing and purchasing strategies based on a Stackelberg game model to jointly maximize the profits of the MNO and the UAV operators. Two pricing schemes have been investigated, including nonuniform pricing and uniform pricing schemes. What's more, a nonuniform pricing algorithm and a distributed spectrum price bargaining algorithm for the two different pricing cases were respectively proposed to achieve the optimal solutions. Simulation results verified the theoretical analysis for the impact of different pricing schemes on the performances of the MNO and the UAV operators. To the best of the authors' knowledge, this is the first work that utilizes blockchain technology for secure spectrum trading for UAV-assisted cellular networks to address the constraint of privacy and security threats.

In Chapter 5, we exploited using laser charging to prolong the UAV's flight time for providing communication coverage in a disaster area as a flying base station. In particular, an energy efficiency maximization problem was formulated for a laser-powered UAV-aided emergency communication scenario with via jointly optimizing UAV's transmission power, flight trajectory as well as the user scheduling. However, such a joint trajectory and adaptive communication design problem is non-trivial to solve due to the closely-coupled relationship of the variables. To tackle this issue, we proposed an efficient iterative algorithm based on block coordinate descent method and successive convex optimization technique to solve the problem iteratively. Numerical results demonstrated that the proposed method could achieve better energy efficiency compared to other benchmark schemes with heuristic UAV trajectories. To the best of the authors' knowledge, this is the first work that preliminarily illustrates the practicability of applying laser charging into UAV communications to address the constraint of low endurance of UAVs considering jointly optimizing user scheduling, UAV's transmission power and trajectory.

In summary, this thesis provides a comprehensive survey on the potentials of integrating UAVs into 5G and beyond networks in which efficient resource management schemes are investigated to address the challenges and issues accompanied with the UAV-assisted wireless communications and networking including network heterogeneity, link disconnection, privacy security and low endurance. These results demonstrate the effectiveness of applying UAVs into current terrestrial networks to offer coverage extension and capacity enhancement. All the contributions and results are expected to advance the state of the art in UAV-assisted wireless communications and networking.

6.2 Future Work

6.2.1 Extensions of Current Research

There are a number of limitations pertaining to the current research, especially when considering the application of the methods developed in this thesis to practical UAV-assisted communication networks. In this subsection, the potential extensions for each chapter in this thesis are described in the following.

- In Chapter 2, the efficient interference management and resource allocation schemes for HAP, LAP and terrestrial networks need to be further studied. Besides, we mainly focused on the potentials of integrating aerial platforms into terrestrial networks. In future work, the space-air-ground integrated networks are worthy of researching. In such multi-layered networks, high latency from satellites needs to be considered.

118

- In Chapter 3, we assumed that UAVs' flight trajectory were predefined with the same speed and direction. In real applications, UAVs' trajectory may be random leading to more severe link disconnections. In addition, the energy constraint for the UAVs has not been considered. Therefore, trajectory optimization and adaptive algorithms should be designed taking into account the power limitation of UAVs in the extended research.

- In Chapter 4, we introduced a conceptual framework of spectrum blockchain but we did not do the experiments on a real blockchain platform. Thus, in the next step, some real tests based on a blockchain application platform such as Hyperledger can be studied. Besides, new consensus algorithms which can improve blockchain's scalability also need to be investigated.

- In Chapter 5, we considered that the UAV moved at a fixed altitude. To enhance UAVs' flexibility, 3D trajectory planning is more practical. In terms of the laser charging technology, how to improve the charging efficiency and how to optimize laser transmitter's placement position are also critical issues.

6.2.2 Promising Future Directions

In this subsection, some promising future directions in terms of UAV-assisted wireless communications and networking are presented in the following.

mmWave and NOMA for UAV Communications

mmWave technology has been identified as a key enabler to provide high-speed data rate for UAV networks owing to some outstanding features such as large bandwidth, low interference, small component size and low cost. Although mmWave communication, in general, suffers high propagation loss and is vulnerable to blockage, such issues are less severe when mmWave is applied for UAV communications due to the flexible UAV mobility and favorable air-ground channel characteristics. In addition, process techniques such as beamforming can concentrate the signal energy from massive MIMO antenna arrays to overcome the high propagation loss at mmWave frequencies. Therefore, the combination of mmWave and massive MIMO can greatly improve the spectral efficiency (SE) of the UAV communications. However, many challenges still need to be addressed for UAV mmWave communication networks. For example, more efficient beamforming training and tracking are needed to account for UAV movement, and channel Doppler effect needs extra consid-

eration. Besides, device electronics at the mmWave is also still much less mature than at lower frequencies.

Except for mmWave communication techniques, as an emerging technique, non-orthogonal multiple access (NOMA) can also be exploited to improve the SE of UAV communication networks significantly. In contrast to the conventional orthogonal multiple access (OMA) schemes (e.g., TDMA), NOMA simultaneously serves multiple users in non-orthogonal resources (in time, frequency, code and space domains) by separating the users in the power domain. Therefore, it is a suitable technology for effectively serving large number of wireless users while enhancing SE. Since NOMA uses the power domain for the multiple access while mmWave provides the multiple access in the spatial domain, the investigation of the coexistence between NOMA and mmWave in UAV communication networks to improve the network capacity further may be a hot research topic.

IRS-Assisted UAV Communications

Recently, intelligent reflecting surface (IRS), also referred as reconfigurable intelligent surface (RIS), has attracted extensive attention in the wireless communication research community, due to its capability of shaping wireless propagation and establishing a programmable radio environment. In particular, an IRS is a meta-surface constituted by many meta-atoms, which are engineered to implement different interactive functions, such as absorption, reflection, refraction, and polarization, for the incoming electromagnetic waves shined on them. IRS-assisted UAV communication offers multitude of benefits including: (i) Reduced energy consumption: Since IRS simply reflects the incident transmission signals and does not require power consuming complex signal processing operations, the energy consumption can be reduced significantly. Besides, IRS can potentially minimize the on-board UAV energy consumption by putting the wireless transmitter at the UAV in sleep mode, in specific scenarios where desired QoS can be met with IRS-only transmissions. What's more, by integrating IRS in UAV-enabled wireless networks, concatenated virtual LoS links between UAVs and mobile users can be formed via passively reflecting the incident signals, which leads to extended coverage area as well as less movement of UAVs. (ii) Efficient spectrum utilization: Since IRS simply reflects the incident transmission signals and does not require an additional frequency channel for transmission, network-wide spectrum consumption can be minimized. (iii) Flexible deployment of metasurfaces in three dimensions: The considered integrated UAV-IRS mode provides flexible placement of IRS in three dimensions and the number of IRS elements provides an additional degree of freedom to improve the channel quality. (iv) Low hardware cost: This IRS surface consists of large arrays of low-cost integrated electronics (e.g., polymer diode/switch or conductive square patches) which re-

flects the incoming signal to the desired direction with minimal hardware costs. Therefore, the integration between the IRS and UAV is expected to pave the way for the development of the B5G network to offer ubiquitous communication services.

However, introducing an IRS into UAV-enabled communication systems also brings challenges for its joint trajectory and resource allocation design. Specifically, due to the existence of the IRS, the composite channel power gain compositing the direct link from the UAV to ground users and the reflected link via IRS is a complicated function of the UAV's trajectory. Furthermore, how to efficiently schedule users to be assisted by the IRS is still unknown and deserves our efforts to explore. Thirdly, as broadband communications have been widely adopted in current cellular networks, the additional reflected path of IRS indeed causes a frequency- and spatial-selective fading channel imposing a significant challenge for the trajectory design of UAV, which was overlooked by existing works based on frequency-flat channel models. These issues are worthy of further research.

UAV Swarm

Individual UAV, with limited computation and storage capabilities, may not be suited for some complex tasks, while UAV swarms are expected to open up new opportunities, which can collaboratively complete complex missions with higher efficiency and lower cost, especially in harsh environments. Specifically, compared with traditional single UAV, UAV swarm has several advantages. One of the first interest of the UAV swarm is to be composed of several smaller drones that can be equipped with different sensors or other equipments providing redundancy that can help to tolerate a certain degree of failure. In addition, a multitude of UAV can cover a larger geographic area than a single one. The UAV swarm featured with high degree of autonomy can also get out from the personnel control and complete the task autonomously through mutual cooperation. Another major advantage of UAV swarm is considered as easily expanding the scalar to execute more complex tasks. By means of distributing tasks and loads to multiple individual drones, the drone swarm can execute tasks in parallel to reduce the execution time with better fault tolerance.

While UAV swarm brings these advantages, it also raises some challenging issues that need to be addressed. It is noted that the UAV swarm must possess a reliable and effective communication network. However, it is hard to be realized in UAV swarm due to the lack of unified network architecture. The traditional communication technologies on fixed networks or slowly moving networks cannot address the unique characteristics of UAV swarm, such as high dynamic topology, intermittent links and capability constraints. Moreover, many UAV swarms adopt open wireless channels in the system, which exposes them to a series of serious network security issues. These topics need to be further studied. Besides, the UAV

swarm performs tasks based on information sharing of the whole network, hence the robustness to make sure the full connection of network is crucial. In the last decade, many UAV swarm cooperation algorithms, including convex optimization, swarm intelligence, and machine learning algorithms are proposed. However, the convex optimization algorithms are applicable only when the targeting problem is convex while the performance of many swarm intelligence algorithms degrades drastically in large-scale complex applications. Machine learning-based algorithms provide good solutions, but require high computation and storage capability. To support intelligent cooperation of the UAV swarm and provide optimal decisions in real-time, digital twin, as one of the key technologies to reflect physical entities with virtual representations, provides the most promising solution. The digital twin- based intelligent cooperation scheme will also become a significant research direction of UAV swarm.

UAV Communications for 6G

As 5G communication networks are now being put into commercialization, technologies for the next-generation (i.e.,6G) communications are also being explored to achieve faster and more reliable data transmissions. From the network advances perspective, providing ubiquitous connectivity to diverse device types is the key challenge for 6G. UAVs will be an important element in 6G wireless communications, since they can facilitate wireless broadcast and support high rate transmissions. In order to support the airborne network formed by UAVs as part of 6G networks, different types of communication are envisaged, which can be labelled as UAV-to-Everything (U2X) communications. The U2X communications will be used to realize the future airborne network of 6G, enabling the UAVs to adopt different transmission modes according to the specific requirements of their corresponding onboard applications. Moreover, UAVs are also the key segments in 6G to achieve 3D connectivity and cell-free communication in which UE will be connected to the whole network instead of a specific cell to reduce handover and afford full coverage and high capacity connectivity.

However, like the emergence of many new technologies when the wireless world moves toward 5G, the new requirements of 6G will also influence the main technology trends in its evolution process. The success of 6G will have to leverage breakthroughs in novel technological concepts. Several major potential technologies have been highlighted by researchers including AI, Terahertz communications, visible light communication, quantum communication, etc. The combination of UAVs with these promising technologies towards 6G needs to be investigated.

Appendix A

A.1 Proof of Theorem 3.1

Assuming that $g_{m,B}$ and $g_{k,B}$ are i.i.d. exponential random variables with unit mean, the ergodic capacity of the mth CUE when sharing the spectrum with the kth DUE is given by

$$
\begin{aligned}
C_m\left(P_m^c, P_k^d\right) &= \mathbb{E}\left[\log_2\left(1 + \gamma_m^c\right)\right] \\
&= \int_0^\infty \int_0^\infty \log_2\left(1 + \frac{P_m^c \alpha_{m,B} g_{m,B}}{\sigma^2 + P_k^d \alpha_{k,B} g_{k,B}}\right) \\
&\quad \times e^{-\left(g_{m,B} + g_{k,B}\right)} dg_{m,B} dg_{k,B},
\end{aligned}
\tag{A.1}
$$

It is observed from the the above expression that $C_m\left(P_m^c, P_k^d\right)$ increases monotonically with P_m^c with fixed P_k^d while $C_m\left(P_m^c, P_k^d\right)$ decreases monotonically with P_k^d with fixed P_m^c. Therefore, we can conclude that the optimal solution of (3.15) can only reside at the upper boundary line of the feasible region defined by $P_m^c = \Phi\left(P_k^d\right)$ from $\left(P_{k,\min}^d, 0\right)$ up to the point $\left(P_{\max}^d, \Phi\left(P_{\max}^d\right)\right)$ or $\left(\Phi^{-1}\left(P_{\max}^c\right), P_{\max}^c\right)$, by acknowledging the fact that $P_m^c = \Phi\left(P_k^d\right)$ is a monotonically increasing function in the range of $\left(P_{k,\min}^d, +\infty\right)$.

Substituting $P_m^c = \Phi\left(P_k^d\right)$ in (A.1), the SINR term γ_m^c is then given by

$$
\begin{aligned}
&\frac{P_m^c \alpha_{m,B} g_{m,B}}{\sigma^2 + P_k^d \alpha_{k,B} g_{k,B}} \\
&= \frac{\alpha_k \alpha_{m,B} g_{m,B}}{\gamma_0^d \alpha_{m,k}\left(\frac{\sigma^2}{P_k^d} + \alpha_{k,B} g_{k,B}\right)}\left(\frac{e^{-\frac{\gamma_0^d \sigma^2}{P_k^d \alpha_k}}}{1 - p_0} - 1\right),
\end{aligned}
\tag{A.2}
$$

which can be shown to monotonically increase with P_k^d in the range $\left(P_{k,\min}^d, +\infty \right)$. Hence, the optimal power allocation solution to the problem (3.15) is the intersection point $\left(P_{\max}^d, \Phi \left(P_{\max}^d \right) \right)$ or $\left(\Phi^{-1} \left(P_{\max}^c \right), P_{\max}^c \right)$, which can be written in a compact form as in (3.28) and (3.29).

Appendix B

B.1 Proof of Theorem 4.1

Since the Problem 4.1 is a convex optimization problem, the duality gap between this problem and its dual optimization problem is zero. Thus, we can deal with Problem 4.1 by solving its dual problem.

The Lagrangian of the Problem 4.1 can be written as

$$\mathscr{L}(b_i, \alpha) = g_i \log_2\left(1 + \frac{b_i}{d_i}\right) - \mu_i b_i + \alpha b_i, \tag{B.1}$$

where α is nonnegative dual variable associated with the constraint $b_i \geq 0$.

The dual function is then defined as $h(\alpha) = \max_{b_i \geq 0} \mathscr{L}(b_i, \alpha)$, and the dual problem is given by $\min_{\alpha \geq 0} h(\alpha)$. Then, the KKT conditions can be written as follows:

$$\frac{\partial \mathscr{L}(b_i, \alpha)}{\partial b_i} = \frac{g_i}{(b_i + d_i)\ln 2} - \mu_i + \alpha = 0, \ \forall i, \tag{B.2}$$

$$\alpha \geq 0, \ b_i \geq 0, \ \forall i, \tag{B.3}$$

$$\alpha b_i = 0. \tag{B.4}$$

From (B.2), it follows

$$b_i = \frac{g_i}{(\mu_i - \alpha)\ln 2} - d_i. \tag{B.5}$$

Suppose $b_i > 0$ when $\mu_i \geq \frac{g_i}{d_i \ln 2}$. Then from (B.4), it follows that $\alpha = 0$. Therefore, (B.5) reduces to $b_i = \frac{g_i}{\mu_i \ln 2} - d_i$. Then $b_i > 0$ results in $\mu_i < \frac{g_i}{d_i \ln 2}$. This contradicts the presumption. Therefore, from (B.3), it follows

$$b_i = 0, \ \text{if } \mu_i \geq \frac{g_i}{d_i \ln 2}. \tag{B.6}$$

Suppose $b_i = 0$ when $\mu_i < \frac{g_i}{d_i \ln 2}$. Then, from (B.5), it follows $\mu_i = \frac{g_i}{d_i \ln 2} + \alpha$. Since $\alpha \geq 0$, it follows $\mu_i \geq \frac{g_i}{d_i \ln 2}$. This contradicts the presumption. Thus, $b_i \neq 0$ for this set of μ_i. Then, from (B.4), it follows $\alpha = 0$. Therefore, from (B.5), it follows

$$b_i = \left(\frac{g_i}{\mu_i \ln 2} - d_i \right), \text{ if } \mu_i < \frac{g_i}{d_i \ln 2}. \tag{B.7}$$

Theorem 4.1 is thus proved.

B.2 Proof of Proposition 4.1

By introducing the dual variables associated with the bandwidth price and amount of total available spectrum constraints, the Lagrangine of Problem 4.4 is given by

$$\mathcal{L}(\boldsymbol{\mu}, \eta, \boldsymbol{\gamma}) = \sum_{i=1}^{N} \mu_i d_i + \eta \left(\sum_{i=1}^{N} \frac{g_i}{\mu_i \ln 2} - \sum_{i=1}^{N} d_i - Q \right) \\ - \sum_{i=1}^{N} \gamma_i \mu_i, \tag{B.8}$$

where η and γ_i are the nonnegative dual variables associated with the constraints $\sum_{i=1}^{N} \frac{g_i}{\mu_i \ln 2} \leq Q + \sum_{i=1}^{N} d_i$ and $\mu_i \geq 0$, respectively.

The dual optimization problem is expressed as the maximization of the Lagrangian

$$\mathcal{V}(\boldsymbol{\mu}, \eta, \boldsymbol{\gamma}) = \max_{\boldsymbol{\mu} \succcurlyeq 0} \mathcal{L}(\boldsymbol{\mu}, \eta, \boldsymbol{\gamma}). \tag{B.9}$$

The dual problem is then given by $\min_{\eta \geq 0, \boldsymbol{\gamma} \succcurlyeq 0} \mathcal{V}(\boldsymbol{\mu}, \eta, \boldsymbol{\gamma})$. The duality gap is zero for the convex problem addressed here, and thus solving its dual problem is equivalent to solving the original problem. Thus the optimal solution needs to satisfy the following KKT conditions:

$$\frac{\partial \mathcal{L}(\mu, \eta, \gamma)}{\partial \mu_i} = d_i - \frac{\eta g_i}{\mu_i^2 \ln 2} - \gamma_i = 0, \forall i, \tag{B.10}$$

$$\eta \left(\sum_{i=1}^{N} \frac{g_i}{\mu_i \ln 2} - \sum_{i=1}^{N} d_i - Q \right) = 0, \tag{B.11}$$

$$\gamma_i \mu_i = 0, \tag{B.12}$$

$$\eta \geq 0, \gamma_i \geq 0, \mu_i \geq 0, \forall i, \tag{B.13}$$

$$\sum_{i=1}^{N} \frac{g_i}{\mu_i \ln 2} - Q - \sum_{i=1}^{N} d_i \leq 0. \tag{B.14}$$

From (B.10), we can derive

$$\mu_i{}^2 = \frac{\eta g_i}{(d_i - \gamma_i)\ln 2}, \forall i. \tag{B.15}$$

To further analyze the dual problem, we firstly provide the following two lemmas.

Lemma A.1. $\gamma_i = 0, \forall i$.

Proof. Suppose that $\gamma_i \neq 0$ for any arbitrary i. Then, from (B.12), we can derive that $\mu_i = 0$. Then, since $g_i > 0$, from (B.15), it follows that $\eta = 0$. Substituting $\eta = 0$ into (B.15), we have $\mu_i = 0, \forall i$. However, this result contradicts the condition in (B.14). Thus, the assumption that $\gamma_i \neq 0$ for any given i does not hold, and we thus have $\gamma_i = 0, \forall i$. ∎

Lemma A.2. $\sum_{i=1}^{N} \frac{g_i}{\mu_i \ln 2} - Q - \sum_{i=1}^{N} d_i = 0$.

Proof. Suppose that $\sum_{i=1}^{N} \frac{g_i}{\mu_i \ln 2} - Q - \sum_{i=1}^{N} d_i \neq 0$. Then, from (B.11), it follows that $\eta = 0$. Substituting $\eta = 0$ into (B.15), we have $\mu_i = 0, \forall i$, which contradicts the condition in (B.14). Therefore, the aforementioned assumption does not hold, and we thus have $\sum_{i=1}^{N} \frac{g_i}{\mu_i \ln 2} - Q - \sum_{i=1}^{N} d_i = 0$. ∎

From Lemma A.1, we have $\gamma_i = 0$ for arbitrary i. Since $\mu_i \geq 0$, thus from (B.15), it follows $\mu_i = \sqrt{\frac{\eta g_i}{d_i \ln 2}}, \forall i$. According to Lemma A.2, it follows that $Q + \sum_{i=1}^{N} d_i = \sum_{i=1}^{N} \frac{g_i}{\mu_i \ln 2}$. Substituting $\mu_i = \sqrt{\frac{\eta g_i}{d_i \ln 2}}$ into it, we can derive

$$\sqrt{\eta} = \frac{\sum_{i=1}^{N} \sqrt{\frac{g_i d_i}{\ln 2}}}{Q + \sum_{i=1}^{N} d_i}. \tag{B.16}$$

Then, it follows

$$\mu_i = \frac{1}{\ln 2} \sqrt{\frac{g_i}{d_i}} \frac{\sum_{i=1}^{N} \sqrt{g_i d_i}}{Q + \sum_{i=1}^{N} d_i}. \tag{B.17}$$

Thus, Proposition 4.1 is proved.

B.3 Proof of Proposition 4.2

This proof consists of two parts: the necessity proof and the sufficiency proof, which are given as follows.

Part I: Sufficiency. The optimal solution to the Problem 4.4 is given by (4.26) with the assumption that that all the indicator functions are equal to 1, i.e., $\mu_i < \frac{g_i}{d_i \ln 2}, \forall i \in$

$\{1, 2, \cdots, N\}$. Submitting (4.26) into these inequalities yields

$$\sqrt{\frac{g_i}{d_i \ln 2}} \frac{\sum_{i=1}^{N} \sqrt{\frac{g_i d_i}{\ln 2}}}{Q + \sum_{i=1}^{N} d_i} < \frac{g_i}{d_i \ln 2}, \forall i \in \{1, 2, \cdots, N\}. \tag{B.18}$$

Then, (B.18) can be rewritten as $Q > \frac{\sum_{i=1}^{N} \sqrt{g_i d_i}}{\sqrt{g_i/d_i}} - \sum_{i=1}^{N} d_i, \forall i \in \{1, 2, \cdots, N\}$. Furthermore, the inequalities given above can be compactly written as

$$Q > \frac{\sum_{i=1}^{N} \sqrt{g_i d_i}}{\min_i \sqrt{\frac{g_i}{d_i}}} - \sum_{i=1}^{N} d_i. \tag{B.19}$$

Thus, the sufficiency of the condition in (4.27) is proved.

Part II: Necessity. This part can be proved by contradiction. For the ease of exposition, we assume that UAV operators are sorted by the following order: $\frac{g_1}{d_1} > \cdots \frac{g_{N-1}}{d_{N-1}} > \frac{g_N}{d_N}$. Then, in Proposition 4.2, the condition becomes $Q > Y_N$, where

$$Y_N = \frac{\sum_{i=1}^{N} \sqrt{g_i d_i}}{\sqrt{\frac{g_N}{d_N}}} - \sum_{i=1}^{N} d_i. \tag{B.20}$$

Now, suppose $Y_{N-1} < Q \leq Y_N$, where Y_{N-1} is shown later in (B.24). Suppose that $\boldsymbol{\mu}^*$ given by (4.26) is still optimal for Problem 4.2 with $Y_{N-1} < Q < Y_N$. Then, since $Q \leq Y_N$, from (4.26) we have $\mu_N^* \geq \frac{g_N}{d_N \ln 2}$ and thus $\left(\frac{g_N}{\mu_N^*} - d_N\right)^+ = 0$. From Problem 4.2, it then follows that $\mu_1^*, \ldots, \mu_{N-1}^*$ is the optimal solution of the following problem

$$\max_{\boldsymbol{\mu} \succcurlyeq 0} \sum_{i=1}^{N-1} \left(\frac{g_i}{\ln 2} - \mu_i d_i\right)^+, \tag{B.21}$$

$$\text{s.t.} \sum_{i=1}^{N-1} \left(\frac{g_i}{\mu_i \ln 2} - d_i\right)^+ \leq Q. \tag{B.22}$$

It is easy to observe that the above problem has the same structure as the Problem 4.2. Therefore, according to Proposition 4.1 and the proof of previous Part I, the optimal solution for this problem can be given by

$$\mu_i^* = \frac{1}{\ln 2} \sqrt{\frac{g_i}{d_i}} \frac{\sum_{i=1}^{N-1} \sqrt{g_i d_i}}{Q + \sum_{i=1}^{N-1} d_i}, \forall i \in \{1, 2, \cdots, N-1\}, \tag{B.23}$$

with the condition that $Q > Y_{N-1}$, where Y_{N-1} is expressed as the threshold for Q above which $\mu_i^* < \frac{g_i}{d_i \ln 2}$, $\forall i \in \{1, 2, \cdots, N-1\}$ holds, i.e.,

$$Y_{N-1} = \frac{\sum_{i=1}^{N-1} \sqrt{g_i d_i}}{\sqrt{\frac{g_{N-1}}{d_{N-1}}}} - \sum_{i=1}^{N-1} d_i. \tag{B.24}$$

Comparing the optimal bandwidth price solution shown in (B.23) with that given in (4.26), we can find that they are different from each other, which contradicts with our assumption that $\boldsymbol{\mu}^*$ is still the optimal solution for Problem 4.2 with the condition $Y_{N-1} < Q \leq Y_N$. Thus, we can conclude that only if the condition $Q > Y_N$ satisfies, the bandwidth prices given by (4.26) are the optimal solutions for Problem 4.2.

Combining the results obtained in Part I and Part II, it is concluded that the bandwidth prices given by (4.26) are the optimal solutions of Problem 4.2 if and only if $Q > \frac{\sum_{i=1}^{N} \sqrt{g_i d_i}}{\min_i \sqrt{g_i/d_i}} - \sum_{i=1}^{N} d_i$. Thus, Proposition 4.2 is proved.

Appendix C

C.1 Proof of Theorem 5.2

The proof of this theorem follows the similar arguments as shown in [257, 263]. First, we define the function

$$f(z) \triangleq \log_2 \left(1 + \frac{\gamma}{G+z} \right), \tag{C.1}$$

for some constant $\gamma \geq 0$ and G. By computing the second derivative of $f(z)$, we obtain the following results,

$$f''(z) = \frac{(\log_2 e)\, \gamma\, (2G + 2z + \gamma)}{(G+z)^2 (G+\gamma+z)^2}. \tag{C.2}$$

Note that in (C.2), if $G \geq -z$, then $f''(z) \geq 0$. Therefore, we can conclude that $f(z)$ is a convex function with $\gamma \geq 0$ and $G \geq -z$. Since the first-order Taylor expansion of a convex function can be regarded as a global under-estimator [261], then for any given point z_0, we have $f(z) \geq f(z_0) + f'(z_0)(z - z_0)$, $\forall z$, where $f'(z_0)$ is the derivative of $f(z)$ at point z_0, and $f'(z_0)$ is given as follows

$$f'(z_0) = \frac{-(\log_2 e)\, \gamma}{(G+z_0)\,(G+\gamma+z_0)}. \tag{C.3}$$

By setting $z_0 = 0$, we have the following inequality,

$$f(z) \geq \log_2 \left(1 + \frac{\gamma}{G} \right) - \frac{(\log_2 e)\, \gamma z}{G\,(G+\gamma)}, \forall z. \tag{C.4}$$

Therefore, for each time slot n, let $\gamma = p[n]\, \gamma_0$, $G = H^2 + \left\| q_j[n] - w_k \right\|^2$, $z = \left\| q(n) - w_k \right\|^2 - \left\| q_j(n) - w_k \right\|^2$, the inequality in (5.49) thus follows. This completes the proof of Theorem 5.2.

C.2   Proof of Theorem 5.3

First, we prove the forward implication of Theorem 5.3 by following a similar approach as in [264, 265]. Without loss of generality, we define ζ^* and $\{\mathbf{Q}^*, \mathbf{V}^*, \mathbf{A}^*, \eta^*, \tau_n^*\} \in \mathscr{F}$ as the optimal energy efficiency and the optimal solutions of the original objective function in (5.7), respectively. Then, the optimal energy efficiency can be expressed as

$$
\begin{aligned}
\zeta^* = \frac{\eta^*}{\tilde{E}_{total}^*} &\geq \frac{\eta}{\tilde{E}_{total}}, \ \forall \{\mathbf{Q}, \mathbf{V}, \mathbf{A}, \eta, \tau_n\} \in \mathscr{F} \\
&\Rightarrow \eta - \zeta^* \tilde{E}_{total} \leq 0 \\
&\quad \eta^* - \zeta^* \tilde{E}_{total}^* = 0.
\end{aligned}
\tag{C.5}
$$

Therefore, we can conclude that $\max\limits_{\mathbf{Q}, \mathbf{V}, \mathbf{A}, \eta, \tau_n} \eta - \zeta^* \tilde{E}_{total} = 0$, and it is achievable by trajectory optimization polices $\{\mathbf{Q}^*, \mathbf{V}^*, \mathbf{A}^*, \eta^*, \tau_n^*\}$. This completes the forward implication.

Next, we prove the converse implication of Theorem 5.3. Suppose $\{\mathbf{Q}_e^*, \mathbf{V}_e^*, \mathbf{A}_e^*, \eta_e^*, \tau_n^{e*}\}$ is the optimal solutions of the equivalent objective function such that $\eta_e^* - \zeta^* \tilde{E}_{total}^{e*} = 0$. Then, for any feasible solutions $\{\mathbf{Q}, \mathbf{V}, \mathbf{A}, \eta, \tau_n\} \in \mathscr{F}$, we can obtain the following inequality:

$$
\eta - \zeta^* \tilde{E}_{total} \leq \eta_e^* - \zeta^* \tilde{E}_{total}^{e*} = 0.
\tag{C.6}
$$

The preceding inequality implies

$$
\begin{aligned}
\frac{\eta}{\tilde{E}_{total}} &\leq \zeta^*, \ \forall \{\mathbf{Q}, \mathbf{V}, \mathbf{A}, \eta, \tau_n\} \in \mathscr{F} \\
\frac{\eta_e^*}{\tilde{E}_{total}^{e*}} &= \zeta^*.
\end{aligned}
\tag{C.7}
$$

In other words, the optimal trajectory planning policies $\{\mathbf{Q}_e^*, \mathbf{V}_e^*, \mathbf{A}_e^*, \eta_e^*, \tau_n^{e*}\}$ for the equivalent objective function are also the optimal solutions for the original objective function. This completes the proof of the converse implication of Theorem 5.3. Thus, the Theorem 5.3 is proved.

C.3   Proof of Theorem 5.4

We follow a similar approach as in [264, 265] to prove the convergence of Algorithm 4. For the sake of notational simplicity, we define the equivalent objective function in (P5.8) as $F(\zeta') = \max_{\mathbf{Q}, \mathbf{V}, \mathbf{A}, \eta, \tau_n} \{\eta - \zeta' \tilde{E}_{total}\}$. Firstly, two propositions are introduced.

Proposition C.1. *$F(\zeta')$ is a strictly monotonic decreasing function in ζ', i.e., $F(\zeta'') > F(\zeta')$ if $\zeta' > \zeta''$.*

Proof. Let $\{\mathbf{Q}', \mathbf{V}', \mathbf{A}', \eta', \tau'_n\} \in \mathscr{F}$ and $\{\mathbf{Q}'', \mathbf{V}'', \mathbf{A}'', \eta'', \tau''_n\} \in \mathscr{F}$ be two distinct optimal solutions for $F(\zeta')$ and $F(\zeta'')$, respectively. Then, if $\zeta' > \zeta''$, we can have

$$
\begin{aligned}
F(\zeta'') &= \max_{\mathbf{Q}, \mathbf{V}, \mathbf{A}, \eta, \tau_n} \left\{ \eta - \zeta'' \tilde{E}_{total} \right\} \\
&= \eta'' - \zeta'' \tilde{E}''_{total} \\
&> \eta' - \zeta'' \tilde{E}'_{total} \\
&\geq \eta' - \zeta' \tilde{E}'_{total} \\
&= F(\zeta').
\end{aligned}
\tag{C.8}
$$

Thus, the proposition is proved. ∎

Proposition C.2. *Let $\{\mathbf{Q}', \mathbf{V}', \mathbf{A}', \eta', \tau'_n\} \in \mathscr{F}$ be an arbitrary feasible solution and $\zeta' = \eta' / \tilde{E}'_{total}$, then $F(\zeta') \geq 0$.*

Proof. Based on the definition of $F(\zeta')$, we can obtain the following results

$$
\begin{aligned}
F(\zeta') &= \max_{\mathbf{Q}, \mathbf{V}, \mathbf{A}, \eta, \tau_n} \left\{ \eta - \zeta' \tilde{E}_{total} \right\} \\
&\geq \eta' - \zeta' \tilde{E}'_{total} = 0.
\end{aligned}
\tag{C.9}
$$

Thus, Proposition C.2 is proved. ∎

Based on the above two propositions, we are now ready to prove the convergence of Algorithm 4. We first prove that the energy efficiency ζ increases in each iteration. Then, we prove that if the number of iterations is large enough, then the energy efficiency ζ converges to the optimal ζ^* such that it satisfies the optimality condition in Theorem 5.3, i.e., $F(\zeta^*) = 0$.

Let $\{\mathbf{Q}[n], \mathbf{V}[n], \mathbf{A}[n], \tau_n\}$ be the optimal policies in the nth iteration. Suppose $\zeta_n \neq \zeta^*$ and $\zeta_{n+1} \neq \zeta^*$ represent the energy efficiency of the considered system in iterations n and $n+1$, respectively. By Theorem 5.3 and Proposition C.2, $F(\zeta_n) > 0$ and $F(\zeta_{n+1}) > 0$ must be true. On the other hand, in the proposed algorithm, we calculate ζ_{n+1} as $\zeta_{n+1} = \eta / \tilde{E}_{total}$. Thus, we can express $F(\zeta_n)$ as

$$
\begin{aligned}
F(\zeta_n) &= \eta - \zeta_n \tilde{E}_{total} \\
&= \tilde{E}_{total}(\zeta_{n+1} - \zeta_n) > 0.
\end{aligned}
\tag{C.10}
$$

Since $\tilde{E}_{total} > 0$, thus we can get $\zeta_{n+1} > \zeta_n$. By combining $\zeta_{n+1} > \zeta_n$ and Proposition C.1, we can show that as long as the number of iterations is large enough, $F(\zeta_n)$ will eventually approach zero and satisfy the optimality condition as stated in Theorem 5.3.

References

[1] J. Wu, S. Guo, H. Huang, W. Liu, and Y. Xiang, "Information and communications technologies for sustainable development goals: State-of-the-art, needs and perspectives," *IEEE Communications Surveys & Tutorials*, vol. 20, no. 3, pp. 2389–2406, 2018.

[2] O. S. Oubbati, M. Atiquzzaman, T. A. Ahanger, and A. Ibrahim, "Softwarization of UAV networks: A survey of applications and future trends," *IEEE Access*, vol. 8, pp. 98 073–98 125, 2020.

[3] E. W. Frew and T. X. Brown, "Airborne communication networks for small unmanned aircraft systems," *Proceedings of the IEEE*, vol. 96, no. 12, pp. 2008–2027, 2008.

[4] Y. Zeng, R. Zhang, and T. J. Lim, "Wireless communications with unmanned aerial vehicles: Opportunities and challenges," *IEEE Communications Magazine*, vol. 54, no. 5, pp. 36–42, 2016.

[5] K. Gomez, S. Kandeepan, M. M. Vidal, V. Boussemart, R. Ramos, R. Hermenier, T. Rasheed, L. Goratti, L. Reynaud, D. Grace *et al.*, "Aerial base stations with opportunistic links for next generation emergency communications," *IEEE Communications Magazine*, vol. 54, no. 4, pp. 31–39, 2016.

[6] S. Hayat, E. Yanmaz, and R. Muzaffar, "Survey on unmanned aerial vehicle networks for civil applications: A communications viewpoint," *IEEE Communications Surveys & Tutorials*, vol. 18, no. 4, pp. 2624–2661, 2016.

[7] S. Chandrasekharan, K. Gomez, A. Al-Hourani, S. Kandeepan, T. Rasheed, L. Goratti, L. Reynaud, D. Grace, I. Bucaille, T. Wirth *et al.*, "Designing and implementing future aerial communication networks," *IEEE Communications Magazine*, vol. 54, no. 5, pp. 26–34, 2016.

[8] A. Fotouhi, H. Qiang, M. Ding, M. Hassan, L. G. Giordano, A. Garcia-Rodriguez, and J. Yuan, "Survey on UAV cellular communications: Practical aspects, standardization advancements, regulation, and security challenges," *IEEE Communications Surveys & Tutorials*, vol. 21, no. 4, pp. 3417–3442, 2019.

[9] Y. Zeng, Q. Wu, and R. Zhang, "Accessing from the sky: A tutorial on UAV communications for 5G and beyond," *Proceedings of the IEEE*, vol. 107, no. 12, pp. 2327–2375, 2019.

[10] M. Mozaffari, W. Saad, M. Bennis, Y.-H. Nam, and M. Debbah, "A tutorial on UAVs for wireless networks: Applications, challenges, and open problems," *IEEE Communications Surveys & Tutorials*, vol. 21, no. 3, pp. 2334–2360, 2019.

[11] M. Erdelj, E. Natalizio, K. R. Chowdhury, and I. F. Akyildiz, "Help from the sky: Leveraging UAVs for disaster management," *IEEE Pervasive Computing*, vol. 16, no. 1, pp. 24–32, 2017.

[12] D. He, S. Chan, and M. Guizani, "Drone-assisted public safety networks: The security aspect," *IEEE Communications Magazine*, vol. 55, no. 8, pp. 218–223, 2017.

[13] S. A. R. Naqvi, S. A. Hassan, H. Pervaiz, and Q. Ni, "Drone-aided communication as a key enabler for 5G and resilient public safety networks," *IEEE Communications Magazine*, vol. 56, no. 1, pp. 36–42, 2018.

[14] J. Liu, Y. Shi, Z. M. Fadlullah, and N. Kato, "Space-air-ground integrated network: A survey," *IEEE Communications Surveys & Tutorials*, vol. 20, no. 4, pp. 2714–2741, 2018.

[15] W. Khawaja, I. Guvenc, D. W. Matolak, U.-C. Fiebig, and N. Schneckenburger, "A survey of air-to-ground propagation channel modeling for unmanned aerial vehicles," *IEEE Communications Surveys & Tutorials*, vol. 21, no. 3, pp. 2361–2391, 2019.

[16] R. Shakeri, M. A. Al-Garadi, A. Badawy, A. Mohamed, T. Khattab, A. K. Al-Ali, K. A. Harras, and M. Guizani, "Design challenges of multi-UAV systems in cyber-physical applications: A comprehensive survey and future directions," *IEEE Communications Surveys & Tutorials*, vol. 21, no. 4, pp. 3340–3385, 2019.

[17] A. A. Khuwaja, Y. Chen, N. Zhao, M.-S. Alouini, and P. Dobbins, "A survey of channel modeling for UAV communications," *IEEE Communications Surveys & Tutorials*, vol. 20, no. 4, pp. 2804–2821, 2018.

[18] H. Wang, H. Zhao, J. Zhang, D. Ma, J. Li, and J. Wei, "Survey on unmanned aerial vehicle networks: A cyber physical system perspective," *IEEE Communications Surveys & Tutorials*, vol. 22, no. 2, pp. 1027–1070, 2019.

[19] D. S. Lakew, U. Sa'ad, N.-N. Dao, W. Na, and S. Cho, "Routing in flying ad hoc networks: A comprehensive survey," *IEEE Communications Surveys & Tutorials*, vol. 22, no. 2, pp. 1071–1120, 2020.

[20] Z. Ullah, F. Al-Turjman, and L. Mostarda, "Cognition in UAV-aided 5G and beyond communications: A survey," *IEEE Transactions on Cognitive Communications and Networking*, vol. 6, no. 3, pp. 872–891, 2020.

[21] Z. Sheng, H. D. Tuan, T. Q. Duong, and L. Hanzo, "UAV-aided two-way multi-user relaying," *IEEE Transactions on Communications*, vol. 69, no. 1, pp. 246–260, 2021.

[22] G. Hu and Y. Cai, "Legitimate eavesdropping in UAV-based relaying system," *IEEE Communications Letters*, vol. 24, no. 10, pp. 2275–2279, 2020.

[23] P. K. Sharma and D. I. Kim, "Secure 3D mobile UAV relaying for hybrid satellite-terrestrial networks," *IEEE Transactions on Wireless Communications*, vol. 19, no. 4, pp. 2770–2784, 2020.

[24] S. Ahmed, M. Z. Chowdhury, and Y. M. Jang, "Energy-efficient UAV relaying communications to serve ground nodes," *IEEE Communications Letters*, vol. 24, no. 4, pp. 849–852, 2020.

[25] Y. Guo, S. Yin, and J. Hao, "Joint placement and resources optimization for multi-user UAV-Relaying systems with underlaid cellular networks," *IEEE Transactions on Vehicular Technology*, vol. 69, no. 10, pp. 12 374–12 377, 2020.

[26] X. Xi, X. Cao, P. Yang, J. Chen, T. Q. Quek, and D. Wu, "Network resource allocation for eMBB payload and URLLC control information communication multiplexing in a multi-UAV relay network," *IEEE Transactions on Communications*, vol. 69, no. 3, pp. 1802–1817, 2020.

[27] Z. Hadzi-Velkov, S. Pejoski, N. Zlatanov, and R. Schober, "UAV-assisted wireless powered relay networks with cyclical NOMA-TDMA," *IEEE Wireless Communications Letters*, vol. 9, no. 12, pp. 2088–2092, 2020.

[28] S. Hosseinalipour, A. Rahmati, and H. Dai, "Interference avoidance position planning in dual-hop and multi-hop UAV relay networks," *IEEE Transactions on Wireless Communications*, vol. 19, no. 11, pp. 7033–7048, 2020.

[29] Q. Hu, Y. Cai, A. Liu, G. Yu, and G. Y. Li, "Low-complexity joint resource allocation and trajectory design for UAV-aided relay networks with the segmented ray-tracing channel model," *IEEE Transactions on Wireless Communications*, vol. 19, no. 9, pp. 6179–6195, 2020.

[30] L. Zhu, J. Zhang, Z. Xiao, X. Cao, X. G. Xia, and R. Schober, "Millimeter-wave full-duplex UAV relay: Joint positioning, beamforming, and power control," *IEEE Journal on Selected Areas in Communications*, vol. 38, no. 9, pp. 2057–2073, 2020.

[31] B. Ji, Y. Li, D. Cao, C. Li, S. Mumtaz, and D. Wang, "Secrecy performance analysis of UAV assisted relay transmission for cognitive network with energy harvesting," *IEEE Transactions on Vehicular Technology*, vol. 69, no. 7, pp. 7404–7415, 2020.

[32] H. Ren, C. Pan, K. Wang, W. Xu, M. Elkashlan, and A. Nallanathan, "Joint transmit power and placement optimization for URLLC-enabled UAV relay systems," *IEEE Transactions on Vehicular Technology*, vol. 69, no. 7, pp. 8003–8007, 2020.

[33] Y. He, D. Zhai, Y. Jiang, and R. Zhang, "Relay selection for UAV-assisted urban vehicular ad hoc networks," *IEEE Wireless Communications Letters*, vol. 9, no. 9, pp. 1379–1383, 2020.

[34] Y. Chen, H. Zhang, and Y. Hu, "Optimal power and bandwidth allocation for multiuser video streaming in UAV relay networks," *IEEE Transactions on Vehicular Technology*, vol. 69, no. 6, pp. 6644–6655, 2020.

[35] H. Li and X. Zhao, "Throughput maximization with energy harvesting in UAV-assisted cognitive mobile relay networks," *IEEE Transactions on Cognitive Communications and Networking*, vol. 7, no. 1, pp. 197–209, 2021.

[36] Y. Ji, Z. Yang, H. Shen, W. Xu, K. Wang, and X. Dong, "Multicell edge coverage enhancement using mobile UAV-relay," *IEEE Internet of Things Journal*, vol. 7, no. 8, pp. 7482–7494, 2020.

[37] P. Ladosz, H. Oh, G. Zheng, and W.-H. Chen, "Gaussian process based channel prediction for communication-relay UAV in urban environments," *IEEE Transactions on Aerospace and Electronic Systems*, vol. 56, no. 1, pp. 313–325, 2019.

[38] L. Xiao, X. Lu, D. Xu, Y. Tang, L. Wang, and W. Zhuang, "UAV relay in VANETs against smart jamming with reinforcement learning," *IEEE Transactions on Vehicular Technology*, vol. 67, no. 5, pp. 4087–4097, 2018.

[39] S. Zhang, H. Zhang, Q. He, K. Bian, and L. Song, "Joint trajectory and power optimization for UAV relay networks," *IEEE Communications Letters*, vol. 22, no. 1, pp. 161–164, 2017.

[40] Q. Zhang, W. Saad, M. Bennis, X. Lu, M. Debbah, and W. Zuo, "Predictive deployment of UAV base stations in wireless networks: Machine learning meets contract theory," *IEEE Transactions on Wireless Communications*, vol. 20, no. 1, pp. 637–652, 2021.

[41] T. Bai, C. Pan, J. Wang, Y. Deng, M. Elkashlan, A. Nallanathan, and L. Hanzo, "Dynamic aerial base station placement for minimum-delay communications," *IEEE Internet of Things Journal*, vol. 8, no. 3, pp. 1623–1635, 2021.

[42] S. Zhang and N. Ansari, "3D drone base station placement and resource allocation with FSO-based backhaul in hotspots," *IEEE Transactions on Vehicular Technology*, vol. 69, no. 3, pp. 3322–3329, 2020.

[43] J. You, S. Jung, J. Seo, and J. Kang, "Energy-efficient 3-D placement of an unmanned aerial vehicle base station with antenna tilting," *IEEE Communications Letters*, vol. 24, no. 6, pp. 1323–1327, 2020.

[44] X. Sun, N. Ansari, and R. Fierro, "Jointly optimized 3D drone mounted base station deployment and user association in drone assisted mobile access networks," *IEEE Transactions on Vehicular Technology*, vol. 69, no. 2, pp. 2195–2203, 2019.

[45] Z. Xiao, H. Dong, L. Bai, D. O. Wu, and X.-G. Xia, "Unmanned aerial vehicle base station (UAV-BS) deployment with millimeter-wave beamforming," *IEEE Internet of Things Journal*, vol. 7, no. 2, pp. 1336–1349, 2019.

[46] H. Kang, J. Joung, J. Ahn, and J. Kang, "Secrecy-aware altitude optimization for quasi-static UAV base station without eavesdropper location information," *IEEE Communications Letters*, vol. 23, no. 5, pp. 851–854, 2019.

[47] L. Zhang, Q. Fan, and N. Ansari, "3-D drone-base-station placement with in-band full-duplex communications," *IEEE Communications Letters*, vol. 22, no. 9, pp. 1902–1905, 2018.

[48] I. Bor-Yaliniz, S. S. Szyszkowicz, and H. Yanikomeroglu, "Environment-aware drone-base-station placements in modern metropolitans," *IEEE Wireless Communications Letters*, vol. 7, no. 3, pp. 372–375, 2017.

[49] L. Wang, B. Hu, and S. Chen, "Energy efficient placement of a drone base station for minimum required transmit power," *IEEE Wireless Communications Letters*, vol. 9, no. 12, pp. 2010–2014, 2020.

[50] J. Liu, H. Zhang, M. Sheng, Y. Su, S. Chen, and J. Li, "High altitude air-to-ground channel modeling for fixed-wing UAV mounted aerial base stations," *IEEE Wireless Communications Letters*, vol. 10, no. 2, pp. 330–334, 2021.

[51] X. Zhong, Y. Huo, X. Dong, and Z. Liang, "QoS-compliant 3-D deployment optimization strategy for UAV base stations," *IEEE Systems Journal*, vol. 15, no. 2, pp. 1795–1803, 2021.

[52] Y.-S. Wang, Y.-W. P. Hong, and W.-T. Chen, "Trajectory learning, clustering, and user association for dynamically connectable UAV base stations," *IEEE Transactions on Green Communications and Networking*, vol. 4, no. 4, pp. 1091–1105, 2020.

[53] M. A. Kishk, A. Bader, and M. S. Alouini, "On the 3-D placement of airborne base stations using tethered UAVs," *IEEE Transactions on Communications*, vol. 68, no. 8, pp. 5202–5215, 2020.

[54] T. Akram, M. Awais, R. Naqvi, A. Ahmed, and M. Naeem, "Multicriteria UAV base stations placement for disaster management," *IEEE Systems Journal*, vol. 14, no. 3, pp. 3475–3482, 2020.

[55] M. J. Sobouti, Z. Rahimi, A. H. Mohajerzadeh, S. A. Hosseini Seno, R. Ghanbari, J. M. Marquez-Barja, and H. Ahmadi, "Efficient deployment of small cell base stations mounted on unmanned aerial vehicles for the internet of things infrastructure," *IEEE Sensors Journal*, vol. 20, no. 13, pp. 7460–7471, 2020.

[56] S. Wan, J. Lu, P. Fan, and K. B. Letaief, "Toward big data processing in IoT: Path planning and resource management of UAV base stations in mobile-edge computing system," *IEEE Internet of Things Journal*, vol. 7, no. 7, pp. 5995–6009, 2020.

[57] Y. Zeng, J. Lyu, and R. Zhang, "Cellular-connected UAV: Potential, challenges, and promising technologies," *IEEE Wireless Communications*, vol. 26, no. 1, pp. 120–127, 2019.

[58] S. Sawadsitang, D. Niyato, P.-S. Tan, and P. Wang, "Joint ground and aerial package delivery services: A stochastic optimization approach," *IEEE Transactions on Intelligent Transportation Systems*, vol. 20, no. 6, pp. 2241–2254, 2018.

[59] K. Dorling, J. Heinrichs, G. G. Messier, and S. Magierowski, "Vehicle routing problems for drone delivery," *IEEE Transactions on Systems, Man, and Cybernetics: Systems*, vol. 47, no. 1, pp. 70–85, 2016.

[60] H. Huang and A. V. Savkin, "A method of optimized deployment of charging stations for drone delivery," *IEEE Transactions on Transportation Electrification*, vol. 6, no. 2, pp. 510–518, 2020.

[61] H. Huang, A. V. Savkin, and C. Huang, "Reliable path planning for drone delivery using a stochastic time-dependent public transportation network," *IEEE Transactions on Intelligent Transportation Systems*, vol. 22, no. 8, pp. 4941–4950, 2021.

[62] D. Wang, P. Hu, J. Du, P. Zhou, T. Deng, and M. Hu, "Routing and scheduling for hybrid truck-drone collaborative parcel delivery with independent and truck-carried drones," *IEEE Internet of Things Journal*, vol. 6, no. 6, pp. 10 483–10 495, 2019.

[63] Q. Guo, J. Peng, W. Xu, W. Liang, X. Jia, Z. Xu, Y. Yang, and M. Wang, "Minimizing the longest tour time among a fleet of UAVs for disaster area surveillance," *IEEE Transactions on Mobile Computing*, to be published. doi: 10.1109/TMC.2020.3038156.

[64] Y. Wu, S. Wu, and X. Hu, "Cooperative path planning of UAVs & UGVs for a persistent surveillance task in urban environments," *IEEE Internet of Things Journal*, vol. 8, no. 6, pp. 4906–4919, 2021.

[65] D. Saha, D. Pattanayak, and P. S. Mandal, "Surveillance of uneven surface with self-organizing unmanned aerial vehicles," *IEEE Transactions on Mobile Computing*, to be published. doi: 10.1109/TMC.2020.3022075.

[66] S. R. Pokhrel, J. Jin, and H. Le Vu, "Mobility-aware multipath communication for unmanned aerial surveillance systems," *IEEE Transactions on Vehicular Technology*, vol. 68, no. 6, pp. 6088–6098, 2019.

[67] H. Huang and A. V. Savkin, "An algorithm of reactive collision free 3-D deployment of networked unmanned aerial vehicles for surveillance and monitoring," *IEEE Transactions on Industrial Informatics*, vol. 16, no. 1, pp. 132–140, 2019.

[68] A. V. Savkin and H. Huang, "A method for optimized deployment of a network of surveillance aerial drones," *IEEE Systems Journal*, vol. 13, no. 4, pp. 4474–4477, 2019.

[69] M. Hu, W. Liu, K. Peng, X. Ma, W. Cheng, J. Liu, and B. Li, "Joint routing and scheduling for vehicle-assisted multidrone surveillance," *IEEE Internet of Things Journal*, vol. 6, no. 2, pp. 1781–1790, 2018.

[70] H. Kim and J. Ben-Othman, "A collision-free surveillance system using smart UAVs in multi domain IoT," *IEEE communications letters*, vol. 22, no. 12, pp. 2587–2590, 2018.

[71] X. Shi, C. Yang, W. Xie, C. Liang, Z. Shi, and J. Chen, "Anti-drone system with multiple surveillance technologies: Architecture, implementation, and challenges," *IEEE Communications Magazine*, vol. 56, no. 4, pp. 68–74, 2018.

[72] H. Fu, S. Abeywickrama, L. Zhang, and C. Yuen, "Low-complexity portable passive drone surveillance via SDR-based signal processing," *IEEE Communications Magazine*, vol. 56, no. 4, pp. 112–118, 2018.

[73] X. Yue, Y. Liu, J. Wang, H. Song, and H. Cao, "Software defined radio and wireless acoustic networking for amateur drone surveillance," *IEEE Communications Magazine*, vol. 56, no. 4, pp. 90–97, 2018.

[74] J. Gu, T. Su, Q. Wang, X. Du, and M. Guizani, "Multiple moving targets surveillance based on a cooperative network for multi-UAV," *IEEE Communications Magazine*, vol. 56, no. 4, pp. 82–89, 2018.

[75] X. Chen, Z. Feng, Z. Wei, F. Gao, and X. Yuan, "Performance of joint sensing-communication cooperative sensing UAV network," *IEEE Transactions on Vehicular Technology*, vol. 69, no. 12, pp. 15 545–15 556, 2020.

[76] Y. Liu, J. Nie, X. Li, S. H. Ahmed, W. Y. B. Lim, and C. Miao, "Federated learning in the sky: Aerial-ground air quality sensing framework with UAV swarms," *IEEE Internet of Things Journal*, vol. 8, no. 12, pp. 9827–9837, 2021.

[77] B. Du, R. Mao, N. Kong, and D. Sun, "Distributed data fusion for on-scene signal sensing with a multi-UAV system," *IEEE Transactions on Control of Network Systems*, vol. 7, no. 3, pp. 1330–1341, 2020.

[78] W. Mei and R. Zhang, "UAV-sensing-assisted cellular interference coordination: A cognitive radio approach," *IEEE Wireless Communications Letters*, vol. 9, no. 6, pp. 799–803, 2020.

[79] B. Wang, Y. Sun, D. Liu, H. M. Nguyen, and T. Q. Duong, "Social-aware UAV-assisted mobile crowd sensing in stochastic and dynamic environments for disaster relief networks," *IEEE Transactions on Vehicular Technology*, vol. 69, no. 1, pp. 1070–1074, 2019.

[80] C. H. Liu, Z. Chen, and Y. Zhan, "Energy-efficient distributed mobile crowd sensing: A deep learning approach," *IEEE Journal on Selected Areas in Communications*, vol. 37, no. 6, pp. 1262–1276, 2019.

[81] W. Li, L. Wang, and A. Fei, "Minimizing packet expiration loss with path planning in UAV-assisted data sensing," *IEEE Wireless Communications Letters*, vol. 8, no. 6, pp. 1520–1523, 2019.

[82] Z. Zhou, J. Feng, B. Gu, B. Ai, S. Mumtaz, J. Rodriguez, and M. Guizani, "When mobile crowd sensing meets UAV: Energy-efficient task assignment and route planning," *IEEE Transactions on Communications*, vol. 66, no. 11, pp. 5526–5538, 2018.

[83] W. Xu, S. Wang, S. Yan, and J. He, "An efficient wideband spectrum sensing algorithm for unmanned aerial vehicle communication networks," *IEEE Internet of Things Journal*, vol. 6, no. 2, pp. 1768–1780, 2018.

[84] X. Liu, M. Guan, X. Zhang, and H. Ding, "Spectrum sensing optimization in an UAV-based cognitive radio," *IEEE Access*, vol. 6, pp. 44 002–44 009, 2018.

[85] Y. Yang, Z. Zheng, K. Bian, L. Song, and Z. Han, "Real-time profiling of fine-grained air quality index distribution using UAV sensing," *IEEE Internet of Things Journal*, vol. 5, no. 1, pp. 186–198, 2017.

[86] D. Wu, D. I. Arkhipov, M. Kim, C. L. Talcott, A. C. Regan, J. A. McCann, and N. Venkatasubramanian, "ADDSEN: Adaptive data processing and dissemination for drone swarms in urban sensing," *IEEE Transactions on Computers*, vol. 66, no. 2, pp. 183–198, 2016.

[87] Y. Zhou, C. Pan, P. L. Yeoh, K. Wang, M. Elkashlan, B. Vucetic, and Y. Li, "Communication-and-computing latency minimization for UAV-enabled virtual reality delivery systems," *IEEE Transactions on Communications*, vol. 69, no. 3, pp. 1723–1735, 2021.

[88] C. Zhan, H. Hu, Z. Wang, R. Fan, and D. Niyato, "Unmanned aircraft system aided adaptive video streaming: A joint optimization approach," *IEEE Transactions on Multimedia*, vol. 22, no. 3, pp. 795–807, 2019.

[89] J. Chakareski, "UAV-IoT for next generation virtual reality," *IEEE Transactions on Image Processing*, vol. 28, no. 12, pp. 5977–5990, 2019.

[90] K. Watanabe and M. Takahashi, "Head-synced drone control for reducing virtual reality sickness," *Journal of Intelligent & Robotic Systems*, vol. 97, no. 3, pp. 733–744, 2020.

[91] M. Chen, W. Saad, and C. Yin, "Echo-liquid state deep learning for 360° content transmission and caching in wireless VR networks with cellular-connected UAVs," *IEEE Transactions on Communications*, vol. 67, no. 9, pp. 6386–6400, 2019.

[92] U. R. Mogili and B. Deepak, "Review on application of drone systems in precision agriculture," *Procedia computer science*, vol. 133, pp. 502–509, 2018.

[93] D. Murugan, A. Garg, and D. Singh, "Development of an adaptive approach for precision agriculture monitoring with drone and satellite data," *IEEE Journal of Selected Topics in Applied Earth Observations and Remote Sensing*, vol. 10, no. 12, pp. 5322–5328, 2017.

[94] P. Tokekar, J. Vander Hook, D. Mulla, and V. Isler, "Sensor planning for a symbiotic UAV and UGV system for precision agriculture," *IEEE Transactions on Robotics*, vol. 32, no. 6, pp. 1498–1511, 2016.

[95] N. Chebrolu, T. Läbe, and C. Stachniss, "Robust long-term registration of UAV images of crop fields for precision agriculture," *IEEE Robotics and Automation Letters*, vol. 3, no. 4, pp. 3097–3104, 2018.

[96] C. M. Gevaert, J. Suomalainen, J. Tang, and L. Kooistra, "Generation of spectral–temporal response surfaces by combining multispectral satellite and hyperspectral UAV imagery for precision agriculture applications," *IEEE Journal of Selected Topics in Applied Earth Observations and Remote Sensing*, vol. 8, no. 6, pp. 3140–3146, 2015.

[97] Indu, R. Singh, H. R. Chaudhary, and A. K. Dubey, "Trajectory design for UAV-to-ground communication with energy optimization using genetic algorithm for agriculture application," *IEEE Sensors Journal*, vol. 21, no. 16, pp. 17 548–17 555, 2021.

[98] D. Bamburry, "Drones: Designed for product delivery," *Design Management Review*, vol. 26, no. 1, pp. 40–48, 2015.

[99] J. Liu, P. Tong, X. Wang, B. Bai, and H. Dai, "UAV-aided data collection for information freshness in wireless sensor networks," *IEEE Transactions on Wireless Communications*, vol. 20, no. 4, pp. 2368–2382, 2021.

[100] B. Duo, Q. Wu, X. Yuan, and R. Zhang, "Anti-jamming 3D trajectory design for UAV-enabled wireless sensor networks under probabilistic los channel," *IEEE Transactions on Vehicular Technology*, vol. 69, no. 12, pp. 16 288–16 293, 2020.

[101] T. D. P. Perera, S. Panic, D. N. K. Jayakody, P. Muthuchidambaranathan, and J. Li, "A WPT-enabled UAV-assisted condition monitoring scheme for wireless sensor networks," *IEEE Transactions on Intelligent Transportation Systems*, vol. 22, no. 8, pp. 5112–5126, 2021.

[102] C. Zhan and Y. Zeng, "Aerial–ground cost tradeoff for multi-UAV-enabled data collection in wireless sensor networks," *IEEE Transactions on Communications*, vol. 68, no. 3, pp. 1937–1950, 2019.

[103] C. Zhan, Y. Zeng, and R. Zhang, "Energy-efficient data collection in UAV enabled wireless sensor network," *IEEE Wireless Communications Letters*, vol. 7, no. 3, pp. 328–331, 2017.

[104] J. Baek, S. I. Han, and Y. Han, "Energy-efficient UAV routing for wireless sensor networks," *IEEE Transactions on Vehicular Technology*, vol. 69, no. 2, pp. 1741–1750, 2019.

[105] D. Ebrahimi, S. Sharafeddine, P.-H. Ho, and C. Assi, "UAV-aided projection-based compressive data gathering in wireless sensor networks," *IEEE Internet of Things Journal*, vol. 6, no. 2, pp. 1893–1905, 2018.

[106] J. Gong, T.-H. Chang, C. Shen, and X. Chen, "Flight time minimization of UAV for data collection over wireless sensor networks," *IEEE Journal on Selected Areas in Communications*, vol. 36, no. 9, pp. 1942–1954, 2018.

[107] C. Zhan, Y. Zeng, and R. Zhang, "Trajectory design for distributed estimation in UAV-enabled wireless sensor network," *IEEE Transactions on Vehicular Technology*, vol. 67, no. 10, pp. 10 155–10 159, 2018.

[108] M. Hua, Y. Wang, Z. Zhang, C. Li, Y. Huang, and L. Yang, "Power-efficient communication in UAV-aided wireless sensor networks," *IEEE Communications Letters*, vol. 22, no. 6, pp. 1264–1267, 2018.

[109] K. L.-M. Ang, J. K. P. Seng, and A. M. Zungeru, "Optimizing energy consumption for big data collection in large-scale wireless sensor networks with mobile collectors," *IEEE Systems Journal*, vol. 12, no. 1, pp. 616–626, 2017.

[110] V. Nazarzehi, A. V. Savkin, and A. Baranzadeh, "Distributed 3D dynamic search coverage for mobile wireless sensor networks," *IEEE Communications Letters*, vol. 19, no. 4, pp. 633–636, 2015.

[111] P. Wu, F. Xiao, C. Sha, H. Huang, and L. Sun, "Trajectory optimization for UAVs' efficient charging in wireless rechargeable sensor networks," *IEEE Transactions on Vehicular Technology*, vol. 69, no. 4, pp. 4207–4220, 2020.

[112] J. Baek, S. I. Han, and Y. Han, "Optimal UAV route in wireless charging sensor networks," *IEEE Internet of Things Journal*, vol. 7, no. 2, pp. 1327–1335, 2019.

[113] N. Zhao, F. R. Yu, L. Fan, Y. Chen, J. Tang, A. Nallanathan, and V. C. M. Leung, "Caching unmanned aerial vehicle-enabled small-cell networks: Employing energy-efficient methods that store and retrieve popular content," *IEEE Vehicular Technology Magazine*, vol. 14, no. 1, pp. 71–79, 2019.

[114] J. Yang, S. Xiao, B. Jiang, H. Song, S. Khan, and S. U. Islam, "Cache-enabled unmanned aerial vehicles for cooperative cognitive radio networks," *IEEE Wireless Communications*, vol. 27, no. 2, pp. 155–161, 2020.

[115] M. Chen, M. Mozaffari, W. Saad, C. Yin, M. Debbah, and C. S. Hong, "Caching in the sky: Proactive deployment of cache-enabled unmanned aerial vehicles for optimized quality-of-experience," *IEEE Journal on Selected Areas in Communications*, vol. 35, no. 5, pp. 1046–1061, 2017.

[116] Y. Zhang, T. T. Liu, H. G. Zhang, and Y. A. Liu, "LEACH-R: LEACH relay with cache strategy for mobile robot swarms," *IEEE Wireless Communications Letters*, vol. 10, no. 2, pp. 406–410, 2021.

[117] J. Shi, L. Zhao, X. Wang, W. Zhao, A. Hawbani, and M. Huang, "A novel deep Q-learning-based air-assisted vehicular caching scheme for safe autonomous driving," *IEEE Transactions on Intelligent Transportation Systems*, vol. 22, no. 7, pp. 4348–4358, 2021.

[118] A. Al-Hilo, M. Samir, C. Assi, S. Sharafeddine, and D. Ebrahimi, "UAV-assisted content delivery in intelligent transportation systems-joint trajectory planning and cache management," *IEEE Transactions on Intelligent Transportation Systems*, vol. 22, no. 8, pp. 5155–5167, 2021.

[119] A. A. Khuwaja, Y. Zhu, G. Zheng, Y. Chen, and W. Liu, "Performance analysis of hybrid UAV networks for probabilistic content caching," *IEEE Systems Journal*, vol. 15, no. 3, pp. 4013–4024, 2021.

[120] T. Zhang, Y. Wang, Y. Liu, W. Xu, and A. Nallanathan, "Cache-enabling UAV communications: Network deployment and resource allocation," *IEEE Transactions on Wireless Communications*, vol. 19, no. 11, pp. 7470–7483, 2020.

[121] J. Ji, K. Zhu, D. Niyato, and R. Wang, "Probabilistic cache placement in UAV-assisted networks with D2D connections: Performance analysis and trajectory optimization," *IEEE Transactions on Communications*, vol. 68, no. 10, pp. 6331–6345, 2020.

[122] H. Wu, F. Lyu, C. Zhou, J. Chen, L. Wang, and X. Shen, "Optimal UAV caching and trajectory in aerial-assisted vehicular networks: A learning-based approach," *IEEE Journal on Selected Areas in Communications*, vol. 38, no. 12, pp. 2783–2797, 2020.

[123] J. Ji, K. Zhu, D. Niyato, and R. Wang, "Joint cache placement, flight trajectory, and transmission power optimization for multi-UAV assisted wireless networks," *IEEE Transactions on Wireless Communications*, vol. 19, no. 8, pp. 5389–5403, 2020.

[124] F. Zhou, N. Wang, G. Luo, L. Fan, and W. Chen, "Edge caching in multi-UAV-enabled radio access networks: 3D modeling and spectral efficiency optimization," *IEEE Transactions on Signal and Information Processing over Networks*, vol. 6, pp. 329–341, 2020.

[125] A. Douik, H. Dahrouj, O. Amin, B. Aloquibi, T. Y. Al-Naffouri, and M. S. Alouini, "Mode selection and power allocation in multi-level cache-enabled networks," *IEEE Communications Letters*, vol. 24, no. 8, pp. 1789–1793, 2020.

[126] A. Bera, S. Misra, and C. Chatterjee, "QoE analysis in cache-enabled multi-UAV networks," *IEEE Transactions on Vehicular Technology*, vol. 69, no. 6, pp. 6680–6687, 2020.

[127] S. Chai and V. K. N. Lau, "Online trajectory and radio resource optimization of cache-enabled UAV wireless networks with content and energy recharging," *IEEE Transactions on Signal Processing*, vol. 68, pp. 1286–1299, 2020.

[128] F. Song, J. Li, M. Ding, L. Shi, F. Shu, M. Tao, W. Chen, and H. V. Poor, "Probabilistic caching for small-cell networks with terrestrial and aerial users," *IEEE Transactions on Vehicular Technology*, vol. 68, no. 9, pp. 9162–9177, 2019.

[129] A. Asheralieva and D. Niyato, "Game theory and Lyapunov optimization for cloud-based content delivery networks with device-to-device and UAV-enabled caching," *IEEE Transactions on Vehicular Technology*, vol. 68, no. 10, pp. 10 094–10 110, 2019.

[130] B. Jiang, J. Yang, H. Xu, H. Song, and G. Zheng, "Multimedia data throughput maximization in internet-of-things system based on optimization of cache-enabled UAV," *IEEE Internet of Things Journal*, vol. 6, no. 2, pp. 3525–3532, 2019.

[131] X. Xu, Y. Zeng, Y. L. Guan, and R. Zhang, "Overcoming endurance issue: UAV-enabled communications with proactive caching," *IEEE Journal on Selected Areas in Communications*, vol. 36, no. 6, pp. 1231–1244, 2018.

[132] N. Zhao, F. Cheng, F. R. Yu, J. Tang, Y. Chen, G. Gui, and H. Sari, "Caching UAV assisted secure transmission in hyper-dense networks based on interference alignment," *IEEE Transactions on Communications*, vol. 66, no. 5, pp. 2281–2294, 2018.

[133] M. E. Mkiramweni, C. Yang, J. Li, and W. Zhang, "A survey of game theory in unmanned aerial vehicles communications," *IEEE Communications Surveys & Tutorials*, vol. 21, no. 4, pp. 3386–3416, 2019.

[134] M. Gapeyenko, V. Petrov, D. Moltchanov, S. Andreev, N. Himayat, and Y. Koucheryavy, "Flexible and reliable UAV-assisted backhaul operation in 5G mmWave cellular networks," *IEEE Journal on Selected Areas in Communications*, vol. 36, no. 11, pp. 2486–2496, 2018.

[135] X. Cao, P. Yang, M. Alzenad, X. Xi, D. Wu, and H. Yanikomeroglu, "Airborne communication networks: A survey," *IEEE Journal on Selected Areas in Communications*, vol. 36, no. 9, pp. 1907–1926, 2018.

[136] S. C. Arum, D. Grace, and P. D. Mitchell, "A review of wireless communication using high-altitude platforms for extended coverage and capacity," *Computer Communications*, vol. 157, pp. 232–256, 2020.

[137] I. Bor-Yaliniz and H. Yanikomeroglu, "The new frontier in RAN heterogeneity: Multi-tier drone-cells," *IEEE Communications Magazine*, vol. 54, no. 11, pp. 48–55, 2016.

[138] H. Shakhatreh, A. H. Sawalmeh, A. Al-Fuqaha, Z. Dou, E. Almaita, I. Khalil, N. S. Othman, A. Khreishah, and M. Guizani, "Unmanned aerial vehicles (UAVs): A survey on civil applications and key research challenges," *IEEE Access*, vol. 7, pp. 48 572–48 634, 2019.

[139] T. Tozer and D. Grace, "High-altitude platforms for wireless communications," *Electronics & Communication Engineering Journal*, vol. 13, no. 3, pp. 127–137, 2001.

[140] D. Grace, M. H. Capstick, M. Mohorcic, J. Horwath, M. B. Pallavicini, and M. Fitch, "Integrating users into the wider broadband network via high altitude platforms," *IEEE Wireless Communications*, vol. 12, no. 5, pp. 98–105, 2005.

[141] D. Grace, N. Daly, T. C. Tozer, A. G. Burr, and D. A. Pearce, "Providing multimedia communications services from high altitude platforms," *International Journal of Satellite Communications*, vol. 19, no. 6, pp. 559–580, 2001.

[142] G. P. White and Y. V. Zakharov, "Data communications to trains from high-altitude platforms," *IEEE Transactions on Vehicular Technology*, vol. 56, no. 4, pp. 2253–2266, 2007.

[143] G. Chen, D. Grace, and T. C. Tozer, "Performance of multiple high altitude platforms using directive HAP and user antennas," *Wireless Personal Communications*, vol. 32, no. 3-4, pp. 275–299, 2005.

[144] G. M. Djuknic, J. Freidenfelds, and Y. Okunev, "Establishing wireless communications services via high-altitude aeronautical platforms: A concept whose time has come?" *IEEE Communications Magazine*, vol. 35, no. 9, pp. 128–135, 1997.

[145] E. Cianca, R. Prasad, M. De Sanctis, A. De Luise, M. Antonini, D. Teotino, and M. Ruggieri, "Integrated satellite-HAP systems," *IEEE Communications Magazine*, vol. 43, no. 12, pp. 33–39, 2005.

[146] D. Grace and M. Mohorcic, *Broadband communications via high altitude platforms*. John Wiley & Sons, 2011.

[147] S. Karapantazis and F. Pavlidou, "Broadband communications via high-altitude platforms: A survey," *IEEE Communications Surveys & Tutorials*, vol. 7, no. 1, pp. 2–31, 2005.

[148] P. Qi, X. Zhao, Y. Wang, R. Palacios, and A. Wynn, "Aeroelastic and trajectory control of high altitude long endurance aircraft," *IEEE Transactions on Aerospace and Electronic Systems*, vol. 54, no. 6, pp. 2992–3003, 2018.

[149] M. J. Patil, D. H. Hodges, and C. E. Cesnik, "Nonlinear aeroelasticity and flight dynamics of high-altitude long-endurance aircraft," *Journal of Aircraft*, vol. 38, no. 1, pp. 88–94, 2001.

[150] E. Cestino, "Design of solar high altitude long endurance aircraft for multi payload & operations," *Aerospace science and technology*, vol. 10, no. 6, pp. 541–550, 2006.

[151] R. A. Martin, N. S. Gates, A. Ning, and J. D. Hedengren, "Dynamic optimization of high-altitude solar aircraft trajectories under station-keeping constraints," *Journal of Guidance, Control, and Dynamics*, vol. 42, no. 3, pp. 538–552, 2019.

[152] F. A. d'Oliveira, F. C. L. d. Melo, and T. C. Devezas, "High-altitude platforms—present situation and technology trends," *Journal of Aerospace Technology and Management*, vol. 8, no. 3, pp. 249–262, 2016.

[153] I. Vandermeulen, M. Guay, and P. J. McLellan, "Distributed control of high-altitude balloon formation by extremum-seeking control," *IEEE Transactions on Control Systems Technology*, vol. 26, no. 3, pp. 857–873, 2017.

[154] P. Sudheesh, M. Mozaffari, M. Magarini, W. Saad, and P. Muthuchidambaranathan, "Sum-rate analysis for high altitude platform (HAP) drones with tethered balloon relay," *IEEE Communications Letters*, vol. 22, no. 6, pp. 1240–1243, 2017.

[155] R. Waghela, C. D. Yoder, A. Gopalarathnam, and A. Mazzoleni, "Aerodynamic sails for passive guidance of high-altitude balloons: Static-stability and equilibrium performance," *Journal of Aircraft*, vol. 56, no. 5, pp. 1849–1857, 2019.

[156] Y. Xu, W. Zhu, J. Li, and L. Zhang, "Improvement of endurance performance for high-altitude solar-powered airships: A review," *Acta Astronautica*, vol. 167, pp. 245–259, 2020.

[157] S. Hu, A. Zhang, and S. Chai, "ASQ-MPHAAS: Multi-payload observation system from high altitude airship," *IEEE Sensors Journal*, vol. 19, no. 24, pp. 12 353–12 362, 2019.

[158] J. Tang, X. Wang, D. Duan, and W. Xie, "Optimisation and analysis of efficiency for contra-rotating propellers for high-altitude airships," *The Aeronautical Journal*, vol. 123, no. 1263, pp. 706–726, 2019.

[159] R. M. Dickinson, "Power in the sky: Requirements for microwave wireless power beamers for powering high-altitude platforms," *IEEE Microwave magazine*, vol. 14, no. 2, pp. 36–47, 2013.

[160] M. D. Zakaria, D. Grace, P. D. Mitchell, T. M. Shami, and N. Morozs, "Exploiting user-centric joint transmission–coordinated multipoint with a high altitude platform system architecture," *IEEE Access*, vol. 7, pp. 38 957–38 972, 2019.

[161] V. V. Mai and H. Kim, "Beam size optimization and adaptation for high-altitude airborne free-space optical communication systems," *IEEE Photonics Journal*, vol. 11, no. 2, pp. 1–13, 2019.

[162] D. Grace, J. Thornton, G. Chen, G. P. White, and T. C. Tozer, "Improving the system capacity of broadband services using multiple high-altitude platforms," *IEEE Transactions on Wireless Communications*, vol. 4, no. 2, pp. 700–709, 2005.

[163] E. Falletti, M. Laddomada, M. Mondin, and F. Sellone, "Integrated services from high-altitude platforms: A flexible communication system," *IEEE Communications Magazine*, vol. 44, no. 2, pp. 85–94, 2006.

[164] A. K. Widiawan and R. Tafazolli, "High altitude platform station (HAPS): A review of new infrastructure development for future wireless communications," *Wireless Personal Communications*, vol. 42, no. 3, pp. 387–404, 2007.

[165] D. Avagnina, F. Dovis, A. Ghiglione, and P. Mulassano, "Wireless networks based on high-altitude platforms for the provision of integrated navigation/communication services," *IEEE Communications Magazine*, vol. 40, no. 2, pp. 119–125, 2002.

[166] A. Ibrahim and A. S. Alfa, "Using Lagrangian relaxation for radio resource allocation in high altitude platforms," *IEEE Transactions on Wireless Communications*, vol. 14, no. 10, pp. 5823–5835, 2015.

[167] A. Mohammed, A. Mehmood, F.-N. Pavlidou, and M. Mohorcic, "The role of high-altitude platforms (HAPs) in the global wireless connectivity," *Proceedings of the IEEE*, vol. 99, no. 11, pp. 1939–1953, 2011.

[168] M. P. Anastasopoulos and P. G. Cottis, "High altitude platform networks: A feedback suppression algorithm for reliable multicast/broadcast services," *IEEE Transactions on Wireless Communications*, vol. 8, no. 4, pp. 1639–1643, 2008.

[169] A. Ibrahim and A. Alfa, *Optimization Methods for User Admissions and Radio Resource Allocation for Multicasting over High Altitude Platforms*. River Publishers, 2019.

[170] M. Alzenad, M. Z. Shakir, H. Yanikomeroglu, and M.-S. Alouini, "FSO-based vertical backhaul/fronthaul framework for 5G+ wireless networks," *IEEE Communications Magazine*, vol. 56, no. 1, pp. 218–224, 2018.

[171] L. Gupta, R. Jain, and G. Vaszkun, "Survey of important issues in UAV communication networks," *IEEE Communications Surveys & Tutorials*, vol. 18, no. 2, pp. 1123–1152, 2015.

[172] I. Bekmezci, O. K. Sahingoz, and Ş. Temel, "Flying ad-hoc networks (FANETs): A survey," *Ad Hoc Networks*, vol. 11, no. 3, pp. 1254–1270, 2013.

[173] A. Al-Hourani, S. Kandeepan, and S. Lardner, "Optimal LAP altitude for maximum coverage," *IEEE Wireless Communications Letters*, vol. 3, no. 6, pp. 569–572, 2014.

[174] M. Mozaffari, W. Saad, M. Bennis, and M. Debbah, "Efficient deployment of multiple unmanned aerial vehicles for optimal wireless coverage," *IEEE Communications Letters*, vol. 20, no. 8, pp. 1647–1650, 2016.

[175] M. Alzenad, A. El-Keyi, F. Lagum, and H. Yanikomeroglu, "3-D placement of an unmanned aerial vehicle base station (UAV-BS) for energy-efficient maximal coverage," *IEEE Wireless Communications Letters*, vol. 6, no. 4, pp. 434–437, 2017.

[176] J. Lyu, Y. Zeng, R. Zhang, and T. J. Lim, "Placement optimization of UAV-mounted mobile base stations," *IEEE Communications Letters*, vol. 21, no. 3, pp. 604–607, 2016.

[177] I. Bor-Yaliniz, M. Salem, G. Senerath, and H. Yanikomeroglu, "Is 5G ready for drones: A look into contemporary and prospective wireless networks from a standardization perspective," *IEEE Wireless Communications*, vol. 26, no. 1, pp. 18–27, 2019.

[178] H. Ahmadi, K. Katzis, and M. Z. Shakir, "A novel airborne self-organising architecture for 5G+ networks," in *2017 IEEE 86th Vehicular Technology Conference (VTC-Fall)*. IEEE, 2017, pp. 1–5.

[179] M. Mozaffari, A. T. Z. Kasgari, W. Saad, M. Bennis, and M. Debbah, "Beyond 5G with UAVs: Foundations of a 3D wireless cellular network," *IEEE Transactions on Wireless Communications*, vol. 18, no. 1, pp. 357–372, 2019.

[180] D. Kreutz, F. M. Ramos, P. Verissimo, C. E. Rothenberg, S. Azodolmolky, and S. Uhlig, "Software-defined networking: A comprehensive survey," *Proceedings of the IEEE*, vol. 103, no. 1, pp. 14–76, 2015.

[181] U. Challita, A. Ferdowsi, M. Chen, and W. Saad, "Machine learning for wireless connectivity and security of cellular-connected UAVs," *IEEE Wireless Communications*, vol. 26, no. 1, pp. 28–35, 2019.

[182] U. Challita, W. Saad, and C. Bettstetter, "Interference management for cellular-connected UAVs: A deep reinforcement learning approach," *IEEE Transactions on Wireless Communications*, vol. 18, no. 4, pp. 2125–2140, 2019.

[183] M. Mozaffari, W. Saad, M. Bennis, and M. Debbah, "Unmanned aerial vehicle with underlaid device-to-device communications: Performance and tradeoffs," *IEEE Transactions on Wireless Communications*, vol. 15, no. 6, pp. 3949–3963, 2016.

[184] B. Li, Z. Fei, and Y. Zhang, "UAV communications for 5G and Beyond: Recent advances and future trends," *IEEE Internet of Things Journal*, vol. 6, no. 2, pp. 2241–2263, 2019.

[185] G. Ding, Q. Wu, L. Zhang, Y. Lin, T. A. Tsiftsis, and Y.-D. Yao, "An amateur drone surveillance system based on the cognitive internet of things," *IEEE Communications Magazine*, vol. 56, no. 1, pp. 29–35, 2018.

[186] A. Asadi, Q. Wang, and V. Mancuso, "A survey on device-to-device communication in cellular networks," *IEEE Communications Surveys & Tutorials*, vol. 16, no. 4, pp. 1801–1819, 2014.

[187] D. Feng, L. Lu, Y. Yuan-Wu, G. Y. Li, S. Li, and G. Feng, "Device-to-device communications in cellular networks," *IEEE Communications Magazine*, vol. 52, no. 4, pp. 49–55, 2014.

[188] M. N. Tehrani, M. Uysal, and H. Yanikomeroglu, "Device-to-device communication in 5G cellular networks: challenges, solutions, and future directions," *IEEE Communications Magazine*, vol. 52, no. 5, pp. 86–92, 2014.

[189] F. Jameel, Z. Hamid, F. Jabeen, S. Zeadally, and M. A. Javed, "A survey of device-to-device communications: Research issues and challenges," *IEEE Communications Surveys & Tutorials*, vol. 20, no. 3, pp. 2133–2168, 2018.

[190] M. M. Azari, G. Geraci, A. Garcia-Rodriguez, and S. Pollin, "UAV-to-UAV communications in cellular networks," *IEEE Transactions on Wireless Communications*, vol. 19, no. 9, pp. 6130–6144, 2020.

[191] C. Zhan and Y. Zeng, "Energy-efficient data uploading for cellular-connected UAV systems," *IEEE Transactions on Wireless Communications*, vol. 19, no. 11, pp. 7279–7292, 2020.

[192] R. Amer, W. Saad, and N. Marchetti, "Mobility in the sky: Performance and mobility analysis for cellular-connected UAVs," *IEEE Transactions on Communications*, vol. 68, no. 5, pp. 3229–3246, 2020.

[193] W. Mei, Q. Wu, and R. Zhang, "Cellular-connected UAV: Uplink association, power control and interference coordination," *IEEE Transactions on Wireless Communications*, vol. 18, no. 11, pp. 5380–5393, 2019.

[194] S. Zhang, H. Zhang, Z. Han, H. V. Poor, and L. Song, "Age of information in a cellular internet of UAVs: Sensing and communication trade-off design," *IEEE Transactions on Wireless Communications*, vol. 19, no. 10, pp. 6578–6592, 2020.

[195] S. Zhang, H. Zhang, B. Di, and L. Song, "Joint trajectory and power optimization for UAV sensing over cellular networks," *IEEE Communications Letters*, vol. 22, no. 11, pp. 2382–2385, 2018.

[196] D. Tse and P. Viswanath, *Fundamentals of wireless communication*. Cambridge university press, 2005.

[197] C. Guo, L. Liang, and G. Y. Li, "Resource allocation for vehicular communications with low latency and high reliability," *IEEE Transactions on Wireless Communications*, vol. 18, no. 8, pp. 3887–3902, 2019.

[198] ——, "Resource allocation for high-reliability low-latency vehicular communications with packet retransmission," *IEEE Transactions on Vehicular Technology*, vol. 68, no. 7, pp. 6219–6230, 2019.

[199] S. Kandukuri and S. Boyd, "Optimal power control in interference-limited fading wireless channels with outage-probability specifications," *IEEE Transactions on Wireless Communications*, vol. 1, no. 1, pp. 46–55, 2002.

[200] C. Guo, L. Liang, and G. Y. Li, "Resource allocation for low-latency vehicular communications: An effective capacity perspective," *IEEE Journal on Selected Areas in Communications*, vol. 37, no. 4, pp. 905–917, 2019.

[201] D. B. West *et al.*, *Introduction to graph theory*. Prentice hall Upper Saddle River, NJ, 1996, vol. 2.

[202] H. W. Kuhn, "The Hungarian method for the assignment problem," *Naval research logistics quarterly*, vol. 2, no. 1-2, pp. 83–97, 1955.

[203] S. D. Muruganathan, X. Lin, H.-L. Maattanen, J. Sedin, Z. Zou, W. A. Hapsari, and S. Yasukawa, "An overview of 3GPP release-15 study on enhanced LTE support for connected drones," *arXiv preprint arXiv:1805.00826*, 2018.

[204] D. Feng, L. Lu, Y. Yuan-Wu, G. Y. Li, G. Feng, and S. Li, "Device-to-device communications underlaying cellular networks," *IEEE Transactions on Communications*, vol. 61, no. 8, pp. 3541–3551, 2013.

[205] N. Hossein Motlagh, T. Taleb, and O. Arouk, "Low-altitude unmanned aerial vehicles-based internet of things services: Comprehensive survey and future perspectives," *IEEE Internet of Things Journal*, vol. 3, no. 6, pp. 899–922, 2016.

[206] F. Shen, G. Ding, Z. Wang, and Q. Wu, "UAV-based 3D spectrum sensing in spectrum-heterogeneous networks," *IEEE Transactions on Vehicular Technology*, vol. 68, no. 6, pp. 5711–5722, 2019.

[207] W. Xu, S. Wang, S. Yan, and J. He, "An efficient wideband spectrum sensing algorithm for unmanned aerial vehicle communication networks," *IEEE Internet of Things Journal*, vol. 6, no. 2, pp. 1768–1780, 2019.

[208] S. Bhattarai, J. J. Park, B. Gao, K. Bian, and W. Lehr, "An overview of dynamic spectrum sharing: Ongoing initiatives, challenges, and a roadmap for future research," *IEEE Transactions on Cognitive Communications and Networking*, vol. 2, no. 2, pp. 110–128, 2016.

[209] J. Lyu, Y. Zeng, and R. Zhang, "UAV-aided offloading for cellular hotspot," *IEEE Transactions on Wireless Communications*, vol. 17, no. 6, pp. 3988–4001, 2018.

[210] L. Wang, H. Yang, J. Long, K. Wu, and J. Chen, "Enabling ultra-dense UAV-aided network with overlapped spectrum sharing: Potential and approaches," *IEEE Network*, vol. 32, no. 5, pp. 85–91, 2018.

[211] J. Yao and N. Ansari, "Caching in energy harvesting aided internet of things: A game-theoretic approach," *IEEE Internet of Things Journal*, vol. 6, no. 2, pp. 3194–3201, 2019.

[212] W. Huang, W. Chen, and H. V. Poor, "Request delay-based pricing for proactive caching: A Stackelberg game approach," *IEEE Transactions on Wireless Communications*, vol. 18, no. 6, pp. 2903–2918, 2019.

[213] S. Hong and H. Kim, "QoE-aware computation offloading to capture energy-latency-pricing tradeoff in mobile clouds," *IEEE Transactions on Mobile Computing*, vol. 18, no. 9, pp. 2174–2189, 2019.

[214] M. Li, T. Q. S. Quek, and C. Courcoubetis, "Mobile data offloading with uniform pricing and overlaps," *IEEE Transactions on Mobile Computing*, vol. 18, no. 2, pp. 348–361, 2019.

[215] N. Zhao, Y. Liang, and Y. Pei, "Dynamic contract incentive mechanism for cooperative wireless networks," *IEEE Transactions on Vehicular Technology*, vol. 67, no. 11, pp. 10 970–10 982, 2018.

[216] Z. Hu, Z. Zheng, L. Song, T. Wang, and X. Li, "UAV offloading: Spectrum trading contract design for UAV-assisted cellular networks," *IEEE Transactions on Wireless Communications*, vol. 17, no. 9, pp. 6093–6107, 2018.

[217] F. Tschorsch and B. Scheuermann, "Bitcoin and beyond: A technical survey on decentralized digital currencies," *IEEE Communications Surveys & Tutorials*, vol. 18, no. 3, pp. 2084–2123, 2016.

[218] A. Dorri, M. Steger, S. S. Kanhere, and R. Jurdak, "BlockChain: A distributed solution to automotive security and privacy," *IEEE Communications Magazine*, vol. 55, no. 12, pp. 119–125, 2017.

[219] T. Salman, M. Zolanvari, A. Erbad, R. Jain, and M. Samaka, "Security services using blockchains: A state of the art survey," *IEEE Communications Surveys & Tutorials*, vol. 21, no. 1, pp. 858–880, 2019.

[220] M. A. Ferrag, M. Derdour, M. Mukherjee, A. Derhab, L. Maglaras, and H. Janicke, "Blockchain technologies for the internet of things: Research issues and challenges," *IEEE Internet of Things Journal*, vol. 6, no. 2, pp. 2188–2204, 2019.

[221] H. Wang, Q. Wang, D. He, Q. Li, and Z. Liu, "BBARS: Blockchain-based anonymous rewarding scheme for V2G networks," *IEEE Internet of Things Journal*, vol. 6, no. 2, pp. 3676–3687, 2019.

[222] M. Li, J. Weng, A. Yang, W. Lu, Y. Zhang, L. Hou, J. Liu, Y. Xiang, and R. H. Deng, "CrowdBC: A blockchain-based decentralized framework for crowdsourcing," *IEEE Transactions on Parallel and Distributed Systems*, vol. 30, no. 6, pp. 1251–1266, 2019.

[223] X. Xu, Q. Liu, X. Zhang, J. Zhang, L. Qi, and W. Dou, "A blockchain-powered crowdsourcing method with privacy preservation in mobile environment," *IEEE Transactions on Computational Social Systems*, vol. 6, no. 6, pp. 1407–1419, 2019.

[224] Y. Zhu, G. Zheng, and K. Wong, "Blockchain-empowered decentralized storage in air-to-ground industrial networks," *IEEE Transactions on Industrial Informatics*, vol. 15, no. 6, pp. 3593–3601, 2019.

[225] V. Sharma, I. You, D. N. K. Jayakody, D. G. Reina, and K. R. Choo, "Neural-blockchain based ultra-reliable caching for edge-enabled UAV networks," *IEEE Transactions on Industrial Informatics*, vol. 15, no. 10, pp. 5723–5736, 2019.

[226] D. Puthal, N. Malik, S. P. Mohanty, E. Kougianos, and G. Das, "Everything you wanted to know about the blockchain: Its promise, components, processes, and problems," *IEEE Consumer Electronics Magazine*, vol. 7, no. 4, pp. 6–14, 2018.

[227] M. S. Ali, M. Vecchio, M. Pincheira, K. Dolui, F. Antonelli, and M. H. Rehmani, "Applications of blockchains in the internet of things: A comprehensive survey," *IEEE Communications Surveys & Tutorials*, vol. 21, no. 2, pp. 1676–1717, 2019.

[228] X. Kang and Y. Wu, "Incentive mechanism design for heterogeneous peer-to-peer networks: A Stackelberg game approach," *IEEE Transactions on Mobile Computing*, vol. 14, no. 5, pp. 1018–1030, 2015.

[229] L. Duan, J. Huang, and B. Shou, "Duopoly competition in dynamic spectrum leasing and pricing," *IEEE Transactions on Mobile Computing*, vol. 11, no. 11, pp. 1706–1719, 2012.

[230] M. Belotti, N. Božić, G. Pujolle, and S. Secci, "A vademecum on blockchain technologies: When, which and how," *IEEE Communications Surveys & Tutorials*, vol. 21, no. 4, pp. 3796–3838, 2019.

[231] C. Stergiou, K. E. Psannis, A. P. Plageras, Y. Ishibashi, and B.-G. Kim, "Algorithms for efficient digital media transmission over IoT and cloud networking," *Journal of Multimedia Information System*, vol. 5, no. 1, pp. 27–34, 2018.

[232] K. E. Psannis, C. Stergiou, and B. B. Gupta, "Advanced media-based smart big data on intelligent cloud systems," *IEEE Transactions on Sustainable Energy*, vol. 4, no. 1, pp. 77–87, 2019.

[233] M. Armbrust, A. Fox, R. Griffith, A. D. Joseph, R. Katz, A. Konwinski, G. Lee, D. Patterson, A. Rabkin, I. Stoica *et al.*, "A view of cloud computing," *Communications of the ACM*, vol. 53, no. 4, pp. 50–58, 2010.

[234] B. Furht and A. Escalante, *Handbook of cloud computing*. Springer, 2010, vol. 3.

[235] N. Abbas, Y. Zhang, A. Taherkordi, and T. Skeie, "Mobile edge computing: A survey," *IEEE Internet of Things Journal*, vol. 5, no. 1, pp. 450–465, 2018.

[236] Y. Mao, C. You, J. Zhang, K. Huang, and K. B. Letaief, "A survey on mobile edge computing: The communication perspective," *IEEE Communications Surveys & Tutorials*, vol. 19, no. 4, pp. 2322–2358, 2017.

[237] P. Mach and Z. Becvar, "Mobile edge computing: A survey on architecture and computation offloading," *IEEE Communications Surveys & Tutorials*, vol. 19, no. 3, pp. 1628–1656, 2017.

[238] R. Yang, F. R. Yu, P. Si, Z. Yang, and Y. Zhang, "Integrated blockchain and edge computing systems: A survey, some research issues and challenges," *IEEE Communications Surveys & Tutorials*, vol. 21, no. 2, pp. 1508–1532, 2nd Quart. 2019.

[239] N. Z. Aitzhan and D. Svetinovic, "Security and privacy in decentralized energy trading through multi-signatures, blockchain and anonymous messaging streams," *IEEE Transactions on Dependable and Secure Computing*, vol. 15, no. 5, pp. 840–852, 2018.

[240] Z. Su, Y. Wang, Q. Xu, M. Fei, Y. Tian, and N. Zhang, "A secure charging scheme for electric vehicles with smart communities in energy blockchain," *IEEE Internet of Things Journal*, vol. 6, no. 3, pp. 4601–4613, 2019.

[241] J. Kang, R. Yu, X. Huang, M. Wu, S. Maharjan, S. Xie, and Y. Zhang, "Blockchain for secure and efficient data sharing in vehicular edge computing and networks," *IEEE Internet of Things Journal*, vol. 6, no. 3, pp. 4660–4670, 2019.

[242] J. Kang, Z. Xiong, D. Niyato, D. Ye, D. I. Kim, and J. Zhao, "Toward secure blockchain-enabled internet of vehicles: Optimizing consensus management using reputation and contract theory," *IEEE Transactions on Vehicular Technology*, vol. 68, no. 3, pp. 2906–2920, 2019.

[243] J. Kang, R. Yu, X. Huang, S. Maharjan, Y. Zhang, and E. Hossain, "Enabling localized peer-to-peer electricity trading among plug-in hybrid electric vehicles using consortium blockchains," *IEEE Transactions on Industrial Informatics*, vol. 13, no. 6, pp. 3154–3164, 2017.

[244] Z. Li, J. Kang, R. Yu, D. Ye, Q. Deng, and Y. Zhang, "Consortium blockchain for secure energy trading in industrial internet of things," *IEEE Transactions on Industrial Informatics*, vol. 14, no. 8, pp. 3690–3700, 2018.

[245] Z. Han, D. Niyato, W. Saad, T. Başar, and A. Hjørungnes, *Game theory in wireless and communication networks: Theory, models, and applications*. Cambridge University Press, 2012.

[246] X. Kang, R. Zhang, and M. Motani, "Price-based resource allocation for spectrum-sharing femtocell networks: A Stackelberg game approach," *IEEE Journal on Selected Areas in Communications*, vol. 30, no. 3, pp. 538–549, 2012.

[247] J. Lee, K. Park, Y. Ko, and M. Alouini, "A UAV-mounted free space optical communication: Trajectory optimization for flight time," *IEEE Transactions on Wireless Communications*, vol. 19, no. 3, pp. 1610–1621, 2020.

[248] T. Zhang, Y. Xu, J. Loo, D. Yang, and L. Xiao, "Joint computation and communication design for UAV-assisted mobile edge computing in IoT," *IEEE Transactions on Industrial Informatics*, vol. 16, no. 8, pp. 5505–5516, 2020.

[249] J. Du, W. Xu, Y. Deng, A. Nallanathan, and L. Vandendorpe, "Energy-saving UAV-assisted multiuser communications with massive MIMO hybrid beamforming," *IEEE Communications Letters*, vol. 24, no. 5, pp. 1100–1104, 2020.

[250] M. B. Ghorbel, D. Rodriguez-Duarte, H. Ghazzai, M. J. Hossain, and H. Menouar, "Joint position and travel path optimization for energy efficient wireless data gathering using unmanned aerial vehicles," *IEEE Transactions on Vehicular Technology*, vol. 68, no. 3, pp. 2165–2175, 2019.

[251] S. Yin, Y. Zhao, L. Li, and F. R. Yu, "UAV-assisted cooperative communications with time-sharing information and power transfer," *IEEE Transactions on Vehicular Technology*, vol. 69, no. 2, pp. 1554–1567, 2020.

[252] S. Yin, L. Li, and F. R. Yu, "Resource allocation and basestation placement in downlink cellular networks assisted by multiple wireless powered UAVs," *IEEE Transactions on Vehicular Technology*, vol. 69, no. 2, pp. 2171–2184, 2020.

[253] Q. Zhang, W. Fang, Q. Liu, J. Wu, P. Xia, and L. Yang, "Distributed laser charging: A wireless power transfer approach," *IEEE Internet of Things Journal*, vol. 5, no. 5, pp. 3853–3864, 2018.

[254] T. Nugent and J. Kare, "Laser power for UAVs," *Laser Motive White Paper-Power Beaming for UAVs*, 2010.

[255] Y. Huo, X. Dong, T. Lu, W. Xu, and M. Yuen, "Distributed and multilayer UAV networks for next-generation wireless communication and power transfer: A feasibility study," *IEEE Internet of Things Journal*, vol. 6, no. 4, pp. 7103–7115, 2019.

[256] J. Qiu, G. David, G. Ding, M. D. Zakaria, and Q. Wu, "Air-ground heterogeneous networks for 5G and beyond via integrating high and low altitude platforms," *IEEE Wireless Communications*, vol. 26, no. 6, pp. 140–148, 2019.

[257] Y. Zeng and R. Zhang, "Energy-efficient UAV communication with trajectory optimization," *IEEE Transactions on Wireless Communications*, vol. 16, no. 6, pp. 3747–3760, 2017.

[258] M. Lahmeri, M. A. Kishk, and M. Alouini, "Stochastic geometry-based analysis of airborne base stations with laser-powered UAVs," *IEEE Communications Letters*, vol. 24, no. 1, pp. 173–177, 2020.

[259] H. Kaushal, V. Jain, and S. Kar, *Free space optical communication.* Gurgaon, Haryana: Springer, 2017.

[260] J. Zhang, Y. Zeng, and R. Zhang, "UAV-enabled radio access network: Multi-mode communication and trajectory design," *IEEE Transactions on Signal Processing*, vol. 66, no. 20, pp. 5269–5284, 2018.

[261] S. Boyd and L. Vandenberghe, *Convex optimization.* Cambridge, U.K.: Cambridge Univ. Press, 2004.

[262] J.-P. Crouzeix and J. A. Ferland, "Algorithms for generalized fractional programming," *Mathematical Programming*, vol. 52, no. 1-3, pp. 191–207, 1991.

[263] Y. Zeng, R. Zhang, and T. J. Lim, "Throughput maximization for UAV-enabled mobile relaying systems," *IEEE Transactions on Communications*, vol. 64, no. 12, pp. 4983–4996, 2016.

[264] W. Dinkelbach, "On nonlinear fractional programming," *Management Science*, vol. 13, no. 7, pp. 492–498, Mar. 1967.

[265] D. W. K. Ng, E. S. Lo, and R. Schober, "Energy-efficient resource allocation for secure OFDMA systems," *IEEE Transactions on Vehicular Technology*, vol. 61, no. 6, pp. 2572–2585, 2012.